DECIPHERING DEPOSITIONAL AND DIAGENETIC PROCESSES IN MARINE SYSTEMS BY APPLICATION OF TRACE METAL AND ISOTOPE GEOCHEMISTRY

By

MICHELLE LEE ABSHIRE

Bachelor of Science in Geology
Oklahoma State University
Stillwater, Oklahoma
2016

Submitted to the Faculty of the
Graduate College of the
Oklahoma State University
in partial fulfillment of
the requirements for
the Degree of
DOCTOR OF PHILOSOPHY
July, 2020

DECIPHERING DEPOSITIONAL AND DIAGENETIC PROCESSES IN MARINE SYSTEMS BY APPLICATION OF TRACE METAL AND ISOTOPE GEOCHEMISTRY

Dissertation Approved:

Dr. Natascha Riedinger

Dissertation Adviser

Dr. James Puckette

Dr. Joseph Donoghue

Dr. Gabriel Cook

ACKNOWLEDGEMENTS

I would like to express my sincere gratitude to my advisor, Dr. Natascha Riedinger, who inspired me to pursue my PhD and continuously encouraged me to push myself further than I ever thought possible. She welcomed me into her large and global scientific family which allowed me to meet the most amazing scientists and travel to parts of the world I never imagined I could visit. I also want to thank my committee members Dr. Joseph Donoghue, Dr. Jim Puckette, and Dr. Gabriel Cook, who supported my science and asked me all of the difficult questions. I am also immensely grateful to the Boone Pickens School of Geology, our Department Head, Dr. Camelia Knapp, and our hugely supportive alumni, many of which had a profound impact on my years at OSU. I am further thankful to the National Science Foundation Graduate Research Fellowship Program which provided funding for the first three years of my research. Also thanks to the American Association of Petroleum Geologists, the Oklahoma Energy Resources Board, and the Geological Society of America for additional funding. The professors and staff at OSU have been nothing short of amazing during my time in Stillwater. In addition to my graduate committee members, several professors have helped me achieve far more than I ever expected. Dr. Tracy Quan has been an ear to listen, a shoulder to cry on, and a brain to pick more times than she might have planned. I appreciate her insight into all things geochemical and academic. Dr. Brendan Hanger and Dr. Ashley Burkett have been so helpful and supportive during my last year at OSU. Dr. Estella Atekwana has also been a huge source of inspiration to me. Mrs. Sandy Earls keeps everything in the department running like a well-oiled machine. Many thanks to John Clymer for his work on the Ohio Shale, and undergraduate lab assistants Chris Jones, Katie Spencer, Jacob Archer, Bre Waterman, and Jessie Wolters who have all been very helpful with lab work. Dr. Anbar, Dr. Romaniello and the METALS lab at Arizona State University have been fantastic resources for all things isotopic. Dr. Severmann and Mrs. Kuzminov at Rutgers State University have also provided resources for my thesis work. I also want to thank my fellow graduate students (past and present) for their support and friendship. There are too many of them to name here, but I think they know who they are.

I am eternally and indescribably grateful to my family who have all stood behind me as my motivation and cheerleading squad for the last 9 years. My daughters, Megan and Vera, have sacrificed their mother to the University for more time than they may have liked, but they seldom complained. To my dad and step-mom Mike and Carol Abshire, and my mother Susan Battle, I'm proud to make you proud. My late grandparents, Joyce and Charley Abshire, and Betty Wilson, all of which I lost since beginning this journey, would be very proud of me for completing a PhD, which will be a first for our family. Finally, I would like to thank my loving fiancé, Chris Bailey, who has supported me in every way possible and never let me give up. I could not have completed this journey without him.

Name: MICHELLE LEE ABSHIRE

Date of Degree: JULY, 2020

Title of Study: DECIPHERING DEPOSITIONAL AND DIAGENETIC PROCESSES IN MARINE SYSTEMS BY APPLICATION OF TRACE METAL AND ISOTOPE GEOCHEMISTRY

Major Field: GEOLOGY

Abstract: While organic-rich shales have been extensively studied as petroleum source rocks, and more recently as unconventional petroleum reservoirs, there is still much that remains unknown about the complex sedimentary and diagenetic processes responsible for black shale formation. Using trace metal concentrations and isotopic inventories, this investigation explores the pathways of trace metal incorporation into organic-rich sediments during deposition and describes the mechanisms which may have been responsible for variations in trace metal contents of three North American black shales deposited during Late Devonian – Early Mississippian time. To interpret ancient ocean redox and productivity, trace metal abundances in marine sediments have been used extensively. However, several oceanographic and diagenetic processes, such as basin restriction or post-depositional oxidation, can modify the primary geochemical signal of the sediment, which in turn may impact paleo-redox and/or -productivity interpretations. Therefore, it is imperative to study the impacts of a dynamic depositional system on trace metal accumulations. On the Namibian Continental Margin (NCM), sediments are deposited in an upwelling zone where large quantities of organic carbon accumulate on the anoxic shelf and are transported to a secondary depocenter on the slope, beneath the oxygen minimum zone. This dynamic environment makes the NCM an ideal location to study an organic-rich depositional system. In this study, the redepositional zone on the NCM was geochemically defined in NCM sediments below the oxygen minimum zone using the concentrations of several redox-sensitive and productivity-related trace metals. It was determined that the U-isotope redox proxy is a particularly useful tool to identify the primary depositional zone of redeposited sediments, despite post-depositional oxidization. The results about the effects of sediment transport and post-depositional oxidation on trace metal contents, the U/TOC ratio, and the U-isotopic composition of organic rich sedimentary deposits presented in this thesis provide new information about how geochemical signals are impacted by post-depositional processes. Understanding the impact of sediment transport and redeposition will assist with the interpretation of geochemical signals in organic-rich shales and may help to identify zones of lateral transport and redeposition related to ancient upwelling margin settings.

TABLE OF CONTENTS

Chapter Page

I. INTRODUCTION 1

1.1 Black Shales 2
1.2 Upwelling Systems 4
1.3 Preservation of Organic matter 7
1.4 Metals as Geochemical Proxies 8
1.5 Uranium and Organic Matter 11
1.6 The Uranium Isotope Redox Proxy 12
1.7 Overview of the Following Chapters 14

II. URANIUM ISOTOPES AS A PROXY FOR PRIMARY DEPOSITIONAL REDOX CONDITIONS IN ORGANIC-RICH MARINE SYSTEMS 17

2.1 Abstract 17
2.2 Introduction 18
2.2.1 Trace Metals and the Geologic Record 18
2.2.2 Namibia Continental Margin 18
2.2.3 Uranium Geochemistry 20
2.3 Methods 21
2.3.1 Sample Digestion, Spiking, and U Isotope Analysis 22
2.4 Results 23
2.4.1 U and TOC Content 23
2.4.2 U Isotope Composition 24
2.5 Discussion 26
2.6 Conclusions 30
2.7 Acknowledgements 31

III. GEOCHEMICAL SIGNATURES OF REDEPOSITIONAL ENVIRONMENTS: THE NAMIBIAN CONTINENTAL MARGIN 32

3.1 Abstract 32
3.2 Introduction 33
3.2.1 Redox-Sensitive Metals 34
3.2.2 Productivity Related Trace Metals 36
3.3 Study Area 38

Chapter Page

3.4 Methods....40
3.4.1 Sampling....40
3.4.2 Aqueous Phase Analysis....40
3.4.3 Solid Phase Analysis....40
3.5 Results and Discussion....42
3.5.1 Shelf Site 25020....42
3.5.2 Shelf Break Site GC 4....47
3.5.3 Upper Slope Site GC 5....48
3.5.4 Effects of Redeposition on Geochemical Signals....50
3.6 Summary and Conclusions....51
3.7 Acknowledgements....52

IV. RECONSTRUCTING THE PALEOCEANOGRAPHIC AND REDOX CONDITIONS RESPONSIBLE FOR VARIATIONS IN URANIUM CONTENT IN NORTH AMERICAN DEVONIAN BLACK SHALES....54

4.1 Abstract....54
4.2 Introduction....55
4.2.1 Black shales, trace metals, and organic matter preservation....55
4.3 Study Areas....58
4.3.1 The Woodford Shale of Oklahoma....58
4.3.2 Cleveland Member of the Ohio Shale of Eastern Kentucky....59
4.3.3 Bakken Shale of Eastern Montana....59
4.4 Methods....60
4.4.1 Sample Collection....60
4.4.2 Sample Analyses....62
4.4.3 Uranium Isotope Analysis....63
4.4.4 Late–Devonian Seawater Average $\delta^{238}U$ Calculation....64
4.5 Results....65
4.5.1 Woodford Shale....65
4.5.2 Cleveland Shale....66
4.5.3 Bakken Shale....66
4.6 Discussion....67
4.7 Conclusion....72
4.6 Acknowledgements....73

V. CONCLUSIONS....74

REFERENCES....77

APPENDICES....101

LIST OF TABLES

Table Page

2.1 Summary of Sample Locations from Namibian Continental Margin 22

4.1 Comparison of geochemical data from Late Devonian Shales 72

A1 Summary of U, TOC, and Isotope Data from Namibian Continental Margin..101

A2 Average Shale Content of Selected Elements 102

A3 Summary of Pore Water Data from Offshore Namibia 103

A4 Summary of TOC and $CaCO_3$ from Namibian Continental Margin 104

A5 Summary of solid-phase data from Namibian Continental Margin 105

A6 Enrichment Factors Namibian Continental Margin 106

A7 Summary of Shale Trace Metal Data 107

A8 Nickel and Copper Content of Woodford Shale 110

LIST OF FIGURES

Figure Page

1.1 Shale Depositional Environments....4

1.2 Mean chlorophyll-a concentration in global surface waters, 1997-2007....6

1.3 Lateral Transport along the Namibian Continental Margin....7

1.4 Trace Metal Behavior as a Function of Redox Conditions....10

1.5 Application of the U-Isotope Redox Proxy....13

2.1 Sediment Profiles of U, TOC, and U-Isotope Data from offshore Namibia....25

2.2 Relationships between U, U-Isotopes and TOC....26

2.3 Conceptual Model of Sediment Transport and U response....28

2.4 Inverse Concentration Plot with U-Isotope data from the Shelf and Slope....30

3.1 Map of Study Area Offshore Namibia....39

3.2 Sediment Profiles of Solid-Phase Redox-Sensitive Metals, TOC, and $CaCO_3$..43

3.3 Pore Water Profiles from Namibian Continental Margin....45

3.4 Sediment Profiles of Solid-Phase Productivity-Related Metals....46

3.5 Conceptual Model of Sediment Transport and Trace Metal Enrichments....51

4.1 Maps of Devonian Shale Core Locations and Paleogeography....61

4.2 Authigenic U, U/TOC, and $\delta^{238}U$ of Woodford Shale....65

4.3 Authigenic U, U/TOC, and $\delta^{238}U$ of Cleveland Shale....66

Figure Page

4.4 Authigenic U, U/TOC, and $\delta^{238}U$ of Bakken Shale 67

4.5 Relationship between U and TOC in Late Devonian Shales 68

CHAPTER I

INTRODUCTION

Organic-rich (black) shales are considered to be of economic importance as a source of petroleum and natural gas, and geologic importance as excellent recorders of past ocean conditions. Despite decades of scientific study, there is still much to discover about the black shale depositional system. The organic matter found in black shales is assumed to be enriched under oxygen-depleted waters, similar to conditions found in highly restricted basins, such as the Black Sea (e.g. Pompeckj, 1901; Demaison and Moore, 1980; Brumsack, 2006). However, some black shales show evidence of bioturbation (e.g. Savrda and Bottjer, 1989), which typically indicates oxygen in the bottom waters (Byers, 1977; Savrda et al., 1984; Savrda and Bottjer, 1986, 1987, 1989; Bromley and Ekdale, 1984; Ekdale and Mason, 1988; Föllmi and Grimm, 1990; Tyson and Pearson, 1991 and references therein). Various processes can lead to high organic carbon preservation in sediments such as high particle sinking velocities, aggregational processes in the water column (e.g. Hedges et al., 2001), rapid burial, and/or intense productivity (e.g. Calvert and Pedersen, 1992). In all cases, oxygen-depleted conditions facilitate the preservation of organic matter as oxygen is exceptionally efficient at the remineralization of organic carbon (e.g. Canfield, 1994; Dean et al., 1994; Dean and Gardner, 1998; Piper and Calvert, 2009).

Common modern depositional environments that host the conditions necessary for large organic carbon accumulations include enclosed basins, semi-restricted basins, and upwelling

systems, (e.g. Brumsack, 2006; Algeo et al., 2008). Similar to organic matter, many redox-sensitive metals can accumulate under reducing and highly productive conditions. For example, uranium (U) accumulates under reducing conditions where U(VI) is reduced to U(IV). This reaction takes place during the microbially-aided oxidation of organic matter. Thus, organic carbon accumulations are often enriched in uranium and U is commonly used as a proxy for organic-richness. However, due to the redox-sensitivity of many metals, post-depositional alteration by bioturbation/bio-irrigation, sediment transport, or changes in bottom water redox conditions may change the oxidation state of metals like U and release them back into the water column. The result of this post-depositional oxidation may be sediments preserved in the geologic record that are enriched in organic carbon without enrichments of redox-sensitive metals. Likewise, the generation and expulsion of hydrocarbons may cause a loss of carbon in shales, leaving a rock enriched in trace metals, relative to TOC.

Modern organic-rich sedimentary environments can serve as natural laboratories in which to observe a shale depositional system. We explore the pathways of trace metal incorporation into sediment during deposition and its association with organic matter, as well as examine post-depositional alteration processes in a modern setting. We then apply the gained knowledge from the Namibia Continental Margin to ancient settings by investigating trace metal concentrations and U-isotopic inventories of Late Devonian-aged black shales from North America, including the Woodford Shale, the Cleveland Shale, and the Bakken Shale. This investigation identifies several possible mechanisms that may be responsible for the trace metal depletions and enrichments found in some black shales.

1.1 Black Shales

Black shales are defined as dark-colored mudrocks containing abundant organic matter and silt- and clay-sized particles that accumulated together (Swanson, 1961; Tourtelet, 1979; Schmoker, 1980; Wignall and Myers, 1988; Lüning and Kolonic, 2003; Piper and Calvert, 2009). A significant percentage of black shales are major source rocks for oil deposits and commonly contain economically viable phosphate deposits (e.g., Piper and Calvert, 2009). Beyond their economic significance, many

black shales represent times of intense change in the oceans, such as oceanic anoxic events (OAEs, e.g. Schlanger and Jenkyns, 1976; Arthur et al., 1990; Leckie et al., 2002; Erba et al., 2004; Baudin, 2005; Jenkyns, 2010; Badin and Riquier, 2014), which are discrete intervals of geological time during which expanded and intensified oxygen minimum zones were present throughout the Earth's ocean basins. Black shales from around the world have been studied extensively to identify OAEs and understand the oceanic and climatic conditions that contributed to wide-spread global anoxia and the preservation of large quantities of organic matter (e.g. Farrimond et al., 1989; Lüning and Kolonic, 2003; Kolonic et al., 2005; Hetzel et al., 2009; Montoya-Pino et al., 2010; Jarvis et al., 2011; Lenniger et al., 2014; Clarkson et al., 2018).

When large quantities of organic matter are preserved in shales, high productivity and oxygen-depleted environmental conditions are considered to be necessary (Swanson, 1961; Tourtelet, 1979; Schmoker, 1980; Meyer and Nederlof, 1984; Wignall and Myers, 1988; Lüning and Kolonic, 2003; Piper and Calvert, 2009). Therefore, organic-rich shale deposits form in specific environments where conditions are favorable for the preservation of organic matter, including enclosed basins, similar to the modern Black Sea, in silled or semi-restricted basins, like the Cariaco Basin off the coast of Venezuela, and in areas with pronounced oxygen minimum zones which can be found in upwelling areas such as offshore Peru or the Benguela upwelling system, offshore Namibia (Figure 1.1) (e.g. Brumsack, 2006; Borchers et al., 2005, Inthorn et al, 2006a, 2006b, Scholz et al., 2011, Algeo and Rowe, 2012).

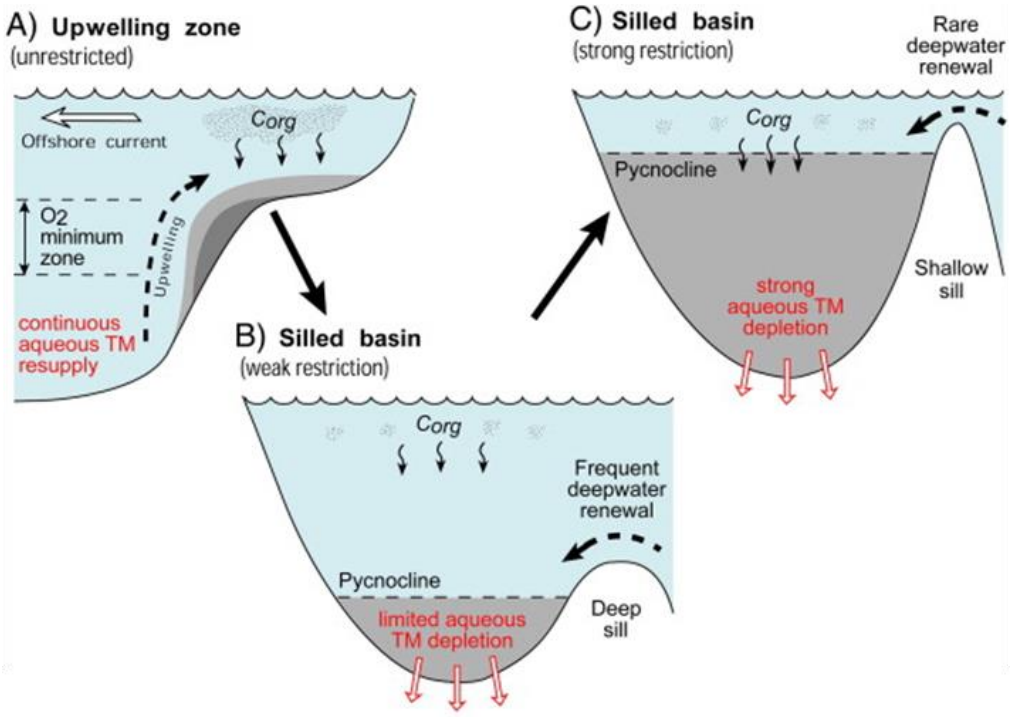

Figure 1.1. Different depositional settings which commonly result in large organic carbon (C_{org}) accumulations include upwelling zones (A) with unrestricted circulation that allows for the continuous resupply of nutrients to the surface waters and trace metals (TM) to the sediments. Partially-restricted silled basins (B) experience frequent deepwater renewal with a deeper pycnocline, and strongly-restricted silled basins (C) have very limited deep-water renewal resulting in a shallow pycnocline and stagnant bottom waters (Algeo and Rowe, 2012).

In a restricted or silled basin, abundant organic matter in the sediments and poor circulation of oxygenated waters into the deep basin allow for the development of stagnant, oxygen-depleted bottom waters (e.g. Deuser, 1971; Algeo and Rowe, 2011). Upwelling areas, on the other hand, are well-ventilated and bottom water anoxia is a result of high productivity and organic matter degradation (e.g. Bailey, 1991).

1.2 Upwelling Systems

In upwelling areas, warm surface waters are pushed seaward by Ekman transport and are replaced by cold, deep water. The upwelled nutrient-rich waters can sustain large phytoplankton populations. The result of this high surface productivity is large deposits of organic carbon in margin

sediments. The decomposition of organic matter in the water column subsequently leads to the consumption of the available oxygen and the development of an oxygen minimum zone (e.g. Bailey, 1991). High rates of primary productivity in surface waters and extensive oxygen minimum zones facilitate the accumulation and preservation of large amounts of organic carbon within the sediments of upwelling areas (Calvert and Pedersen, 1992). Thus, ocean upwelling zones are very important to the marine carbon cycle (Müller and Suess, 1979; Pedersen and Calvert, 1990; Inthorn, 2005). There are four major eastern boundary upwelling zones in the modern oceans: the California margin upwelling zone, the Canary Current upwelling zone (offshore northwest Africa), the Peru margin upwelling zone, and the Namibian Continental Margin (Philander and Yoon, 1982; Shannon and Nelson, 1996; Berger and Wefer, 2002). While upwelling areas make up only 0.3% of the global ocean, they are responsible for approximately 2% of global marine productivity (Carr, 2001). The Namibian Continental Margin (NCM) is the most productive upwelling margin in the modern ocean (Shannon and Nelson, 1996, Figure 1.2).

Along the Namibian Continental Margin (NCM), southeasterly trade winds induce upwelling of nutrient-rich deep waters (e.g. Shannon and Nelson, 1996), which are delivered to the photic zone. The upwelling along the NCM induces strong primary production (Figure 1.2, Mollenhauer et al., 2002), which is estimated at a rate of 0.37 Gt carbon per year with the average chlorophyll concentration in surface waters above the NCM around 2-3 mg/m^3 (Carr, 2001). The productivity in the waters above the NCM is only a small fraction of the total global productivity which is estimated at 40 Gt C per year (Carr, 2001 and references therein). The highest productivity is located in waters above the shelf with additional high productivity in filaments of nutrient-rich water that extends seaward above the continental slope (Carr, 2001, Mollenhauer et al., 2002).

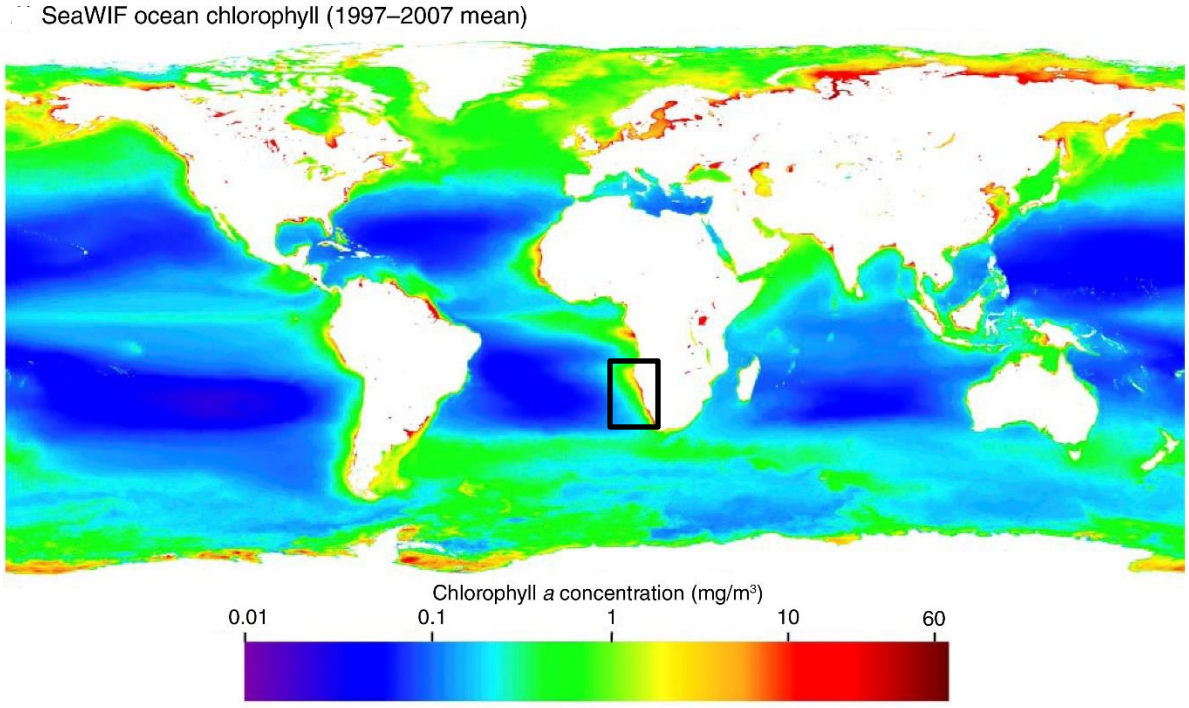

Figure 1.2. Chlorophyll-a concentration in global surface waters averaged from 1997 through 2007. High concentrations of chlorophyll-a are apparent in the coastal waters offshore southwestern Africa in the Benguela Upwelling Area (black square). Modified after Huston and Wolverton (2009).

A study by Inthorn et al. (2006) used beam attenuation to monitor the movement of sediments throughout the NCM. The study revealed that there is extensive particle transport occurring along the NCM in nepheloid layers, which are discrete layers of water with enhanced particle content, relative to surrounding waters. Three types of nepheloid layers have been previously described and include (A) surface nepheloid layers (SNL), which are generally associated with the productive surface layer (e.g. Gardner et al., 1993; Gundersen et al., 1998; Oliveira et al., 2001), (B) intermediate nepheloid layers (INL), which are a result of the accumulation or transport of particles in intermediate waters in association with strong density gradients (e.g. Azetsu-Scott et al., 1995; Cacchione and Drake, 1986; McCave et al., 2001; Pak et al., 1980), and (C) bottom nepheloid layers (BNL), which are found in the lowermost water column and are maintained by turbulent mixing in the bottom boundary layer (e.g. Bacon and Rutgers van der Loeff, 1989; Graf and Rosenberg, 1997; McCave, 1996). In the NCM,

organic rich particles from sediment below the highly productive shelf are transported off shore in nepheloid layers. This lateral transport and redistribution of particles creates a secondary area of intense organic carbon accumulation on the upper slope depocenter (Figure 1.3).

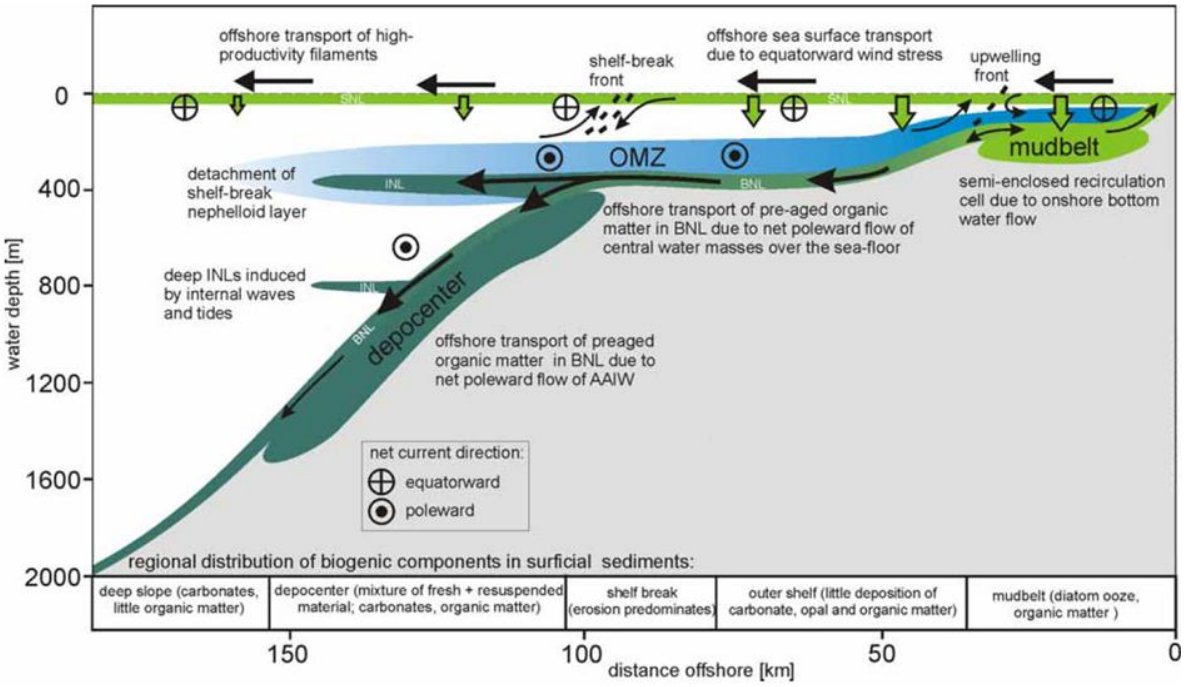

Figure 1.3. Conceptual model of the Namibia Continental Margin at 25.5°S with organic carbon enrichments in the sediments (mudbelt and depocenter) and the oxygen minimum zone (OMZ, blue) above the shelf, shelf break and slope. The general flow direction (encircled dots and crosses, black arrows), nepheloid layer distribution (green), intensity of primary production and carbon export to the seafloor (green arrows) and the composition of seafloor sediments. BNL: Bottom nepheloid layer, INL: Intermediate nepheloid layer, SNL: Surface nepheloid layer (Modified after Inthorn, 2005).

1.3 Preservation of Organic Matter

It is considered that the preservation of organic matter in the marine environment is < 0.5% efficient (Hedges and Keil, 1995). Although it has been suggested that productivity, sediment accumulation rate, bottom water redox conditions, and organic matter source are the primary variables, the precise mechanisms controlling the preservation of marine organic matter remain unclear (Henrichs,

1992, 1993; Hedges and Keil, 1995). Organic matter remineralization takes place in both oxic and anoxic conditions (Westrich and Berner, 1984; Cowie and Hedges, 1992; Lee, 1992; Kristensen and Holmer, 2001). However, marine organic matter is more easily remineralized in oxic waters and thus more likely preserved in sediments underlying anoxic bottom waters (Hedges et al., 1999; Aller, 1994; Hartnett et al., 1998). Accumulation rate is one of the environmental variables most commonly inferred to have an effect on organic matter preservation (e.g. Pedersen and Calvert, 1991). Rapid accumulation helps to protect accumulating sediments from dissolved oxidizing agents resulting in potentially less remineralization (Henrichs, 1992). However, increased clastic or carbonate input may dilute TOC content (Müller and Suess, 1979). Measured increases in TOC content of a shale may indicate periods of enhanced surface productivity, expansion of bottom water anoxia, and/or changes in sedimentation rate (Emerson, 1985; Canfield, 1989,1994; Pedersen and Calvert, 1990; Piper and Calvert, 2009). To distinguish between the processes responsible for elevated total organic content (TOC) in a shale, geochemical proxies are a commonly applied and useful tool to reconstruct past depositional conditions.

1.4 Metals as Geochemical Proxies

There are many major and minor elements that have been historically used as proxies for a multitude of environmental conditions including redox, nutrient supply, productivity, provenance, temperature, climate, and ocean circulation. For example, in the 1960's oxygen isotopes were measured to interpret paleotemperatures (e.g. Craig, 1965). In the 1970's the isotopic composition of sulfur in marine evaporites was studied as a redox proxy used to reconstruct the oxygenation of Earth's early atmosphere (e.g. Holland, 1978). Later, during the 1980's and 1990's, a new approach to paleoenvironmental reconstructions included the investigation of heavy metal (e.g. Ni, Mo, V) compositions of marine organisms and sedimentary rocks (e.g. Brumsack, 1980; Barnes and Cochran, 1990; Morford and Emerson; 1999). As early as 2001, the use of non-traditional stable isotopes of redox-sensitive metals began to be recognized as potentially important tools for paleoredox reconstructions (Barling et al, 2001). More recently, additional non-traditional isotope systems have

been studied with great potential as paleoredox indicators including U (Stirling et al., 2007), rhenium (Re) (Miller et al., 2015), thallium (Tl) (Owens et al., 2017b), and mercury (Hg) (Zheng et al., 2018).

The sources of trace metals (TM), that is, metals in low abundances compared to the overall element composition, to sediments are categorized as having either a lithogenic, biogenic, or seawater source (Calvert and Pedersen, 1993; Tribovillard et al., 2006; Piper and Calvert, 2009). Weathering and erosion of continents delivers trace metals to oceans primarily via rivers, groundwater, and wind-blown sediments (e.g. Rex and Goldberg, 1958; Martin and Meybeck, 1979; Calvert and Pedersen, 1993). Some metals are also delivered to the oceans via submarine hydrothermal activity (Bonatti et al., 1976; Lyle, 1976; Dymond and Corliss, 1977; Corliss et al., 1979; Von Damm, 1990).

Certain metals, such as Zn, Ni, Cd, and Cu, can act as nutrients and are taken up into cellular organisms within the water column (Bruland, 1983; Borchers et al., 2005). The cellular uptake of metals into planktonic organisms creates a nutrient-like profile in the water column, meaning that the photic zone is depleted of these metals and concentration of the metals increases with depth. The metals which were incorporated into the organisms are then delivered to the seafloor within the sinking biodetritus (Brongersma-Sanders, 1980; Böning et al., 2015). Accumulations of trace metals such as Ba, Cu, and Ni in sediments can identify periods of high primary productivity because these metals are generally associated with biocycling processes and bioproductivity (Knauer and Martin, 1973; Brongersma-Sanders, 1980; Bruland, 1983; Collier and Edmond, 1983; Brumsack, 1986; Dean et al., 1997; Whitfield, 2002; Böning et al., 2004; Borchers et al., 2005; Piper and Calvert, 2009). The trace metal content of sediments is reliant upon several factors: the supply of trace metals to the bottom water, a removal mechanism to precipitate these metals into the solid phase (such as the precipitation of metal sulfides, changes in valence state, adsorption, and biological processes, (Krauskopf, 1956), and the rate of sedimentation (Manheim, 1961; Brongersma-Sanders, 1966).

The metals which are most commonly used in redox reconstructions (i.e. Mo, V, U) are typically sourced to sediments by precipitation from seawater during redox reactions (Calvert and

Pedersen, 1993; Nameroff, 1996; Crusius et al., 1996; Morford and Emerson, 1999). Large accumulations of trace metals such as Fe, Mn, Mo, V, and U in sediments and sedimentary rocks can be diagnostic of deposition under oxic, suboxic, anoxic, or sulfidic/euxinic conditions (Figure 1.4, Brumsack, 1989, 2006; Algeo and Maynard, 2004; Tribovillard, 2006; Piper and Calvert, 2009). The redox environments are defined here and in subsequent chapters as having > 2.0, 2.0 – 0.2, and < 0.2 ml O_2 l^{-1} H_2O for oxic, suboxic, and anoxic environments, respectively, with sulfidic/euxinic conditions marked by 0 ml O_2 l^{-1} H_2O and measurable quantities of free H_2S (Edwards, 1985; Tyson and Pearson, 1991).

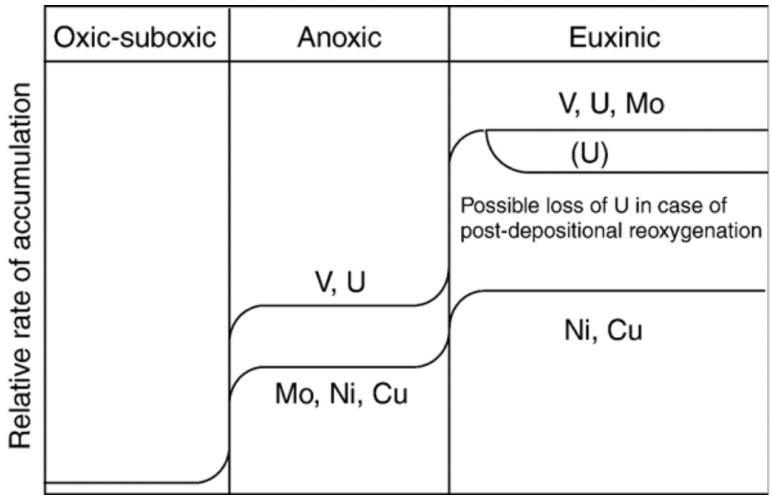

Figure 1.4. Solid-phase enrichments of Ni, Cu, Mo, U, and V in oxic-suboxic, anoxic, and euxinic/sulfidic environments (Tribovillard et al., 2006).

There are many factors which can alter paleoenvironmental interpretations of a single proxy, thus it is critical to support the paleoenvironmental interpretations of a single geochemical proxy with other proxy elements. The comparison of a suite of geochemical proxies helps to compensate for the effects of diagenetic alteration and improves interpretations of paleoenvironments. For example, post-depositional oxidation can remove some redox-sensitive metals from previously anoxic sediments; this

can be accomplished by a shift in bottom water redox conditions (Morford et al., 2001; Algeo and Maynard, 2004; Tribovillard et al., 2006) or by the introduction of oxygenated water into the sediments through bioirrigation (Aller, 1994; Zheng et al, 2000; Volkenborn et al., 2007). Additionally, the amount of redox-sensitive trace metals which can be drawn into sediments is dependent in part on the trace metal availability in the watermass (Algeo, 2004; Algeo and Lyons, 2006; Algeo and Tribovillard, 2009; Algeo and Rowe, 2012; Zhu et al., 2018). The rate of deepwater renewal can limit the supply of TM to bottom waters such that in a restricted setting, the bottom water becomes depleted of TMs. However, in an open ocean setting, trace metal supply to the sediments is unrestricted. Reducing environments within upwelling zones with continuous deep water renewal allows for greater trace metal enrichments in the sediments (Figure 1.1).

1.5 Uranium and Organic Matter

The association of trace metals and organic carbon is well known and has been observed throughout the geologic record (e.g. Cochran et al., 1986; Anderson, 1987; Algeo and Maynard, 2004; Cumberland et al., 2016). Uranium concentration is very important to the petroleum industry because U is so commonly found enriched in organic-rich shales. The petroleum industry uses gamma-ray logs to read the radioactivity of rocks below the Earth's surface, and usually this radioactivity comes from elements such as K, Th, and U which are incorporated into the rock. Gamma-ray log response in a black shale is usually high in rocks with a large amount of TOC because of the association of organic matter and uranium (e.g., Mo et al., 1973; Schmoker, 1981; Herron, 1991). As a result, gamma-ray logs have traditionally been employed as an indicator for interpreting TOC content when used in petroleum exploration (e.g., Herron, 1991; Schovsbo, 2002; Lüning and Kolonic, 2003).

Despite assumed similar depositional environments, U as an indicator of organic-richness cannot always be used reliably; some black shale deposits demonstrate little to no correlation between TOC and uranium content (e.g., Lüning and Kolonic, 2003). Low gamma-ray response has been noted

in several black shale formations including the organic carbon-rich Llandeilo-Caradoc shale in the Welsh Basin (Lev et al., 2000), and the Posidonia Shale of southern Germany (Mann et al., 1986).

Some alteration of the U/TOC ratio can occur during deposition. For example, the presence of phosphorites can increase U in sediment that is unrelated to organic matter (Veeh et. al., 1974; Burnett and Veeh, 1977; Starinsky et al, 1982). Burial rate can also play a role in the enrichment or depletion of U in sediment, as higher sedimentation rates can result in lower U contents while slower sedimentation rates allow for more U to be incorporated into sediment at the sediment-water interface (SWI, Klinkhammer and Palmer, 1991). Other factors to take into account are the amount of dissolved oxygen in the water column or pore water, duration of anoxia, and the position of redox boundaries, as U is very redox-sensitive and will quickly oxidize and be released into seawater upon the introduction of oxygen into the sediment (Lüning and Kolonic, 2003). Additionally, burrowing/bioturbating organisms can introduce oxygen into anoxic, U-rich sediments (Aller 1994; Zheng et al., 2002). This can release U back into the water column through the oxidation of the reduced U (Zheng et al., 2002). Post burial, thermal maturation and other diagenetic effects can increase the U/TOC ratio by removing organic carbon through hydrocarbon generation and migration and leaving uranium behind (Lüning and Kolonic, 2003). Uranium isotopes can track specific pathways of U incorporation into sediment and may help to narrow down or identify the possible processes at work (Weyer et al., 2008; Basu et al., 2014; Stylo et al., 2015; Lau et al., 2019).

1.6 The Uranium Isotope Redox Proxy

Uranium isotope fractionation varies through the processes by which uranium is incorporated into sediment, such as changes in speciation and redox-reactions, including microbially-aided reduction (Weyer et al., 2008; Basu et al., 2014; Stirling et al., 2015; Stylo et al., 2015), and these variations have been used in recent studies to quantify the extent of past marine anoxia (Montoya-Pino et al., 2010; Dahl et al., 2014, 2017; Kendall et al., 2015; Wang et al., 2016; White et al., 2018; Gothmann et al., 2019; Tostevin et al., 2019). The ratio between the two most abundant isotopes of U, ^{238}U and ^{235}U, is

expressed as $\delta^{238}U$ (equation 2.2). Sediments deposited under anoxic (no dissolved oxygen) and euxinic/sulfidic (anoxic with free hydrogen sulfide) conditions have $\delta^{238}U$ values that are isotopically heavier than seawater. Conversely, sediments deposited under oxic conditions tend to have U-isotopic compositions close to or slightly isotopically lighter than seawater (Figure 1.5, Weyer et al., 2008; Tissot and Dauphas, 2015; Rolison et al., 2017). The redox conditions interpreted using U isotopes can be validated by the use of other redox proxy trace metals such as molybdenum (Mo) and vanadium (V).

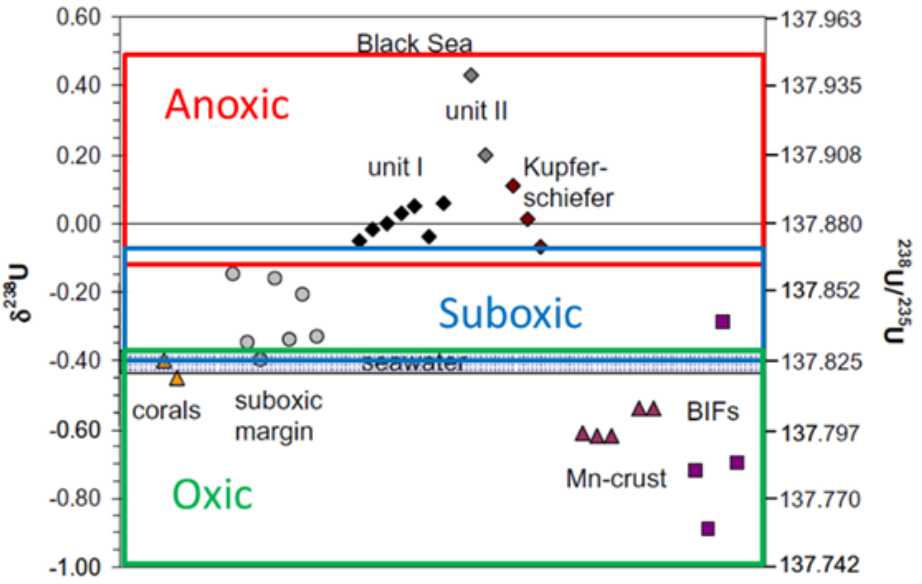

Figure 1.5. Early work on the U-isotope redox proxy demonstrated that anoxic/euxinic sedimentary rocks and sediments show higher $\delta^{238}U$ values while more oxic sediment plots lighter. Significant positive isotopic fractionation occurs between seawater and organic-rich shales (Black Sea, Unit-I and Unit-II and Kupferschiefer), while significant negative fractionation from seawater is observed in ferromanganese crusts/nodules and banded iron formations (BIFs). Suboxic sediments (from the Peruvian continental margin) displays less positive fractionation from seawater and corals display little to no fractionation. Modified after Weyer et al. (2008).

Having an accurate seawater U-isotopic composition is critical to the interpretation of $\delta^{238}U$ values in sediments, as the fractionation of U from seawater identifies depositional redox conditions. The isotopic composition of seawater is recorded in carbonate rock (Weyer et al., 2008; Romaniello et

al., 2013; Andersen et al., 2014; Zhang et al., 2018; Gothmann et al., 2019) and the fractionation away from seawater is used to determine the redox conditions under which non-carbonate sediments are deposited. Thus, many studies have focused on the measurement of U-isotopes in modern and ancient carbonate rock to understand the isotopic compositions of the oceans through time. Carbonate associated $\delta^{238}U$ values have been used to track past global ocean redox through known oceanic anoxic events (Montoya-Pino et al., 2010; Brennecka et al., 2011; Dahl et al., 2014; Lau et al., 2016), where anoxic water masses expanded to cover large areas of the seafloor. The large amount of isotopically heavy U incorporated into anoxic sediments during the anoxic events caused negative $\delta^{238}U$ excursions in seawater which were recorded in carbonate rock. Dahl et al. (2017) used this same approach to describe an oxygenation event using positive seawater $\delta^{238}U$ excursions recorded in carbonate rocks. More recently, however, Chen et al. (2018) demonstrated that there is a slight positive offset of $\delta^{238}U$ values of 0.2-0.3‰ imposed on carbonate rock through early diagenesis, and this diagenetic effect should be considered when interpreting ancient $\delta^{238}U$ signatures.

1.7 Overview of the Following Chapters

In the following chapters we have compared the geochemical signatures of several time-equivalent black shales with varying TOC and trace metal contents to a modern analogue for a black shale depositional system to study the impact of sediment transport and early diagenetic alteration on the trace metal content, the U/TOC ratio, and the U-isotopic composition. We found that the Namibian Continental Margin may be a satisfactory analogue for some, but not all, black shale depositional systems.

The second chapter of this thesis represents the first manuscript produced by the thesis research (Michelle L. Abshire, Stephen J. Romaniello, Amy M. Kuzminov, Jessica Cofrancesco, Silke Severmann, and Natascha Riedinger: *Uranium isotopes as a proxy for primary depositional redox conditions in organic-rich marine systems,* published in *Earth and Planetary Science Letters*, 2020). In this chapter we present the U content, TOC content, and U-isotopic composition of surface sediments

along an offshore transect on the Namibia Continental Margin (NCM). The study revealed that the primary process responsible for the decoupling of U and TOC was the reoxygenation of organic-rich sediments as they are transported laterally from the anoxic shelf to the oxic slope of the NCM. Furthermore, in the manuscript we discussed that the U-isotopic signature of the redeposited sediments was the same as that of the primary depositional site and was only slightly impacted by transport and redeposition.

For the second manuscript (Michelle L. Abshire, Jeremy D. Owens, Jessica Cofrancesco, Maik Inthorn, and Natascha Riedinger: *Geochemical Signatures of Redepositional Environments: The Namibian Continental Margin,* submitted to *Marine Geology*), which comprises chapter III, we analyzed a suite of trace metals along the NCM including redox proxies Mn, Fe, Mo, and V, and productivity proxies Ni, Cu, and Ag. The sediments at each sampling location along the NCM offshore transect contained unique geochemical signatures, which allowed for the geochemical identification of the redepositional zone.

Chapter IV consists of the third manuscript (Michelle Abshire, Stephen Romaniello, Clinton Scott, John Clymer, Silke Severmann, James Puckette, and Natascha Riedinger: *Reconstructing the paleoceanographic and redox conditions responsible for variations in uranium content in North American Devonian Black Shales*, in preparation for *Marine and Petroleum Geology*) in which we compare U enrichments, U/TOC ratios, and U-isotopic compositions of three age-equivalent North American black shales: The Woodford Shale of Oklahoma, the Cleveland Shale of Kentucky, and the Bakken Shale of Montana. To identify the depositional and oceanographic conditions present in each basin during the Late Devonian Period, each shale formation is compared to previously published TOC, U content, and U-isotope data from modern upwelling and restricted basin settings.

With a presently changing climate and concerns over expanding oxygen minimum zones and increased ocean anoxia (Stramma et al., 2008; Falkowski et al., 2011; Schmidtko et al., 2017), it is critical to refine geochemical proxies in modern settings to better understand the pathways of proxy

metals into sediments and how geochemical signals may be altered under dynamic marine environmental conditions. With a more robust understanding of the geochemical response to varying ocean redox and productivity, we are more prepared to interpret the changes of past ocean systems, and thus better equipped to anticipate the impacts of future climate change on marine environments.

CHAPTER II

URANIUM ISOTOPES AS A PROXY FOR PRIMARY DEPOSITIONAL REDOX CONDITIONS IN ORGANIC-RICH MARINE SYSTEMS

2.1 Abstract

In marine sediments, authigenic uranium (U) enrichments and U isotope compositions are important tools for interpreting changes in redox conditions; however, their use as paleoproxies requires a comprehensive understanding of the dominant processes that contribute to sediments becoming enriched or depleted. This study focuses on the U content and $^{238}U/^{235}U$ ratio of organic-rich surface sediments from the Namibian continental margin, where high productivity results in an expanded oxygen minimum zone (OMZ). The investigated core sample sites are located on the shelf, shelf break, and slope where bottom water redox conditions vary from anoxic to suboxic to oxic, respectively. While all cores have relatively high total organic carbon (TOC) contents (up to 12 wt. %), each location displays a unique U to TOC relationship. Shelf sediment exhibit a fair correlation between U and TOC, while the shelf break and slope sediments show a pronounced decoupling of U and TOC. On the Namibian Continental Margin, particle-rich nepheloid layers transport organic-rich deposits from within the OMZ, through oxic water, to be redeposited on the slope. Due to the sensitivity of U to changes in redox conditions, this lateral movement results in the release of the reduced U phases back into the water column through oxidation while transporting the partially remineralized organic carbon to the slope. Oxidation of

U during transport does not alter the average primary $^{238}U/^{235}U$ isotopic signature in redeposited sediment, and the combination of high TOC, low U content and high $\delta^{238}U$ values may become a useful tool for the identification of the boundaries of ancient OMZs.

2.2 Introduction

2.2.1 Trace metals and the geologic record

The association of trace elements, such as uranium (U), and total organic carbon (TOC) in organic-rich sedimentary deposits is well-known and has been observed in both the modern marine environment and in the geological record (Cochran et al., 1986; Anderson, 1987; Algeo and Maynard, 2004; Cumberland et al., 2016). While perturbations in this association have been reported to some extent (Cumberland et al., 2016, and references therein), many of the mechanisms behind the decoupling of U and TOC in continental margin settings are not well-documented. In this study we examine organic-rich sediments of the Namibian Continental Margin (NCM) offshore of Namibia, Southwest Africa, and variations in U content in three organic-rich (TOC >3 wt.%) sample sites. Solid phase U content, TOC content, and isotope composition of U in sediments of the NCM were measured and redox proxies of solid-phase U concentration and U isotope ratios were used to understand how well the original depositional redox conditions are recorded in the geologic record, even after the lateral transport and/or post-depositional oxidation of the deposits.

2.2.2 Namibian Continental Margin

Ocean upwelling systems, such as the Benguela upwelling system off the coast of Namibia, account for 9% of all marine organic carbon burial (Berner, 1982). Typically, the organic carbon content of sediment in upwelling zones reaches 5% or more by weight and the annual flux of carbon to the sea floor in Earth's upwelling areas combined has been estimated to be about 10 million tons/year (Berger and Wefer, 2002). In the NCM, high surface ocean productivity and decomposition of organic matter in the water column, as well as the oxidation of hydrogen sulfide,

results in an extended oxygen minimum zone (OMZ) (e.g. Brüchert et al., 2003; Borchers et al., 2005). The OMZ reaches the seafloor along the shelf and shelf break and extends out into the water column over the continental slope. Consequently, sediments on the shelf experience anoxic bottom water, while shelf break and slope sediments deposit under suboxic and oxic bottom water, respectively, with the OMZ several hundreds of meters above the slope. Anoxic, suboxic and oxic conditions are operationally defined here as having <0.2, 0.2–2.0, and >2.0 ml O_2 L^{-1} H_2O, respectively (Tyson and Pearson, 1991). Despite the varying degrees of bottom water oxygenation, high amounts of TOC (2.5-12 wt.%) are observed at all three sites. The sedimentation rate in the NCM has been estimated to be about 1 mm yr^{-1} (Bremner and Willis, 1993), and strong upwelling along this margin has been present since at least the Pliocene-Pleistocene boundary (Berger and Wefer, 2002). Seasonal variability in the upwelling cells responsible for the high primary productivity and expansion of the oxygen minimum zone is pronounced in the northern upwelling area (Chapman and Shannon, 1985). Within our study area, however, the OMZ remains present on the shelf and becomes more pronounced during the highly productive austral summer (Bruchert et al., 2003). The strong coastal upwelling and high primary productivity has been ongoing in this region since at least the early Pleistocene (Berger and Wefer, 2002).

Organic matter accumulation and burial on the Namibian shelf and upper slope are strongly controlled by lateral transport within nepheloid layers, which are layers within the water column with enhanced particle content relative to the surrounding water (Giraudeau et al., 2000). At the NCM, the transport of sediment from the shelf to the slope is controlled primarily by intermediate nepheloid layers (INL), that is, accumulation or transport of particles in intermediate waters in association with strong density gradients, and bottom nepheloid layers (BNL), which are found closer to the sea floor and are maintained by turbulent mixing (Giraudeau et al., 2000; McPhee-Shaw et al., 2004; Inthorn et al., 2006a,b). Previous studies have evaluated suspended particulate matter and particulate organic matter (Inthorn et al., 2006b) and employed radiocarbon dating of

seafloor sediments (Mollenhauer et al., 2007) to conclude that the lateral transport of sediment in nepheloid layers contributes more organic matter to the slope than the direct vertical settling of particles from the surface layer.

2.2.3 Uranium geochemistry

Uranium has two common oxidation states; soluble U(VI) and insoluble U(IV) (Langmuir, 1978). Under reducing bottom water conditions insoluble U(IV) is incorporated into marine sediment along with organic matter at the sediment-water interface (e.g. Langmuir, 1978; Klinkhammer and Palmer, 1991; Spirakis, 1996; McManus et al., 2005, 2006; Tribovillard et al., 2006). Under oxic bottom water conditions U is incorporated by diffusion from pore water within reducing sediments (Anderson, 1982). The reduction pathway into marine sediment is a significant sink in the global U budget (Barnes and Cochran, 1990; Klinkhammer and Palmer, 1991). Because of the relationship between U and organic matter, U has been considered a reliable proxy for organic carbon in marine settings (Anderson, 1982; Spirakis, 1996; McManus et al., 2005).

In recent years, U isotopes have emerged as novel and complementary redox proxy for the reconstruction of past ocean anoxia. Uranium has three naturally-occurring isotopes, ^{238}U and ^{235}U, which are primordial with half-lives of 4.5 and 0.7 billion years, respectively (e.g. Jaffey et al., 1971), and radiogenic ^{234}U, which is the decay product of ^{238}U and has a half-life of ~246 thousand years (e.g. Cheng et al., 2013). The $^{238}U/^{235}U$ isotope composition varies through the processes by which U is incorporated into sediment. Uranium isotope fractionation occurs during adsorption, changes in speciation, or due to changes in redox chemistry, including microbially-aided reduction (Weyer et al, 2008; Basu et al., 2014; Stirling et al., 2015; Stylo et al., 2015). Redox reactions result in reduced U(IV) becoming enriched with the heavier isotope (Montoya-Pino et al., 2010; Basu et al., 2014; Stirling et al., 2015; Stylo et al., 2015), due to the nuclear field shift effect (Andersen et al., 2017, and references therein) which affects the size and shape of the nucleus (Yang and Liu, 2016). Sediments found in anoxic environments typically have higher $^{238}U/^{235}U$ than sediments

from less-reducing environments, such as suboxic and certainly oxic settings (Andersen et al., 2017, and references therein). Thus, the $^{238}U/^{235}U$ ratio in ancient rock has recently become an important tool in determining the extent of past ocean oxygenation (e.g. Brennecka et al., 2011a; Lau et al., 2017; Zhang et al., 2018). The $^{234}U/^{238}U$ is often used as a tool in Pleistocene chronology by comparing known seawater $^{234}U/^{238}U$ composition with measured $^{234}U/^{238}U$ in sediments as excess ^{234}U decays (Henderson, 2002). Fractionation of ^{234}U from ^{238}U is a result of α-recoil during the decay of ^{238}U.

2.3 Methods

Sediment cores were retrieved using a multicorer device as part of the May 2015 Regional Graduate Network in Oceanography (RGNO) program in Namibia. Sediment cores offshore of Namibia were collected at locations on the shelf (25020), shelf break (GC 4) and slope (GC 5). Sampling sites were specifically chosen for their relation to the OMZ and, therefore, geochemical potential (Table 2.1). Depth measurements of ocean water temperature, salinity, and bottom water oxygen levels were also collected onboard the ship. Cores were immediately sliced onboard the ship in 1-2 cm intervals for the length of the entire core (24-28 cm). The sediments were then transferred into 50 mL centrifuge tubes and the head space was purged with nitrogen gas before sealing in order to prevent oxygen exposure. The sediment samples were stored frozen at -20°C in order to impede microbial activity. Total organic carbon (TOC) content of the sediments was measured after addition of dilute HCl to remove any carbonate material, using an Elemental Analyzer (EA, Costech) at Oklahoma State University (OSU) (For further details of sample preparation and TOC analysis, see Cofrancesco, 2016).

Table 2.1. Position, water depth, bottom water oxygen concentration, and depositional environment for sites 25020 (shelf), GC 4 (shelf break) and GC 5 (slope). Samples were collected in May, 2015 (modified after Cofrancesco, 2016).

Core Name	Latitude	Longitude	Water depth (m)	Bottom water oxygen (mL/L)*	Depositional Environment
25020	25°00.000'S	14°28.200'E	116	<0.05#	Anoxic shelf
GC 4	25°20.660'S	13°46.480'E	302	1.11	Suboxic shelf break
GC 5	25°30.000'S	13°27.000'E	795	3.36	Oxic slope

* Oxygen data from Cofrancesco (2016). # CTD detection limit is 0.05 mL/L.

2.3.1 Sample digestion, spiking, and U isotope analysis

Approximately 100 mg of powdered sample were digested using trace-metal grade nitric (3 ml), hydrofluoric (200 µl) and perchloric (3 ml) acids in PFTE vials, and heated at 170°C until fully dissolved. Samples were then evaporated until dry and residue was dissolved in 5% HNO3. Elemental concentrations were analyzed using inductively coupled plasma-mass spectrometry (ICP-MS, iCapQc, ThermoScientific) at OSU. Standard reference material NIST 2702 was digested and analyzed alongside Namibian sediment samples to monitor reproducibility. Average values of replicate digestions were well within recommended ranges with relative standard deviation for U being <2%. The authigenic fraction of U is estimated using the calculation:

$$U_{auth} = U_{sample} - [U/Al_{detrital} * Al_{sample}], \text{ (equation 2.1)}$$

assuming a detrital U:Al ratio of 15×10-6 (McManus et al., 2005). The authigenic fraction is reported as a percentage of the total U content in each sample.

All digested samples to be analyzed for U isotope composition were double spiked with IRMM 3636a $^{236}U/^{233}U$ mixed isotopic double spike (e.g. Stirling et al., 2007) of known isotopic composition. The target $^{236}U:^{235}U$ spiking ratio in the sample:spike mixture was 3:2. The spiking ratio utilized for these samples is lower than that observed in other labs.

After spiking, U was separated from matrix with column chromatography using Uteva ion exchange resin (Potter et al., 2005). Aliquots of the purified U samples were analyzed on the iCap ICP-MS to quantify U concentration of the sample and estimate the U recovery prior to $^{238}U/^{235}U$ ratios being analyzed on the Neptune MC-ICP-MS using CRM112a as the bracketing standard. By using less spike and running at lower concentration of U, it introduces a greater range of error for the samples. However, one benefit of running the samples at a lower concentration and with less spike is that it reduces the chances of carryover between samples and also reduces the chances of creating an instrument memory of these isotope ratios. These measurements were conducted at the Department of Marine and Coastal Sciences at Rutgers University in New Brunswick, New Jersey. Uranium isotope composition is expressed in terms of $\delta^{238}U$ in per mil (‰) deviation from a universal reference material CRM-112a and the internal analytical error is reported as ± 2SD. The equations used to calculate $\delta^{238}U$ and $\delta^{234}U$ are as follows:

$$\delta^{238}U = [(^{238}U/^{235}U)_{sample} / (^{238}U/^{235}U)_{CRM112a} - 1] \times 1000 \text{ (equation 2.2)},$$

$$\delta^{234}U = [(^{234}U/^{238}U)_{sample} / (^{234}U/^{238}U)_{equilibrium} - 1] \times 1000 \text{ (equation 2.3)},$$

where $^{234}U/^{238}U_{equilibrium} = 5.472 \times 10^{-5}$ (e.g. McCulloch and East, 2000). Measured isotope composition values had average 2SD errors of 0.13‰ for $\delta^{238}U$ measurements and 19.66‰ for $\delta^{234}U$ measurements while analysis of standards yielded an internal precision of 0.20‰ ($\delta^{238}U$) and 5.21‰ ($\delta^{234}U$).

2.4 Results

2.4.1 U and TOC content

In the NCM sediments, solid-phase U is predominantly authigenic with U_{auth} exceeding 95% of U present in all samples (Table A1). Total U contents decrease systematically from highest concentrations on the shelf in the core of the OMZ, to intermediate on the suboxic shelf break and lowest on the deepest, oxic slope site (Figure 2.1). Similar to U, TOC contents are highest on the

shelf; however, TOC contents are higher on the upper slope compared to the shelf break, despite the upper slope having higher oxygen concentration. The U content in the shelf break samples ranges from 38.5-50.2 ppm. On the upper slope (Site GC 5), high TOC content was measured ranging from 5.8-7.7 wt.%; however, in contrast to the shelf and shelf break sites, these samples have relatively low U of 5.7-12.2 ppm. The TOC content of the shelf sediments ranges from 7-12 wt.% and U content increases with depth from 5.1 to 95.4 ppm (Figure 2.1). The TOC content at the shelf break (Site GC 4) is lower than in the shelf sediments with values ranging from 2.5-3.4 wt.%.

2.4.2 U isotope composition

The $\delta^{238}U$ in the shelf deposits (Site 25020) underlying anoxic bottom water is in the range of -0.24 to 0.12‰ (average $\delta^{238}U$ value near -0.03 ± 0.15‰) for sediments below 2 cm depth (Figure 2.1). These isotope compositions are significantly higher than $\delta^{238}U$ of seawater ($\delta^{238}U_{seawater}$ = -0.41 ± 0.03; Weyer et al., 2008). Only sediments in the surface 2 cm have isotope compositions that are within error or slightly lower than seawater $\delta^{238}U$ (-0.55‰ ± 0.13‰ to -0.64‰ ±0.07‰). Shelf sediments display a general trend down core from lighter to heavier $\delta^{238}U$ values, which are associated with higher U content with depth. Shelf break deposits (Site GC 4) under suboxic bottom water show $\delta^{238}U$ compositions that are only slightly higher than $\delta^{238}U_{seawater}$, despite consistent U enrichment, with measured $\delta^{238}U$ values ranging from -0.42 to -0.12‰ (average $\delta^{238}U$ of -0.18 ± 0.13‰). The U isotopic composition of upper slope sediments underlying oxic bottom waters (Site GC 5) is consistently higher than $\delta^{238}U_{seawater}$ ranging from -0.22 to 0.18‰ (average $\delta^{238}U$ of -0.09 ± 0.10‰). In contrast to the anoxic site, the highest $\delta^{238}U$ values at the oxic site occur near the surface at around 5 cm depth, approaching seawater values at depth. Uranium concentrations at the oxic site are relatively low (<5 ppm) with only minimal authigenic enrichment. The $\delta^{234}U$ of the shelf sediment are very near $\delta^{234}U_{seawater}$ ($\delta^{234}U_{seawater}$ = 145‰; Henderson, 2002) with little variation. Slope sediments have $\delta^{234}U$ values that are consistently at,

or just below, seawater values. Shelf break sediments, however, have $\delta^{234}U$ values that are substantially and consistently below $\delta^{234}U_{seawater}$ ranging between 8‰ and 19‰. A table with all data used in this study is available in the appendix (Table A1).

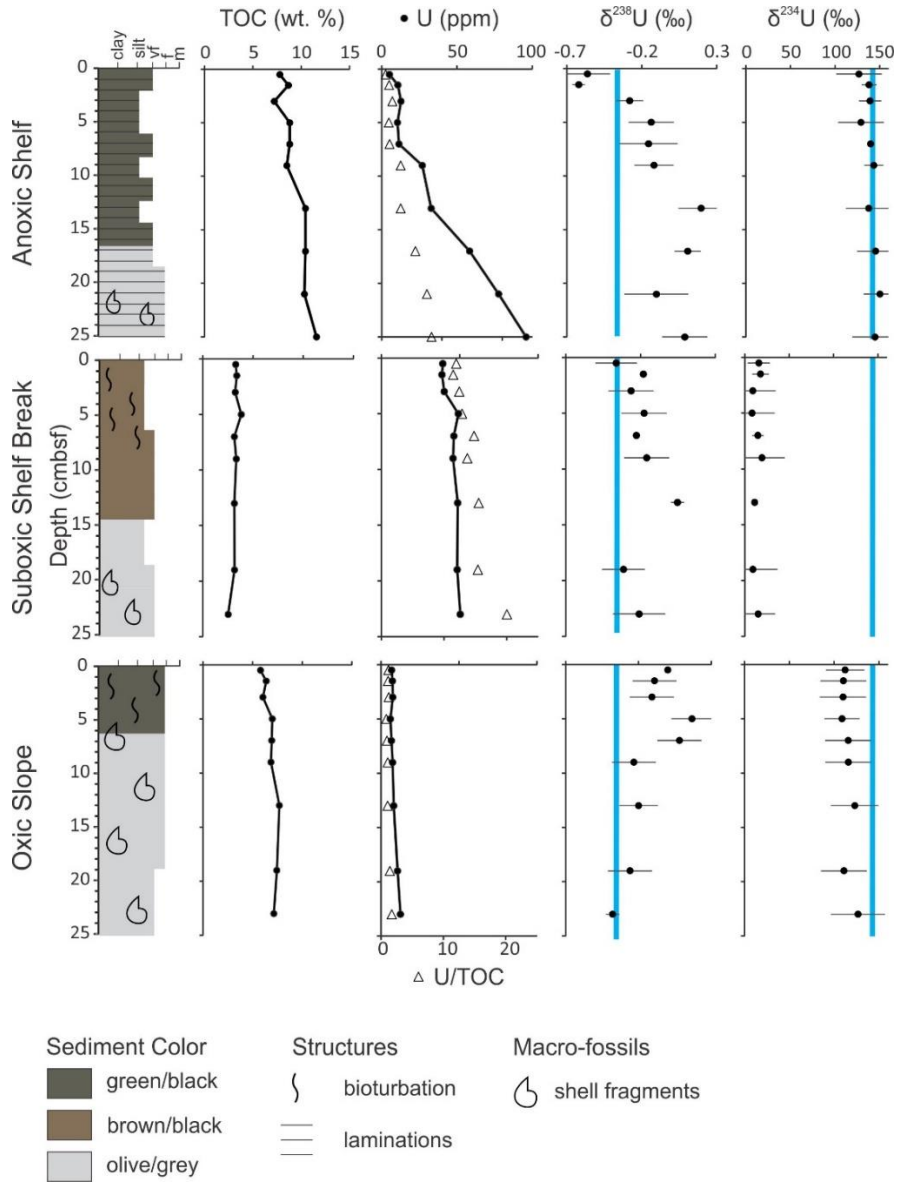

Figure 2.1. Total organic carbon (TOC), solid phase uranium (U), U/TOC ratio, and U isotopes ($\delta^{238}U$, $\delta^{234}U$) on the shelf (Site 25020), shelf break (Site GC 4), and upper slope (Site GC 5). All three cores have high TOC, a wide range of U contents, and U/TOC ratios that appear strongly controlled by U content. Namibian sediments are dominated by higher $\delta^{238}U$, relative to $\delta^{238}U_{seawater}$ of -0.41 ± 0.03‰ (Weyer et al., 2008). The $\delta^{234}U$ values on the shelf and slope are relatively similar.

Shelf break sediment, however, show significant fractionation away from seawater ($\delta^{234}U_{seawater}$ = 145‰; Henderson, 2002). Error bars = 2SD. Seawater isotopic composition is shown as a blue bar. Lithological interpretation by Cofrancesco (2016).

2.5 Discussion

The sediments at the slope site (GC5) show nearly uniform U content throughout the length of the core (Figure 2.1), suggesting that U is undergoing only modest early diagenetic enrichment in the upper 25 cm of sediment at this oxic site. The different types of sedimentary U content profiles can be explained by sediment redeposition. Previous studies have shown that on the Namibian Continental Margin vertical settling of fresh organic matter from productivity in the overlying water column is only a minor contributor of organic carbon to these slope sediments with the majority of organic material being delivered via nepheloid layers from the shelf (McPhee-Shaw et al., 2004; Inthorn et al., 2006b). The result of this transport is a decoupling of U and TOC and a unique U/TOC ratio at the slope site (Figure 2.2A).

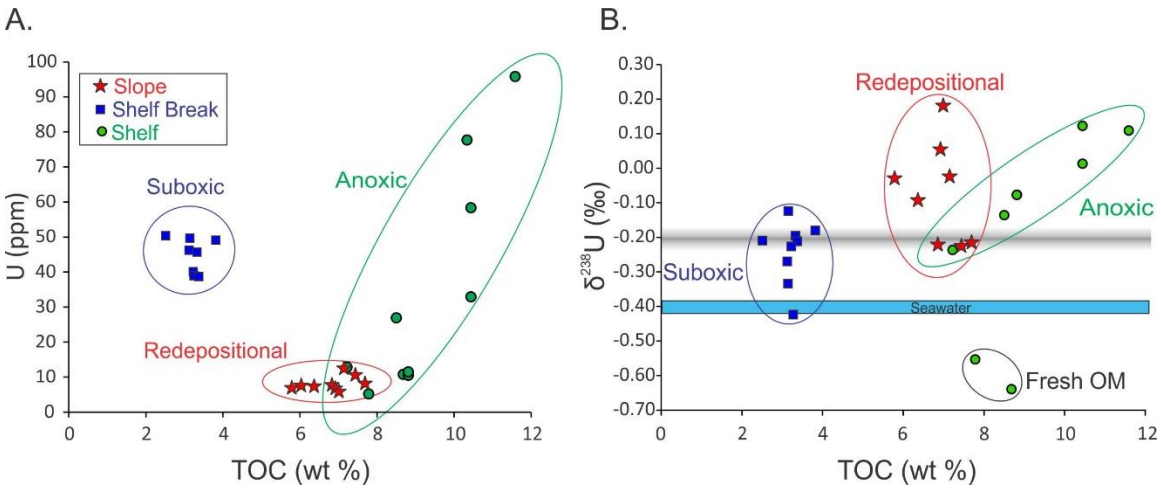

Figure 2.2. There are three distinctive zones that emerge when U content (A) and $\delta^{238}U$ (B) are plotted against TOC. The $\delta^{238}U$ value of -0.20‰, shown here as a grey line, delineates the approximate boundary between suboxic and anoxic deposition (Andersen et al., 2017). Blue bar shows seawater $\delta^{238}U$ average value -0.41‰ ± 0.03‰ (Weyer et al., 2008). The two circled shelf sediment samples with lower $\delta^{238}U$ values are likely indicative of fresh organic matter (OM).

Similar to the U/TOC contents, each sample location can be operationally grouped according to the $\delta^{238}U$/TOC ratio (Figure 2.2B), with the exception of two samples with fresh organic matter from the uppermost sediments on the shelf (refer to text in Figure 2.2B). The uppermost samples at the shelf site show unusually negative $\delta^{238}U$ values between -0.5 and -0.7‰. These values could be explained by absorption of U to Mn-oxides, which is accompanied by a -0.2‰ fractionation (Brennecka et al. 2011b). Another, more likely explanation for the extremely negative $\delta^{238}U$ values may be the absorption of ^{238}U-depleted U to fresh organic matter. Holmden et al. (2015) observed low $\delta^{238}U$ values between -0.5 and -1.24‰ in plankton tow and sediment trap samples in the highly productive Saanich Inlet, although the isotope fractionation mechanism in the plankton tow is not yet known. The $\delta^{238}U$ values reported by Holmden et al. (2015) are consistent with the deposition of fresh, labile organic matter found on the anoxic shelf.

Below 2 cm depth, the shelf sediments show an enriched ^{238}U isotope composition ($\delta^{238}U$ > -0.20‰) similar to those reported for other anoxic environments (Andersen et al., 2017 and references therein). Similarly, slope deposits are also enriched in the heavier isotope relative to seawater, despite oxic bottom water. This supports the notion that the sediments were originally deposited under anoxic conditions before being redeposited downslope. During transport and redeposition, organic carbon-laden particles are exposed to oxygenated water, causing solid-phase U to be oxidized from insoluble U(IV) to soluble U(VI) and released back into seawater (Figure 2.3). Despite oxidation, the remaining U in the sediment is isotopically heavier than seawater. Preservation of the original isotope composition during water column transport agrees with laboratory experiments conducted by Wang et al. (2015) which demonstrated little to no U isotope fractionation when solid phase U(IV) is oxidized to U(VI) under neutral pH conditions.

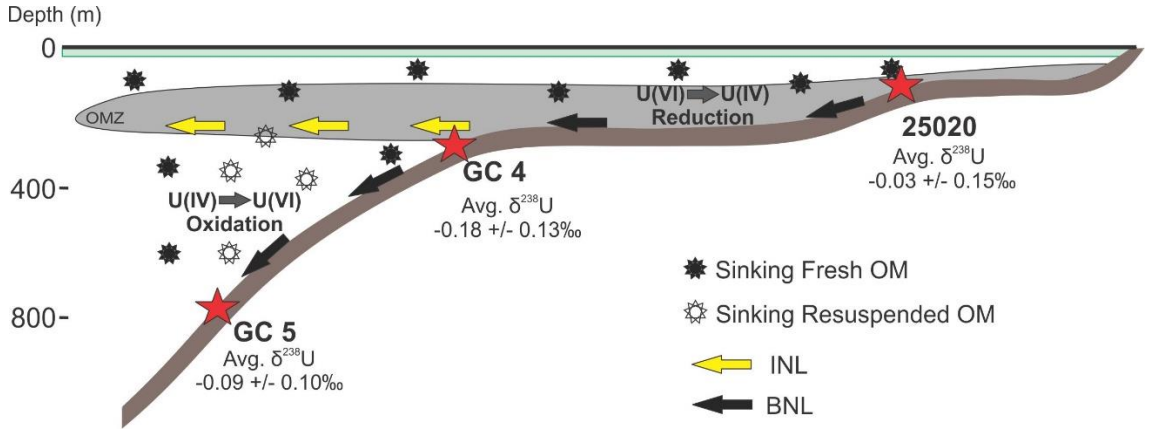

Figure 2.3. Conceptual model of sediment transport and U response in the NCM. The degradation of large amounts of organic matter (OM) in the productive surface ocean (light green bar) results in an expanded oxygen minimum zone (OMZ). In the NCM, organic-rich deposits are transported from the shelf via the intermediate nepheloid layer (INL) and bottom nepheloid layer (BNL). OM contributions to the sea floor come from sinking, fresh material as well as resuspended organic matter. Sample locations on the shelf (Site 25020), shelf break (Site GC 4) and slope (Site GC 5) are marked with red stars (modified after Inthorn, 2005).

The range of $\delta^{238}U$ values in sediment at the shelf break (-0.12‰ to -0.42‰) is similar to values previously reported from Peru margin suboxic sediment (-0.16‰ to -0.41‰; Weyer et al., 2008) and represents deposition under suboxic conditions. At the shelf break site (GC4), where little to no material from the shelf is redeposited and erosion outpaces sedimentation (Mollenhauer et al., 2007), any U present is likely preserved due to the suboxic bottom water conditions. The $\delta^{234}U$ values measured at this site are approaching secular equilibrium, suggesting that shelf break sediment is far older than shelf and slope sediment. Exposure of older material on the shelf break is consistent with a highly erosive regime on the shelf break. Erosive patterns were reported by Mollenhauer et al. (2007) who observed erosive surfaces in parasound sediment echosounder profiles. Thus, the age and long term exposure of the shelf break sediment is likely the primary reason for the loss of TOC and for the decoupling of U and TOC at this site.

At the Namibian Continental Margin, the $\delta^{238}U$ is recorded in the organic-rich shelf sediments during early diagenesis. These deposits are then transported via nepheloid layers (Inthorn

et al., 2006a,b; Mollenhauer et al., 2007), beyond the shelf break, and redeposited on the slope under oxic bottom water. Although some part of the organic matter in the slope sediments results from overlying productive waters, the majority of organic material on the slope is delivered from the shelf via nepheloid layers (McPhee-Shaw et al., 2004; Inthorn et al., 2006b). While most U is lost due to oxidation during and after transport, the primary depositional $\delta^{238}U$ signature is preserved (Figure 2.3). Thus, this study shows that the $\delta^{238}U$ of organic-rich sediment can be a useful proxy for determining the primary depositional redox environment prior to transport, oxidation, and redeposition. Additionally, the $\delta^{238}U$ redox proxy may be used to determine primary depositional conditions when post-depositional bottom conditions change, and oxygen is introduced to the sediment by, for example, bioturbation. Therefore, we expect that the U isotope proxy will track primary depositional conditions when post-depositional redox conditions change.

One important observation that was made during the course of this study is the apparent Rayleigh distillation-style fractionation of U during transport and oxidation, and this should be addressed. The U in shelf sediment follows the expected trend for microbially-mediated U reduction (e.g. Sterling et al., 2015) in that the reductive incorporation of U into sediment results in isotopically heavier U.

The same enrichment in ^{238}U also appears to be occurring as U is oxidized and removed, following a Rayleigh distillation model, suggesting that lighter U(IV) is preferentially removed from sediment during transport (Figure 2.4). This is something of a conundrum as U in oxic settings is typically isotopically similar to, or lighter than, seawater (e.g. Weyer et al., 2008). The combination of high TOC, low U content, and heavier isotopic composition may be used to specifically detect the lower boundaries of an OMZ where downslope transport has occurred.

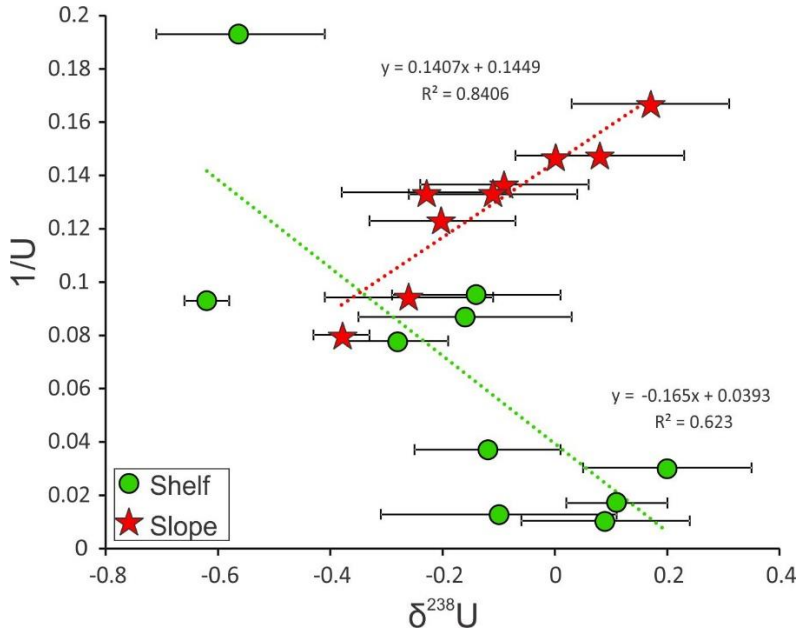

Figure 2.4. Inverse concentration plot showing the increasing $\delta^{238}U$ values with both reduction and oxidation in anoxic shelf sediments (green circles) and oxic slope sediments (red stars). Linear relationships between 1/U and $\delta^{238}U$ indicate mixing or fractionation. The green line follows the predicted trend for U(VI) reduction. The red line shows the unexpected fractionation of U isotopes during transport and redeposition, resulting in isotopically light U being preferentially removed from sediment.

2.6 Conclusions

The content of U in marine sediment has long been used as a proxy for organic-richness of sedimentary rock, however, there are many cases in which perturbations in the U/TOC ratio has been observed (e.g. Wignall and Myers, 1988; Lüning and Kolonic, 2003). Our shelf break data show that lower TOC does not necessarily equate to lower enrichments of U. Likewise, high TOC can be found without enrichments of U, as seen in NCM slope sediment where U has been disproportionally lost during particle transport in nepheloid layers. The $\delta^{238}U$ composition of U in marine sediments is a complementary tool for the reconstruction of the depositional conditions of ancient shales where there may be some conflict as to whether or not oxygenated bottom water was present at the time of sediment deposition. This could be the case when biological evidence, such as fossils or bioturbation, typical for oxic bottom water, is in conflict with high organic carbon

content that indicate anoxic conditions, as observed in the organic-rich Jurassic Kimmeridge Clay (Wignall and Myers, 1988). However, because oxidation is congruent, and isotope fractionation occurs during incongruent reduction, several reduction and oxidation steps may still change $\delta^{238}U$, for example, in sediments which have undergone transport and redeposition. The ability to identify primary depositional redox conditions of ancient rocks, and those zones in which post-depositional oxidation have occurred, can give better certainty to paleoenvironmental reconstructions and may allow for a better understanding of ancient ocean conditions.

2.7 Acknowledgements

This manuscript is based upon work supported by the National Science Foundation (NSF) Graduate Research Fellowship Program under Grant No. 1746055. Any opinions, findings, and conclusions or recommendations expressed in this manuscript are those of the authors and do not necessarily reflect the views of the National Science Foundation. The authors would like to thank C. Jones and T. Wu for help and assistance in the lab, and J. Donoghue, J. Puckette, and G. Cook for valuable conversations, and T. Dahl and an anonymous reviewer for insightful comments during the review process. This is an Oklahoma State University - Boone Pickens School of Geology contribution # 2019-107.

CHAPTER III

GEOCHEMICAL SIGNATURES OF REDEPOSITIONAL ENVIRONMENTS: THE NAMIBIAN CONTINENTAL MARGIN

3.1 Abstract

Trace metal abundances in marine sediments have been used extensively to interpret periods of ancient ocean redox conditions and elevated primary productivity. However, sediment reworking that results in post-depositional oxidation can modify the primary geochemical signal of the sediment, which in turn may impact paleo-redox and/or -productivity interpretations. In the case of sediments on the Namibian Continental Margin (NCM), lateral transport and redeposition contribute to the accumulation of organic matter on the margin slope. To better constrain the geochemical effects of lateral transport on the NCM, we examined the trace metal signature (including solid-phase Fe, Mo, V, Ni, Cu and Ag, and pore water Fe, Mo, and V) in sediment surface cores (~25 cm) along a transect from shelf to slope through the primary and secondary depositional zones of the margin. Despite varying bottom water redox conditions ranging from anoxic (upper shelf), to suboxic (shelf break), to oxic (upper slope), each site has elevated organic carbon contents (1.1-11.6 wt.%), due to high surface water primary productivity and lateral transport of organic material from the shelf to the upper slope. Productivity proxies Ni, Cu, and Ag parallel the organic carbon accumulations largely irrespective of the local redox conditions. In contrast, the contents of V, Mo, and Fe respond to the local bottom water redox conditions at each

site, being enriched under strongly reducing conditions and less-enriched under more oxic bottom waters despite the large organic carbon accumulations at all three investigated sites. Thus, the degree of trace metal enrichment and total organic carbon content at each site on the NCM can not only be used to reconstruct primary depositional bottom water redox conditions, but also to identify zones of sediment redeposition. Using multiple sample sites along an offshore transect allows for the identification of intense lateral transport and redeposition of organic-rich sediments that is taking place along the margin. The relative concentrations of both redox-sensitive and productivity-related trace metals suggest that the decoupling of trace metals and organic carbon enrichments occasionally observed in the geological record could be explained by the process of lateral transport and redeposition.

3.2 Introduction

Trace metals have been well-established as redox and/or productivity proxies in sediments and sedimentary rock (Calvert and Pedersen, 1993; Morford and Emerson, 1999; Lipinski et al., 2003; Algeo and Maynard, 2004; Cruse and Lyons, 2004; Borchers et al., 2005; Brumsack, 2006; Piper and Calvert, 2009; Algeo and Rowe, 2012; Owens et al., 2016, 2017). This is due to the processes responsible for the incorporation of trace metals into sediments and, ultimately, the sedimentary record. Trace metals have three major pathways into the sediment: 1) the precipitation of seawater sourced metals related to redox conditions (Calvert and Pedersen, 1993; Nameroff, 1996; Crusius et al., 1996; Morford and Emerson, 1999), 2) biologically sourced metals delivered to sediment within organic matter (Algeo and Maynard, 2004; Brumsack, 2006; Piper and Calvert, 2009; Böning et al., 2015), and 3) delivery of metals contained within detrital materials from continental weathering (Emerson and Huested, 1991; Borchers et al., 2005; Tribovillard et al., 2006; Scott et al., 2017). The variations in organic carbon content and trace metal abundances in the sedimentary record reflect water column productivity and/or the redox state of the benthic water conditions during deposition (Böning et al., 2004, 2005; Borchers et al., 2005; Algeo and Lyons,

2006; Tribovillard et al., 2006; Böning et al., 2015; Little et al., 2015). Thus, trace metal accumulations have been considered relatively reliable proxies that are useful in determining depositional redox and surface water productivity conditions using the enrichments of these elements beyond detrital background concentrations. Geochemical proxies, however, have some environmental limits on accumulation and may be subject to post-depositional and early/late diagenetic alteration. For example, trace metal supply can affect the geochemical signal which can be due to basin restriction (Algeo, 2004; Algeo and Lyons, 2006, Formolo et al., 2014; Zhu et al., 2018) or drawdown due to global redox conditions (Reinhard et al., 2013; Gill et al., 2011; Owens et al., 2016; Sahoo et al., 2016). Likewise, bioturbation (Aller, 1994; Zheng et al, 2000; Volkenborn et al., 2007) and sediment resuspension (Aller et al., 1986; Kowalski et al. 2013; Abshire et al., 2020), which is presently occurring along the Namibian Continental Margin (NCM), can introduce oxygen into previously anoxic sediments, thus releasing some redox-sensitive metals.

3.2.1 Redox-Sensitive Metals

Redox-sensitive trace metals, such as molybdenum (Mo), iron (Fe), and vanadium (V), are often enriched in organic-rich sediment (e.g., Goldschmidt, 1954, Brumsack, 2006 and references therein) and are used in determining modern and ancient depositional redox conditions (e.g. Emerson and Huested, 1991; Calvert and Pedersen, 1993; Algeo and Maynard, 2004; Cruse and Lyons, 2004; Brumsack, 2006; Tribovillard et al., 2006; Piper and Calvert, 2009; Lyons et al., 2009; Algeo and Rowe, 2012; Owens et al., 2016, 2017). The relative abundance of specific trace metals can assist in differentiating between redox conditions on a local and/or global scale (e.g., Algeo and Maynard, 2004; Tribovillard et al., 2004, 2005; Lyons et al., 2009; Sahoo et al., 2016; Owens et al., 2016). The use of Mo as a redox proxy is based on its distinctive geochemical behavior in both oxic and sulfidic environments (Emerson and Huested, 1991; Algeo and Lyons, 2006). In average shale, approximating typical weathered upper continental crust, Mo is found in very low concentrations (1-1.5 ppm, Wedepohl, 1991, Table A2). Conversely, Mo is the most

abundant transition metal in oxic seawater (Collier, 1985) and Mo speciation is dominated by the Mo(VI) species in the form of molybdate. Removal of Mo from oxic seawater occurs via adsorption to Fe- and Mn- (oxyhydr)oxides (Shaw et al., 1990). The adsorbed particles sink to the seafloor and, under reducing conditions, Fe- and Mn-(oxyhydr)oxide minerals are reduced with dissolved Mo increasing in the surrounding solution (Shaw et al., 1990, Crusius et al., 1996; Morford and Emerson, 1999). There is a geochemical switch to convert Mo from molybdate (Mo(VI)-O) to particle-reactive thiomolybdate (Mo(IV)-S), which requires the presence of an increased amount of dissolved sulfide. This is the geochemical condition that must occur for enrichments of Mo to be recorded into the sediment as Mo(IV) (Helz et al., 1996; Erickson and Helz, 2000; Zheng et al., 2000; Helz et al., 2011; Poulson-Brucker et al., 2009). Consequently, the extent of Mo accumulation in sediment has been used in many studies to identify local euxinic environments (Helz et al., 1996; Nameroff et al., 2002; Lipinski et al., 2003; Cruse and Lyons, 2004; Borchers et al., 2005; Algeo and Lyons, 2006; Scott and Lyons, 2012).

Vanadium is found enriched in the sediments of both suboxic and anoxic environments (Shaw et al, 1990; Emerson and Huested, 1991). In oxygenated seawater, V exists as V(V), in the form of the vanadate oxyanion and can easily adsorb onto Fe- and Mn-(oxyhydr)oxides (Calvert and Piper, 1984; Wehrli and Stumm, 1989; Emerson and Huested, 1991). Under mildly reducing conditions, V(V) is reduced to V(IV) and forms vanadyl ions, hydroxyl species, and insoluble hydroxides (Van der Sloot et al., 1985). In the presence of free HS^- under strongly reducing conditions, V(IV) is further reduced to V(III) and precipitated in the solid oxide or hydroxide phase (Breit and Wanty, 1991; Emerson and Huested, 1991; Wanty and Goldhaber, 1992). Because of the two-step reduction process necessary for V fixation in the sediment, V concentrations, when combined with Mo concentrations, are used to identify anoxic and euxinic environments at local and global scales (Algeo and Maynard, 2004; Owens et al., 2016).

In oxic seawater, Fe and Mn precipitate as Fe and Mn oxyhydroxides, thus Fe and Mn are found in concentrations below 1 nM in oxic seawater (Bruland and Lohan 2006, and references therein). Reactive Fe may be mobilized from suboxic sediments, transported, and sequestered during Fe sulfide precipitation in a euxinic water column as pyrite. Based on this process, transport of reactive Fe from the shelf downslope has been observed in the Black Sea (Severmann et al., 2008) and the Peruvian OMZ (Scholz, 2018). Due to the behavior of Fe under various redox conditions, the presence of dissolved iron in pore waters, solid-phase total iron content, and the Fe/Al ratio, which records active Fe enrichment (Werne et al., 2002; Lyons et al., 2003; Raiswell et al., 2018), are commonly used as redox indicators in marine environments (Raiswell and Berner, 1985; Lyons et al., 2003; Cruse and Lyons, 2004; Lyons and Severmann, 2006; Raiswell et al., 2018). Sediments with Fe/Al ratios above 0.66 are considered to be enriched (Raiswell et al., 2018), reflecting deposition in a sulfidic environment, such as the Black Sea (Lyons and Severmann, 2006).

3.2.2 Productivity Related Trace Metals

Productivity-related trace metals accumulate in sediments deposited under upwelling waters due to a high flux of organic matter with enhanced organic carbon preservation at depth (e.g. Böning et al., 2004). Metals such as nickel (Ni), copper (Cu), and silver (Ag) are generally associated with biocycling processes and bioproductivity (Bruland, 1983; Borchers et al., 2005) and are primarily delivered to marine sediments directly within, or adsorbed to, sinking biodetritus (Brongersma-Sanders, 1980; Böning et al., 2015).

Under oxic conditions, Ni is primarily preserved as soluble Ni-carbonate ($NiCO_3$) or adsorbed to humic and fulvic acids, however, Ni may also be present as soluble Ni^{2+} cations or $NiCl^+$ ions (Calvert and Pedersen, 1993; Whitfield, 2002; Algeo and Maynard, 2004). Copper is typically present in oxic settings as organometallic ligands and, to a lesser degree, as soluble $CuCl^+$ ions (Calvert and Pedersen, 1993; Whitfield, 2002; Algeo and Maynard, 2004). The productivity-

related trace metals incorporated into sediments of upwelling margin settings, such as the Chilean and Peruvian margins, are primarily preconcentrated in biodetritus and delivered to the sediments by settling through an oxygen minimum zone (OMZ, Böning et al., 2004, 2005). As organic matter degrades, incorporated metals may be released into pore waters (Moore et al., 1988). Under sulfidic conditions, pore water metals may be incorporated into sediment as insoluble sulfides (Moore et al., 1988; Huerta-Diaz and Morse, 1990, 1992; Morse and Luther, 1999), and remain in the sediment.

While present understanding of the marine geochemical cycling of Ag is relatively limited, when compared to some other trace metals, recent studies have demonstrated that elevated Ag content in sediment may be a reliable indicator of ocean surface productivity (Crusius and Thomson, 2003; Friedl and Pedersen, 1998, 2001; Hendy and Pedersen, 2005; McKay and Pedersen, 2008; Wagner et al., 2013). Similar to Ni and Cu, Ag is taken up in the bodies of micro-organisms in surface waters (Fisher and Wente, 1993) and delivered to the seafloor along with the sinking biodetritus (Friedl and Pedersen, 1998; Böning et al., 2004). Large solid-phase accumulations of Ag (>> average shale values of 0.07 ppm, Table A2) may be due to an accumulation of Ag in the bottom waters via the degradation of settling biodetritus (Böning et al., 2005; Kay and Pedersen, 2008; Morford et al., 2008). In highly-reducing conditions, Ag can form Ag_2S, which is an extremely insoluble sulfide (Dyrssen and Kremling, 1990; Friedl and Pedersen, 2001) and is found enriched in sulfidic sediment through this reduction pathway.

To determine the effects of redeposition on trace metal signals, we present with this study the solid phase and pore water geochemistry of redox- and productivity-related trace metals in sediments on the NCM. A combined approach of bottom-water oxygenation measurements, redox-sensitive and productivity-related trace metal analysis, and total organic carbon content measurements can provide useful insights to aid in paleoenvironmental reconstructions of organic-

rich depositional systems to better constrain ancient environments that may have experienced sediment redeposition.

3.3 Study Area

The perennial upwelling that occurs in the NCM supports some of the highest rates of primary productivity in the present-day oceanic system (Chapman and Shannon, 1985; Summerhayes et al., 1995; Brüchert et al., 2000; Berger and Wefer, 2002; Mollenhauer, 2002) which creates extreme water column oxygen depletion and periodic sulfidic bottom water due to the degradation of sinking biodetritus (Carr, 2002; Borchers et al., 2005). The resulting oxygen minimum zone (OMZ) stretches from the shelf, across the upper continental margin and beyond the shelf break (Chapman and Shannon, 1985). Within the OMZ, oxygen-deficient conditions augment the preservation of large quantities of organic carbon in the sediment (van der Weijden et al., 1999). Seasonal variability in the upwelling cells responsible for the high primary productivity and the consequential expansion of the OMZ is pronounced in the northern parts of the upwelling area (Chapman and Shannon, 1985; Mollenhauer et al., 2002). Our study area, which is significantly south of the Intertropical Convergence Zone, is only slightly affected by seasonal variability in upwelling strength (Shannon, 1985) and the OMZ remains present throughout the year, becoming more pronounced during the summer months (Brüchert et al., 2003). The strong coastal upwelling and high primary productivity have been occurring in this region since at least the early Pleistocene (Berger and Wefer, 2002).

The phytoplankton populations that thrive in the coastal waters above the Namibian shelf are dominated by diatoms, dinoflagellates, and radiolarians (Summerhayes, 1995) resulting in shelf sediments consisting primarily of organic carbon-rich diatomaceous ooze (Bremner, 1983; Summerhayes, 1995; Mollenhauer, 2002). Waters above the shelf break and upper slope contain an abundance of coccolithophores and foraminifera (Giraudeau et al., 1993) delivering a small, but not negligible, amount of organic material to the sediments below (McPhee-Shaw et al., 2004;

Inthorn et al., 2006b). The upper slope depocenter (Figure 3.1) is primarily supplied with organic carbon from the shelf, which is delivered via lateral (offshore) sediment transport in nepheloid layers resulting in the formation of a secondary organic carbon depocenter (Inthorn et al., 2006a,b; Mollenhauer, 2007). The lateral transport and redeposition of sediments on the NCM make this an ideal area to investigate the impact of dynamic depositional conditions in organic-rich sediments on the trace metal inventory.

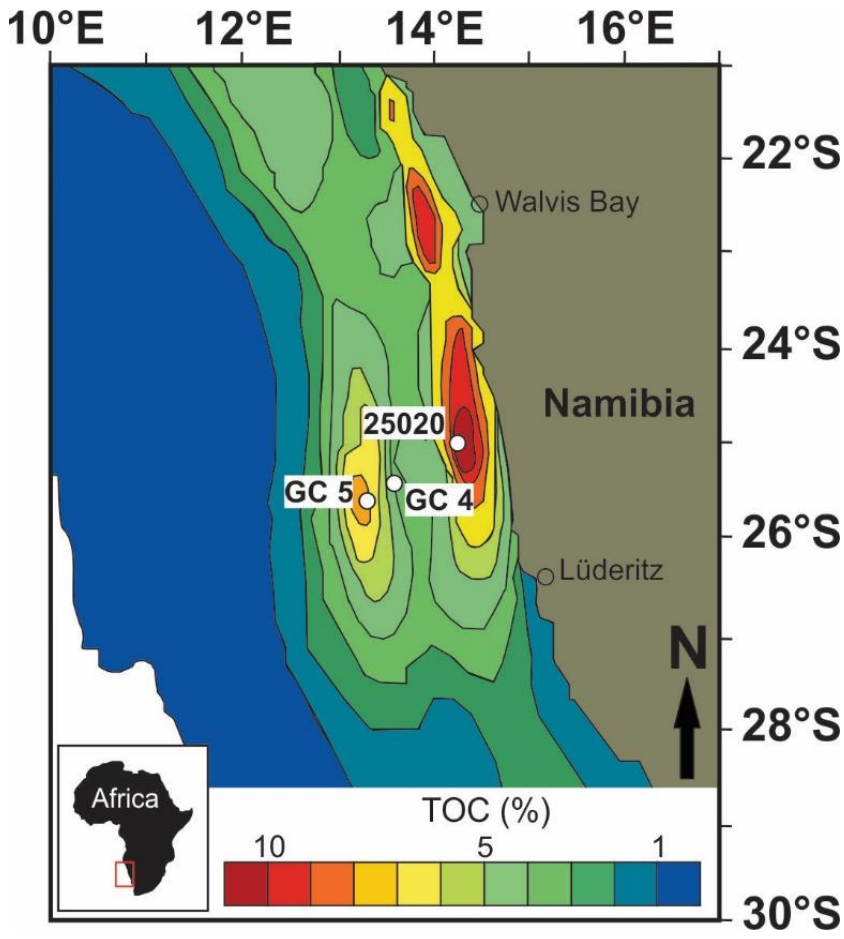

Figure 3.1: Map of the study area showing the areas of intense organic carbon preservation (warmer colors) in the sediments (modified after Mollenhauer et al., 2002). Sample sites 25020 (outer shelf), GC 4 (shelf break), and GC 5 (upper slope) are labeled as white circles.

3.4 Methods

3.4.1 Sampling

Sediment cores were collected for geochemical analyses from the NCM offshore southwestern Africa (Figure 3.1) onboard the research vessel RV MIRABILIS as part of the May 2015 Regional Graduate Network in Oceanography (RGNO) program. Coring sites 25020, GC 4 and GC5 are located on the outer shelf, shelf break, and upper slope, respectively. Surface sediment cores were retrieved using a multi-core (MUC) device from the three sample sites (Table 2.1) and were immediately sliced onboard the ship into 1-2 cm intervals, transferred into centrifuge tubes, and the headspace was purged with nitrogen gas. Bottom water was immediately extracted from the top of the core using a syringe and pore waters were extracted from each tube containing sediments via Rhizons (Seeberg-Elverfeld et al., 2005). All extracted water samples were acidified with trace metal grade (TMG) nitric acid and were stored at 4°C.

3.4.2 Aqueous Phase Analysis

Measurements of ocean water temperature, salinity, and bottom water oxygen levels were obtained from the research vessel using a Conductivity Temperature Depth (CTD) device with an oxygen sensor that had a detection limit of 0.05 mL O_2 L^{-1} H_2O.

Bottom and pore water samples were analyzed for trace metal concentrations using an inductively-coupled plasma-mass spectrometer (ICP-MS, ThermoFisher Scientific, iCAP Qc) at Oklahoma State University. Sample aliquots were diluted 25-fold with 2% supra-pure nitric acid prior analysis. A standard reference material NIST 1643f was analyzed with each set of samples for quality control. The standard deviation for all elements was better than 5%.

3.4.3 Solid Phase Analysis

Total organic carbon (TOC) content of the NCM sediment was measured using an Elemental Analyzer (EA, Costech) at Oklahoma State University (OSU) and were previously reported in Abshire et al. (2020).

Samples for analyses of Al, Mn, Fe, V, Mo, Ni and Cu from all cores were completely digested using a CEM Mars 6 microwave with 5 ml of ~9 M trace metal grade (TMG) nitric acid to remove organic matter followed by TMG hydrochloric, nitric, and hydrofluoric acids. Sample preparation and analyses on a Thermo Element II ICP-MS were carried out in the Geochemistry group at the National High Magnetic Field Laboratory at Florida State University. A set of standard reference materials (NIST 2702, SDO1, and SCO1) were digested and analyzed with each set of samples and, in all cases, reported elements were within the published analytical error.

Samples analyzed for Ag content from all cores were digested using TMG nitric, hydrofluoric, and perchloric acids and heated to 170°C until fully dissolved. Samples were then evaporated until dry and residue was dissolved in 5% TMG nitric acid. The Ag content was measured on a ThermoScientific iCAP Qc ICP-MS at Oklahoma State University. Standard reference material NIST SRM 2702 was digested and analyzed alongside samples with less than 3% error.

Since aluminum can be used as an indicator of the aluminosilicate fraction of a sedimentary deposit, indicating the extent of input from continental weathering (e.g., Brumsack, 1989; Calvert and Pedersen, 1993; Morford and Emerson, 1999; Piper and Perkins, 2004), Trace metal/Aluminum (TM/Al) ratios will be reported alongside trace metal data. Additionally, enrichment factors (EF) for each solid phase element were calculated based on the average enrichment at each site, relative to average shale composition (e.g. Borchers et al., 2005; Brumsack, 2006; Bennett and Canfield, 2020). The calculation for EFs is as follows:

$$EF_X = (X/Al)_{sample} / (X/Al)_{shale}, \text{ (equation 3.1).}$$

The enrichment factor is relative to average shale as defined by Turekian and Wedepohl (1961) and average shale concentrations for studied elements are given in Table A2. All generated data are summarized in Table A3 (pore water), Table A4 (TOC and $CaCO_3$) Table A5 (solid phase trace metals), and Table A6 (calculated enrichment factors). Pore water Ni and Cu were below detection limits (0.08 ppb and 0.22 ppb, respectively) in all samples.

3.5 Results and Discussion

3.5.1 Shelf Site 25020

Shelf sediments are finely laminated below the highly productive surface water and anoxic bottom water (O_2 below detection limit; Abshire et al., 2020) on the shelf of the NCM (Site 25020) (Figure 3.2A). Terrestrial input to the study area is low (Shannon and Nelson, 1996; Borchers et al., 2005) and measured Al contents of the shelf sediments are below 2.3 wt.%. (as low as 0.7 wt.%), thus trace metal enrichments are interpreted as having negligible detrital components. The low pore water iron (Fe_{PW}) concentration at the sediment-water interface (SWI) and slight (~0.09µM) increase in bottom water Fe is explained by the upward diffusion of reduced Fe (Canfield, 1989a; Severmann et al., 2010; Scholz et al., 2011). Pore water iron remains low to a depth of 3 cm (Figure 3.3A) where there is an apparent release of iron from the solid phase as a result of the reductive dissolution of Fe (oxyhydr)oxide minerals (e.g., Froelich et al., 1979; Canfield, 1989a).

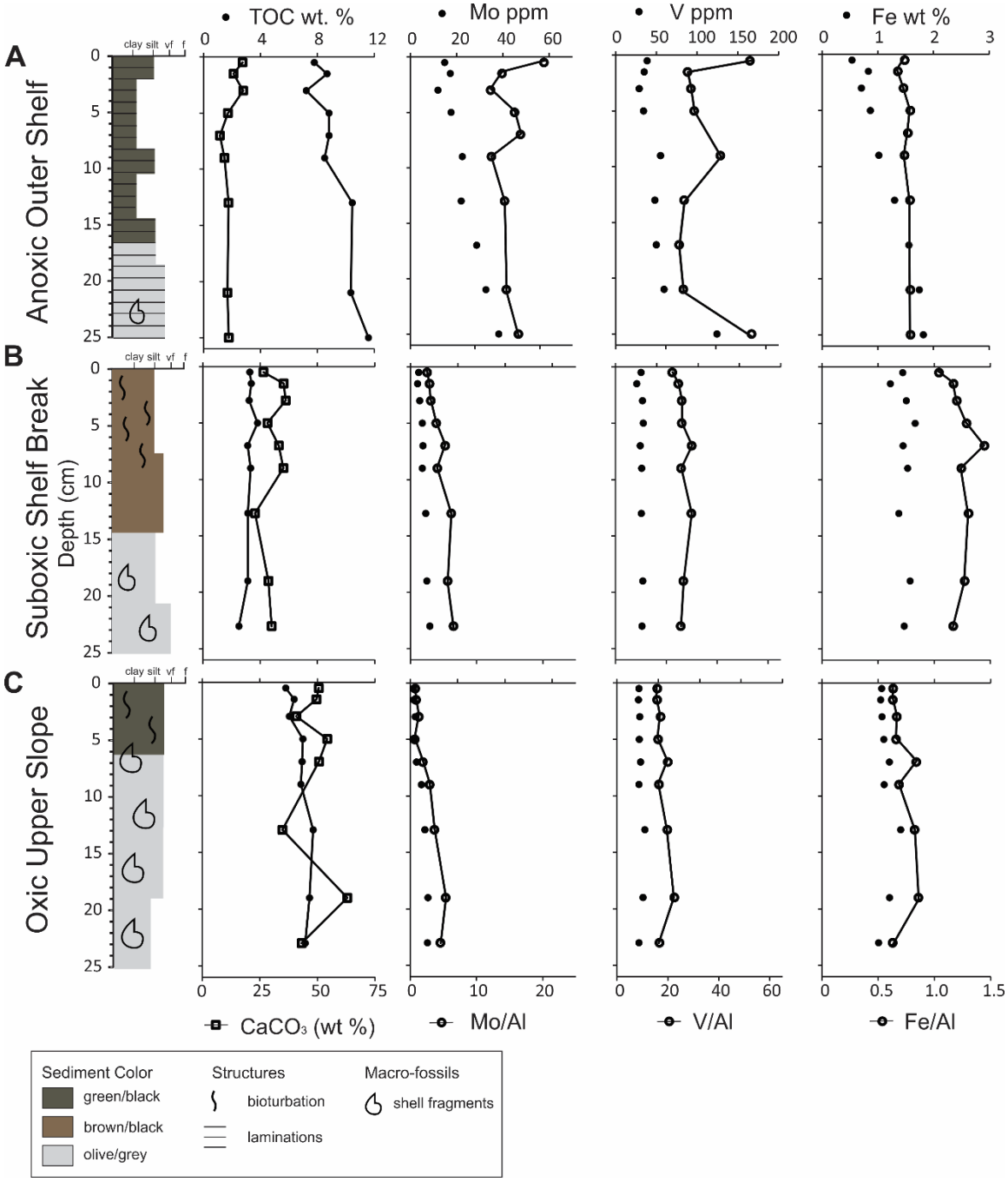

Figure 3.2. Core descriptions, total organic carbon (TOC), and redox-sensitive trace metal content of sediment from the A. anoxic shelf (site 25020), B. suboxic shelf break (site GC 4), and C. oxic upper slope (site GC 5). Trace metal/Aluminum (TM/Al) ratios are plotted alongside trace metal concentrations to normalize TM values against any lithogenic variation (e.g. Calvert and Pedersen, 1993). Trace metal measurements are represented by solid circles; TM/Al ratios are plotted as open circles with lines. Sedimentary core descriptions and TOC data are from Cofrancesco (2016) and Abshire et al. (2020).

The observed decrease in Fe_{PW}, along with the increase in solid-phase Mo, V, and Fe suggests the presence of dissolved sulfide (Berner, 1970; Raiswell and Canfield, 2012) and the likely subsequent formation of iron sulfide minerals (e.g., pyrite) below 3 cm depth. While there are no sulfide data available for this study, the sediments had a strong sulfide odor (see also Cofrancesco, 2016). Furthermore, the sulfide concentration below 3 cm sediment depth must be greater than the threshold required for the geochemical switch which allows Mo to be scavenged from the pore water (Figure 3.3A) as thiomolybdate (Helz et al., 1996; Erickson and Helz, 2000; Zheng et al., 2000; Poulson-Brucker et al., 2009; Helz et al., 2011) and, consequently, to accumulate in the solid-phase (Figure 3.2A, Table A5). Manganese content remains low throughout the depth of the outer shelf core (38-159 ppm, average 77.4 ppm), as well as in the cores on the shelf break and upper slope (Table A5), when compared to Chilean (Böning et al., 2005) and Peruvian upwelling margin sediments (Brumsack, 2006).

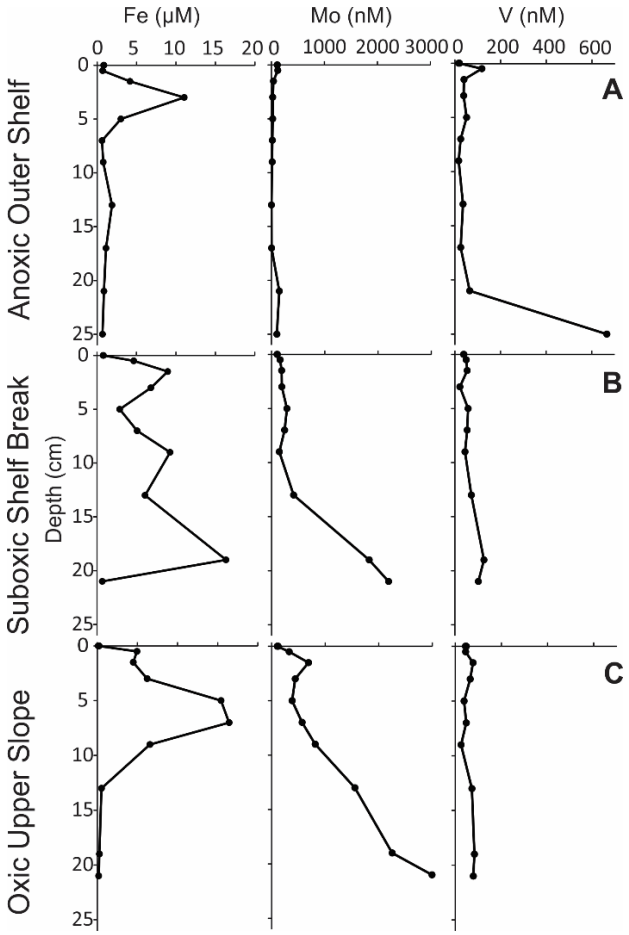

Figure 3.3 Pore water concentration of iron (Fe), molybdenum (Mo) and vanadium (V) from sediment cores collected from the A. anoxic shelf (site 25020), B. suboxic shelf break (site GC 4), and C. oxic upper slope (site GC 5). Pore water Ni and Cu were measured and were below detection limit in all sampled pore waters.

High productivity in surface waters above the shelf (Mollenhauer et al., 2002) is mirrored in the elevated concentration of organic carbon at this site (up to 11.6 wt.%). The Ni, Cu, and Ag content all increase with depth indicating potentially higher periods of productivity in the past (Figure 3.4A), similar to findings from similar water depths along the NCM by Borchers et al. (2005). However, Al content also increases with depth in the shelf sediments which suggests that, in addition to higher productivity, that there may have been more detrital input in the past. Previous studies have suggested, in modern shelf sediments, the dominant source for trace metal accumulation is biogenic (Ni, Cu, and Ag) or related to seawater input (U and Mo) (Borchers et al.,

2005). Since productivity-related metals are incorporated into organic matter in the water column (Brongersma-Sanders, 1980; Böning et al., 2015), and the redox-sensitive metals are enriched in the sediment, geochemical signals of the offshore Namibia shelf suggest a strong correlation between the preservation of the organic material and the reducing conditions during deposition (Borchers et al., 2005).

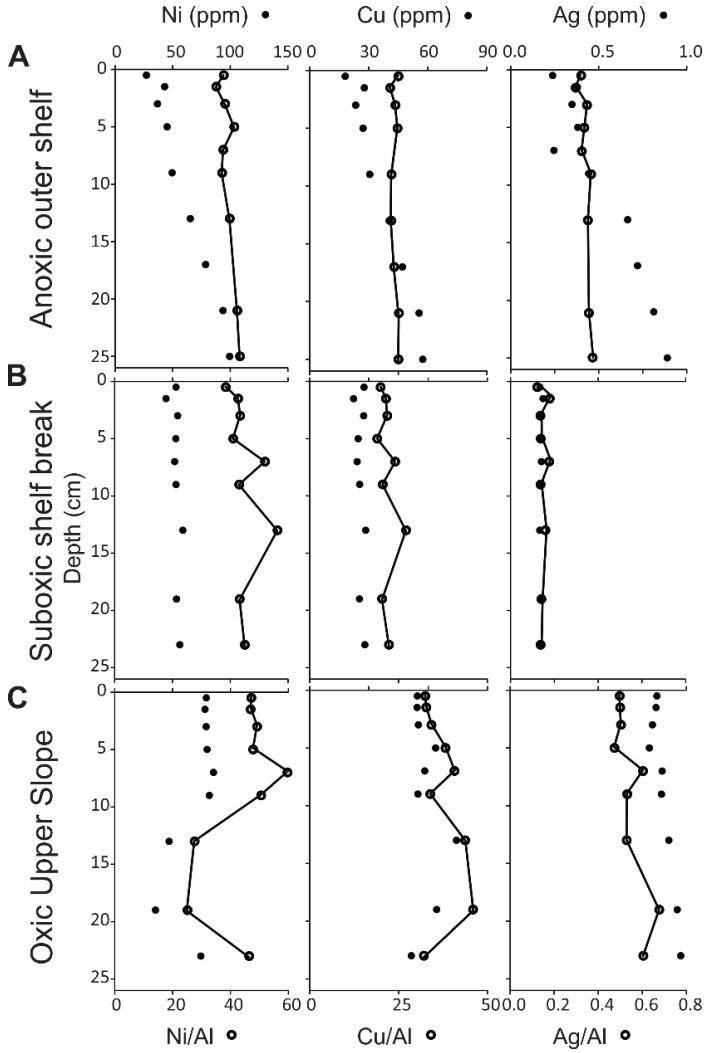

Figure 3.4. Productivity-related solid phase trace metal results from A) anoxic shelf (site 25020), B) suboxic shelf break (GC 4) and C) oxic upper slope (GC 5). Metal concentrations are plotted with a solid black circle and TM/Al ratios are plotted as open circles with lines.

3.5.2 Shelf Break Site GC 4

On the shelf break (site GC 4) suboxic bottom water (Table 2.1), high surface water productivity (Mollenhauer et al., 2002), and net erosion due to bottom currents (Mollenhauer et al., 2007) create a dynamic and unusual depositional environment. Erosion is the dominant control on organic matter deposition and outpaces accumulation at the shelf break site, resulting in the exposure of relatively old organic carbon at the sediment surface (Mollenhauer et al., 2007, Abshire et al., 2020). The moderate $CaCO_3$ content in the shelf break sediments is attributed to the observed shell fragments present in the core (Figure 3.2B). Pore waters contain a variable amount of iron that fluctuates significantly with depth (Figure 3.3B), indicating possible disturbances by burrowing organisms that were observed at the shelf break site (Figure 3.2B). The benthic organisms are likely introducing slightly oxygenated bottom water (1.11mL O_2 L^{-1}, Abshire et al., 2020) into the sediments through bio-irrigation (Aller, 1994; Kristensen, 2000), thus oxidizing the sediments and releasing Fe, V, and Mo into the pore water (Aller, 1994; Canfield, 1994).

Productivity proxy contents of Ni, Cu and Ag, as well as TOC contents (average 3 wt.%) are all comparatively lower in the shelf break sediments, versus the shelf site, and concentrations of these metals remain consistent throughout the sediment column (Figure 3.4B). The reduced productivity-related metal content may be related to the known significant erosion, but may also indicate a smaller contribution of fresh organic matter from surface productivity in this location. The redox-sensitive trace metal data are consistent with a previous study that reported high U/TOC ratios in the shelf break sediment (Abshire et al., 2020). Abshire et al. (2020) showed a range of uranium isotope ($^{234}U/^{238}U$) values in NCM shelf break sediment that approached secular equilibrium, implying that the shelf break sediment is significantly older than sediment from the outer shelf and upper slope of the NCM – a result of the erosional regime that dominates the shelf break (Mollenhauer et al., 2007) and the subsequent exposure of recalcitrant organic material to suboxic conditions. The apparent disconnect between TOC and redox-sensitive trace metals

observed in NCM shelf break sediments has also been observed in the geologic record (e.g., Lüning and Kolonic, 2003; Scott et al., 2017). The erosional exposure of recalcitrant organic matter may provide an alternative explanation to late diagenetic or catagenetic carbon loss in shales with pronounced TM enrichments relative to TOC.

3.5.3 Upper Slope Site GC 5

In sediments at site GC 5 on the upper slope, the absence of laminations and the direct measurements of dissolved oxygen in the bottom water (Table 2.1) place the depositional conditions under a fully oxic regime. The upper slope sediments show relatively high $CaCO_3$ content, which is attributed to the shell fragments within the sediments below 6 cm depth (Figure 3.2C). Low Mo, V, and Fe content (Figure 3.2C) and enrichment factors (Table A6) reflect deposition under oxic conditions. Interestingly, TOC contents are high (5.8-7.7 wt.%), considering organic carbon is assumed to not usually be well-preserved under oxic conditions (Demaison and Moore, 1980; Tyson, 1987; Canfield, 1989b; Piper and Calvert, 2009). Reducing conditions below the SWI are indicated by a moderate increase in Fe_{PW} (up to 16 µM) at 5-7 cm core depth, likely due to the alteration of iron oxides, after which Fe_{PW} decreases sharply (Figure 3.3C). The observed decrease in Fe_{PW} may be related to the presence of dissolved sulfides at depth. However, although pore water sulfide concentrations were not measured, H_2S likely did not exceed concentrations of 11 µM to activate the geochemical switch for Mo precipitation (Helz et al., 1996; Erickson and Helz, 2000; Poulson-Brucker et al., 2009) as Mo enrichments are very minor (Figure 3.2C). The solid phase Mo content in the upper slope sediments is low, while dissolved Mo accumulates in the pore water with Mo_{PW} reaching concentrations up to nearly 3000 nM (Figure 3.3C). The pore water Mo profile indicates upward diffusion of Mo with a source in the deeper sediments. Such a deep Mo source could suggest higher Mo accumulation during interglacial cycles.

Elevated quantities of productivity proxy elements Ni, Cu, and Ag at the upper slope site (Figure 3.4C) suggest that the high TOC content of the upper slope sediments (up to 7.7 wt.%) is

related to high productivity in the water column. However, with oxic conditions at the SWI and in the water column for several hundred meters below the OMZ, it is unlikely that productivity alone is responsible for such observed enrichments. The increased concentrations of productivity-related metals in the sediments at the upper slope site do not positively correlate with enrichments of redox-sensitive trace metals as seen on the shelf. Lateral transport of organic-rich sediment from the anoxic shelf on the NCM (Inthorn et al., 2006a,b; Mollenhauer, 2007) might be responsible for enrichments of Ni, Cu, and Ag (average EFs = 5, 7, and 62, respectively, Table A6). In contrast to the shelf and shelf break sites in this study, Cu does not behave similarly to Ni at the upper slope site. Instead, Cu and also Ag show larger enrichments than Ni, relative to the shelf site, suggesting that some Ni may be lost more easily during the partial remineralization of the organic matter during vertical transport through a long oxic water column below the OMZ. Alternatively, Cu and Ag might be more efficiently scavenged from the water column by particulate organics and/or Fe-Mn (oxyhydr)oxides during transport. The Ag content of the NCM upper slope sediment is exceptionally high, with Ag reaching up to 0.97 ppm (Figure 3.4C) when compared to the average shale Ag content of ~0.07 ppm (Turekian and Wedepohl, 1961, Wedepohl, 1971, Table A2). Our data suggest that observations of NCM sediments are similar to those from the Northwestern United States Continental Margin (Morford et al., 2008), Peruvian Margin (Böning et al., 2004), Central Chilean Margin, and Western Canadian Margin (McKay and Pedersen, 2008) where Ag is scavenged by sinking particles, especially within OMZs, resulting in a greater flux of solid-phase Ag to the sediment under a deeper water column (Böning et al., 2004; Morford et al., 2008; McKay and Pedersen, 2008). Furthermore, it has been shown that in East Atlantic Ocean waters dissolved Ag correlates with silica (Flegal et al., 1995) and increases with water depth (Martin et al., 1983). These observations are similar to barium (Ba) as a productivity indicator, where Ba is scavenged within the water column requiring certain water column depths to appropriately represent organic carbon accumulation in the sediments (e.g. Dymond et al., 1992; Von Breymann et al., 1992; Klump et al., 2000; Nameroff et al., 2002; McKay and Pedersen; 2008; Horner et al., 2015). Due

to the nutrient-type distribution of Ba and Ag in the water column (Bruland and Lohan, 2006 and references therein), concentrations are greater in deeper waters. Thus, the amount of silver scavenged by sinking particulate organic matter is related to the availability of Ag with increasing water depth as well as particle travel time through the water column.

3.5.4 Effects of Redeposition on Geochemical Signals

Offshore sediment transport along the NCM results in the release of some redox-sensitive trace metals as sediments are settling through an oxic water column and is reflected in the preserved geochemical properties of the redepositional zone (Figure 3.5). Upon redeposition on the upper slope, the partially-remineralized organic matter remains, retaining the productivity-related trace metals (Ni, Cu, and Ag) despite oxic conditions. Redox-sensitive elements Mo and V are highly influenced by water column conditions and thus deviations in their abundance occur through redeposition. The enrichments of Ni, Cu, and Ag in the upper slope sediment suggest a resistance of these metals to oxidation during transport and the addition of a smaller amount of fresh organic matter from the productive water column above the upper slope. All of the geochemical and sedimentological signals observed in the NCM upper slope sediments – bioturbation, high organic carbon contents, enrichments in productivity proxy metals, and depletion in the redox-sensitive metals (when compared to the average shale, Turekian and Wedepohl, 1961) – characterize the sediments of the redepositional site. Such a distinct geochemical signature, when found in ancient rock, could be used to identify a paleo-redepositional setting from beneath an upwelling OMZ especially when considering the global location of the setting (i.e. eastern margins of the ocean basin).

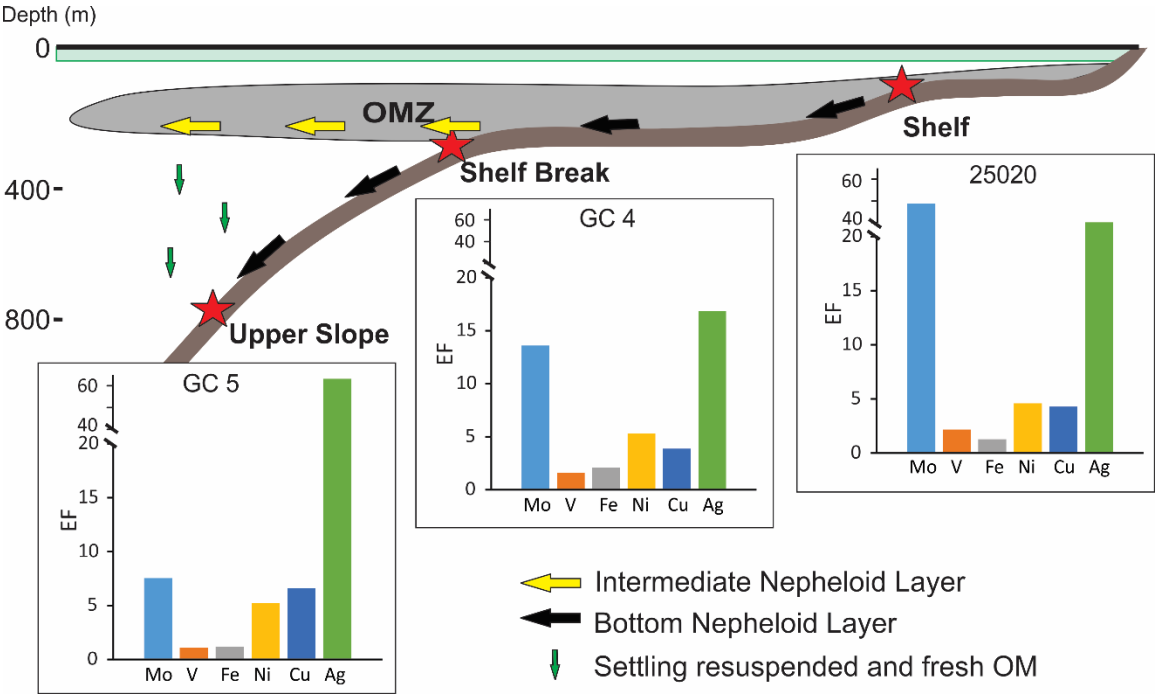

Figure 3.5. Conceptual model showing the direction of sediment transport in intermediate (yellow arrows) and bottom (black arrows) nepheloid layers, settling of suspended and fresh organic matter (green arrows), the position of the OMZ, and the enrichment factors (EF) of solid-phase elements Mo, V, Fe, Ni, Cu, and Ag at each sample site (red stars, modified after Inthorn, 2005).

3.6 Summary and Conclusions

Lateral transport of organic-rich sediments resulted in highly varied geochemical signals along the NCM. Through these observations we can define the geochemical and sedimentary properties of a redepositional zone, which will be significant for paleoceanographic studies. The redepositional area at the upper slope on the NCM is characterized by bioturbated, organic-rich (>5 wt.%) sediments with relatively low Mo contents compared to the shelf and shelf break, no significant enrichments of Fe and V, substantial enrichments of Ni, Cu, and especially high Ag content (Figure 3.5).

Silver is a promising paleoproductivity proxy, although it is coupled to the water column depth. Similar to Ba, Ag is best applied to sediments deposited at great water depths. Moreover, Ag scavenging seems to be dependent on the amount of Ag available in the water column (e.g.,

Flegal et al, 1995), which may vary with different ocean settings (and thus likely with overall water column mixing). Unlike barium, which is subject to remobilization from marine sediments during diagenesis (e.g., McManus et al., 1994; Torres et al., 1996; Riedinger et al., 2006), the consistent Ag concentration throughout the NCM sediment columns suggests that Ag may be more resistant to diagenetic alteration. We therefore postulate that Ag can provide, in addition to paleoproductivity reconstruction, information about water depth and water mixing properties, when applied in combination with other paleo proxies.

While not all ocean upwelling systems undergo intense lateral redeposition processes to the extent of the modern NCM, a more complete understanding of the sedimentary controls on geochemical signals in organic carbon-rich deposits from modern sediments will help to better constrain the depositional environments of ancient organic-rich deposits. Our data suggest that the distinct multi-proxy geochemical signatures observed in the NCM system could be a tool for identifying redepositional environments recorded in ancient rocks. This observation could potentially help constrain some of the difficulties interpreting organic-rich shales that display evidence of benthic life, such as the Jurassic Kimmeridge Clay (e.g. Wignall and Myers, 1988) and the Jurassic Posidonia Shale (e.g. Röhl et al., 2001) and may have various redox conditions throughout the basin both spatially and through time. Due to the expansion of OMZs in the past several decades, and predictions of continued ocean deoxygenation (Stramma et al., 2008, Schmidtko et al., 2017), understanding how proxy metals are incorporated into sediment under a variety of depositional conditions is critical to the interpretation of past OAEs and predictions of future changes to ocean oxygenation.

3.7 Acknowledgements

This manuscript is based upon work supported by the National Science Foundation (NSF) Graduate Research Fellowship Program under Grant No. 1746055. Any opinions, findings, and conclusions or recommendations expressed in this manuscript are those of the authors and do not

necessarily reflect the views of the National Science Foundation. Grants to JDO (NSF OCE and NASA Exobiology) helped to fund the FSU and National High Magnetic Field Laboratory (DMR-1157490) analysis. The authors thank the Regional Graduate Network in Oceanography program, the Research Discovery Camp, and the crew of the Research Vessel Mirabilis. We gratefully acknowledge T. Wu for help and assistance in the lab, C. Scott, J. Donoghue, J. Puckette, and G. Cook for helpful conversation and insight, and Christian März and two anonymous reviewers for their constructive comments on a previous draft, which greatly improved the manuscript.

CHAPTER IV

RECONSTRUCTING THE PALEOCEANOGRAPHIC AND REDOX CONDITIONS RESPONSIBLE FOR VARIATIONS IN URANIUM CONTENT IN NORTH AMERICAN DEVONIAN BLACK SHALES

4.1 Abstract

While organic-rich shales have become increasingly important in recent years as unconventional petroleum reservoirs, the complex sedimentary and early-diagenetic processes responsible for highly variable geochemical signals in shales are still not fully understood. Trace metals, which are commonly used as redox or productivity proxies, are found enriched to differing degrees in many black shales. For instance, one commonly applied proxy for redox and organic-richness is uranium (U). Typically, in shales, uranium contents display a linear relationship to total organic carbon (TOC). This relationship is related to the processes and mechanisms responsible for the incorporation of U into the sediment during the deposition and remineralization of organic matter. Although mostly linear, the U to organic carbon relation can vary in some instances. For example, some shales display uncharacteristically low U content despite having high TOC content. This low U/TOC ratio can occur in a shale if sediments were exposed to oxygen post-deposition. Other shales have large enrichments of U relative to TOC, which may be a result of catagenesis and organic carbon loss through hydrocarbon generation and migration.

Here we examine the U to TOC ratios and U-isotope composition of three Late Devonian-

Early Mississippian shales, the Woodford Shale, the Cleveland Shale, and the Bakken Shale with two study sites in Oklahoma, one site in Eastern Kentucky, and one site in Montana, respectively.

The U/TOC ratios of each shale are unique from one another exhibiting formation average ratios that range from 3 in the Cleveland Shale to 9 in the Woodford Shale, while the U-isotope data indicate that all three formations were deposited under anoxic conditions. The observed variations in U to TOC ratios and U-isotopic compositions help to define subtle changes in oceanographic conditions during deposition. These three shales, when compared to modern anoxic basins and upwelling areas, have distinct geochemical compositions which indicates that, while lithologically similar, each study site represents a distinctly different depositional environment. The comparison of geochemical signals preserved in ancient shales to those signals observed in modern marine depositional systems allows for an enhanced understanding of the U and TOC relationship, and ultimately of the complex and dynamic shale depositional system.

4.2 Introduction

4.2.1 Black shales, trace metals, and organic matter preservation

Black shales form in specific depositional environments such as enclosed basins, similar to the modern Black Sea (e.g. Brumsack, 2006), within oxygen minimum zones (OMZs), similar to the OMZ located along the modern Namibian Continental Margin (e.g. Borchers et al., 2005), or are deposited during oceanic anoxic events (OAEs; e.g. Jenkyns, 2010). In all cases where large quantities of marine organic matter are preserved in sediments, high productivity and an oxygen-depleted environment are commonly assumed to be necessary (Swanson, 1961; Tourtelet, 1979; Schmoker, 1980; Meyer and Nederlof, 1984; Wignall and Myers, 1988; Lüning and Kolonic, 2003; Piper and Calvert, 2009).

Certain trace metal to total organic carbon (TOC) ratios are commonly used to determine the level of basin restriction in marine systems (Algeo and Rowe, 2012). For example, Algeo and

Lyons (2006) proposed a method for estimating the degree of basin restriction by observing that the amount of Mo drawn into sediments in anoxic environments depends on (A) the amount of available Mo in the water, and (B) the amount of sedimentary organic matter. The results of the Algeo and Lyons (2006) study showed that the ratio of Mo to TOC in the sediment reflected the availability of the metal in the watermass. When bottom waters are well connected to open ocean water, the Mo/TOC ratios were high. In the case of silled or restricted basins, the Mo/TOC ratios were lower, due to the drawdown of molybdenum into euxinic sediments (Algeo and Lyons, 2006). Inferences have also been made about the extent of bottom water euxinia due to basin restriction by evaluating U/Mo ratios (Algeo and Tribovillard, 2009, Zhu et al., 2018), suggesting that Mo is drawn into sulfidic sediments at higher concentrations than U. However, euxinic bottom water does not necessarily indicate basin restriction. For example, the modern Namibian Shelf experiences intermittent euxinic bottom waters while being entirely unrestricted (Copenhagen, 1953; Chapman and Shannon, 1985; Emeis et al., 2004; Brüchert et al., 2003). In either case, U behaves similarly to Mo in that it accumulates in sulfidic sediments. However, U also accumulates in anoxic sediments where free sulfides are not present (Zheng et al., 2002a,b; McManus et al., 2005). Therefore, low U content in organic-rich sediments may be a good indicator for extended periods of basin restriction, regardless of the presence of sulfides, as the U content in sediments is limited by the availability of U in the watermass.

The uranium content of sediment can be used, in concert with other redox-sensitive trace elements, to distinguish between oxic and anoxic bottom water conditions in modern and paleo-marine depositional systems (e.g. Barnes and Cochran, 1990; Klinkhammer and Palmer, 1991; Calvert and Pedersen, 1993; Chaillou et al., 2002; Algeo and Maynard, 2004; Cruse and Lyons, 2004; Algeo and Rowe, 2012). In an oxic marine environment, U(VI) is soluble and forms stable carbonate complexes (Langmuir, 1978). In a reducing environment, U(VI) is reduced to insoluble U(IV), which is incorporated into marine sediment along with organic matter at the sediment-water

interface (Langmuir, 1978; Klinkhammer and Palmer, 1991; Spirakis, 1996; Lüning and Kolonic, 2003; McManus et al., 2005, 2006; Tribovillard et al., 2006; Algeo and Tribovillard, 2009), during the reduction of uranium by remineralization of organic matter. Uranium reduction takes place in the absence of oxygen, is intensified in the presence of sulfides (Klinkhammer and Palmer, 1991; Lovely et al., 1991; Lovley, 1993; Spirakis, 1996; Algeo and Maynard, 2004) and is enhanced by metal-reducing microbes (Stirling et al., 2015; Stylo et al., 2015).

The ratio of ^{238}U and ^{235}U in marine sediments and sedimentary rocks has recently emerged as a complementary redox proxy for the reconstruction of past ocean anoxia. Uranium isotope fractionation occurs during adsorption, changes in speciation, or due to changes in redox chemistry, which includes microbially-aided U reduction (Weyer et al, 2008; Basu et al., 2014; Stirling et al., 2015; Stylo et al., 2015), and the U-isotope composition of sediments will vary through these processes. Redox reactions result in reduced U(IV) becoming enriched with the heavier isotope (Montoya-Pino et al., 2010; Basu et al., 2014; Stirling et al., 2015; Stylo et al., 2015), due to the nuclear field shift effect (Andersen et al., 2017, and references therein). Sediments deposited in anoxic environments have been typically observed to contain higher $^{238}U/^{235}U$ than sediments from less-reducing or oxidizing environments (Weyer et al., 2008; Montoya-Pino 2010; Brennecka et al., 2011a; Basu et al., 2014; Stirling et al., 2015; Stylo et al., 2015; Lau et al., 2017; Zhang et al., 2018), with the exception of upper slope sediments from the Namibian Continental Margin, which are enriched in the heavier isotope under oxic conditions due to sediment transport and redeposition (Abshire et al., 2020). Furthermore, the U-isotope system may be used to differentiate between depositional environments (restricted euxinic basin vs. continental shelf) by determining the degree of fractionation from seawater (Anderson et al., 2014, 2017).

In restricted basins, such as the Black Sea, uranium isotopic compositions in the water column and bottom waters are isotopically lighter than average seawater (Anderson et al., 2014; Noordmann et al., 2015). The result of extended periods of basin restriction and long deep water

residence time results in a sedimentary isotopic composition that is lighter than sediments deposited under similar redox conditions where waters are better circulated, thus reflecting the overall depletion of the heavier isotope from the watermass (Anderson et al., 2014, 2017). When examining the isotopic composition of an organic-rich rock and attempting to resolve depositional redox conditions from U-isotopic signals, it is important to consider the impacts of basin restriction and redox on proxy signals, as they may be altered by basin restriction and the eventual drawdown of the heavier isotope into persistently anoxic sediments.

In this study we examine the uranium content, total organic carbon (TOC) content, and U-isotopic composition of three late Devonian shales deposited in three different depositional settings: The Woodford Shale of Oklahoma, the Cleveland Member of the Ohio Shale of eastern Kentucky, and the Upper and Lower Bakken Shales of eastern Montana.

4.3 Study Areas

4.3.1 The Woodford Shale of Oklahoma

The Woodford Formation is a black, organic-rich shale of Late Devonian age consisting of varying proportions of terrigenous, pelagic, and authigenic constituents (Comer, 2008). The Woodford Shale is easily recognized in subsurface logs due to its high radioactivity and persistent hydrocarbon shows, and is a source-rock for much of the oil produced in Oklahoma (e.g. Cardott and Lambert, 1985). Because of the economic potential of the Woodford as a petroleum source rock, the depositional environment responsible for the widespread formation of Woodford Shale has been heavily studied. However, there is still some disagreement in literature as to the oceanographic conditions necessary for the accumulation of the organic carbon found within the shale, as well as to describe some sedimentological features and lithologies found throughout the formation. A study by Heckel (1977) cites the presence of large phosphate nodules and laminations found throughout the Woodford Shale as evidence for strong upwelling conditions in a margin

setting. Algeo and Tribovillard (2009) agree with an upwelling depositional environment for Oklahoma Woodford Shale and suggested, based on molybdenum/uranium covariations, that the Late Devonian seaways of Oklahoma were open to the ocean, which allowed for the free exchange of nutrients and trace metals. In contrast to the findings of previous studies, Turner and Slatt (2016) concluded that the lower Mo/TOC ratios of a lower section of Woodford Shale indicated a period of basin restriction, followed by upwelling, as indicated by higher Mo/TOC ratios and phosphate nodules only present in the uppermost section.

4.3.2 Cleveland Member of the Ohio Shale of Eastern Kentucky

The Cleveland Shale Member of the Ohio Shale Group is a Late Devonian aged organic-rich shale in the Appalachian Basin (Ettensohn, 1987; Pashin and Ettensohn, 1995). The shale contains minor carbonate concretions and pyrite (Robl et al., 1983). Throughout the Devonian Period the Appalachian Basin was connected to the Michigan and Illinois Basins as well as the ancient Rheic Ocean by marginal sills (Algeo et al., 2008; Algeo and Rowe, 2012). Redox conditions in the Appalachian Basin during the time of deposition of the Cleveland Shale member may have been affected by changes in circulation patterns due to sea-level fluctuations, which would have caused a shallowing of sills restricting the flow of seawater into the basin (Pashin and Ettonsohn, 1995; Algeo et al., 2007; Algeo and Rowe, 2012). Such a sill shallowing could have resulted in the slowing of the rate of the deep-water renewal of trace metals (Algeo and Rowe, 2012), resulting in the lower Mo/TOC ratios measured within the Cleveland Member (Algeo et al., 2007; Algeo and Rowe, 2012).

4.3.3 Bakken Shale of Eastern Montana

The Late Devonian-Early Mississippian Bakken Formation is present in the subsurface of the Williston Basin spanning from Northeastern Montana, North Dakota, Southwestern Manitoba and Southern Saskatchewan (Smith and Bustin, 1996; Angulo and Buatois, 2009). The formation

consists of three members: the upper black shale member, a middle member containing sandstone, siltstone, and dolomite, and a lower black shale member that is lithologically similar to the upper member (Meissner, 1984, Webster, 1984; Egenhoff et al., 2011; Egenhoff and Fishman, 2013, Borcovsky et al., 2017). The upper and lower shale members are the primary source rocks for Bakken reservoirs as well as some overlying and underlying units (Gerhard et al., 1990; Chen et al., 2009; Egenhoff and Fishman, 2013) and are the intervals of interest for this study. During the time of Bakken deposition, the Williston Basin was located in the tropics along the western margin of what would become North America (e.g., Gerhard et al., 1990; Nordeng, 2009). Rising sea levels inundated the basin and likely created stratified water conditions allowing for anoxic bottom water and the accumulation of large amounts of organic carbon (Smith and Bustin, 1996; Nordeng, 2009), although the depth of the water column and extent of stratification is still debated (Smith and Bustin, 1996). Changes in the extent of stratification throughout the basin may have important impacts on the geochemical signals and the amount of organic carbon preserved in the shale. It was proposed that some of the deeper facies contained in the southern Williston basin show evidence of restriction relative to those in the north where the waters were better connected to the open ocean via the Elk Point Trough (Algeo and Tribovillard, 2009).

4.4 Methods

4.4.1 Sample collection

In order to compare three relatively age-equivalent shale formations, four Late Devonian-Mississippian aged cores were examined from the three study locations. To examine the Woodford Shale, samples from two cores were selected, the George Core and the Poe Core. The George core containing Woodford Shale was collected from Noble County, Oklahoma on the Cherokee Platform, and the Woodford Poe core was collected from Hughes County, Oklahoma in the Arkoma Basin (Figure 4.1). Samples were taken from each core in approximate 5-foot intervals with variabilities in sampling resolution due to core availability and areas of interest. A rock saw was

used to cut a cube or wedge from the center of the slab being cautious not to include any outer edges to avoid contamination by drilling fluids. Deionized water was used to lubricate the saw. Woodford cores were chosen based on availability and location and are housed in the Oklahoma State University Core Laboratory in Stillwater, Oklahoma.

Figure 4.1. Maps of the four core locations (represented by red stars): Two Woodford Shale cores from Oklahoma, one Cleveland Shale core from Kentucky, and one Bakken Shale core from Montana. A) Map of the United States (Modified from USGS, National Map) and B) Paleogeographic map of North America during the Late Devonian Period (Modified after Blakey, 2016).

To study the Cleveland Shale, Core K-56676 was sampled. The core was collected in Letcher County, Kentucky (Figure 4.1) by EQT Production Company and is currently housed in the Kentucky Geological Survey Core Repository in Lexington, Kentucky. The core represents 115 feet of Cleveland Shale and was sampled every ~5 feet, depending on core availability.

Bakken Shale samples were collected from USGS core code E701, the Blue Sky well, for a previous study and U and TOC values reported here were previously included in the supplementary material of Scott et al. (2017). Splits of the samples used in the previous study were provided by the United States Geological Survey (USGS) for isotopic analysis.

4.4.2 Sample Analyses

All Woodford and Cleveland core samples were crushed into fine powder using a ball mill with a tungsten carbide canister and balls. Total carbon (TC) and total inorganic carbon (TIC) were measured using an Eltra 2000 Carbon Sulfur Determinator at Oklahoma State University (OSU). The measured TIC was subtracted from the TC with the difference being total organic carbon (TOC, wt. %).

Elemental concentrations of Woodford and Cleveland Shale samples were analyzed using inductively coupled plasma-mass spectrometry (ICP-MS, iCapQc, ThermoScientific) at OSU. Due to the anticipated high volume of organics in shale samples, approximately 100 mg of each powdered sample was combusted at 900°C in a furnace for 12 h to remove the organic content. Ashed samples were digested under temperature and pressure (PicoTrace Digestion system) using trace-metal grade nitric (3 ml), hydrofluoric (2 ml) and hydrochloric (3 ml) acids. Samples were heated at 180°C until fully dissolved and evaporated. Samples were reconstituted in 5% trace metal grade nitric acid. Standard reference material (USGS SDO-1) was digested and analyzed alongside

Woodford and Cleveland shale samples to monitor reproducibility. Average values of replicate digestions were well within recommended ranges with the error for U <5%.

All Bakken shale samples used in this study were prepared and measured for trace metal content and TOC by the United States Geological Survey and methods and results are reported in Scott et al. (2017). A powder split of samples from core E701 were provided by the USGS and were digested alongside Woodford and Cleveland samples for the purpose of U-isotope analysis.

The authigenic fraction of U (Uauth) in all shale samples is estimated using the calculation:

$$U_{auth} = U_{sample} - [U/Al_{detrital} * Al_{sample}], \text{ (equation 4.1)}$$

assuming a detrital U:Al ratio of 15×10^{-6} (McManus et al., 2005). The authigenic fraction is reported in the results table (Table A7). However, because U_{auth} is calculated using Al to determine dilution by detrital components, and both U and TOC are subject to dilution by the same detrital components, U_{auth} will not be used when comparing U to TOC because the Al-normalization may introduce variance in trace element-TOC relationships (Algeo and Lyons, 2006).

4.4.3 Uranium Isotope Analysis

All digested shale samples to be analyzed for U isotope composition were treated with an ultra-pure double-spike IRMM3636 (e.g. Stirling et al., 2007) with a concentration of 10.7 ppb ^{233}U and 10.7 ppb ^{236}U. In Woodford Shale samples, the target ^{236}U:^{235}U spiking ratio in the sample:spike mixture was 3:2. The spiking ratio utilized for these samples is lower than that observed in other labs. This practice was intended to prevent carryover between samples and reduce the chance of creating an instrument memory of the isotope ratios. The U was then separated from the matrix with column chromatography using Uteva ion exchange resin (Potter et al., 2005). Aliquots of the purified U samples were then analyzed on an iCap ICP-MS to quantify U concentration of the sample and estimate the U recovery prior to $^{238}U/^{235}U$ ratios being analyzed on the Neptune multi-

collector (MC) ICP-MS. These measurements on Woodford Shale samples were conducted at the Department of Marine and Coastal Sciences at Rutgers University in New Brunswick, New Jersey.

For Cleveland and Bakken shales, digested samples for uranium isotope analysis were treated with IRMM3636 to a spike to sample ratio of .4 ml to 250ng of U. Samples were dried down to equilibrate the spike and taken up in 3M nitric acid. The samples were then pre-concentrated via element-specific column chemistry, then treated with concentrated HNO_3 and 30% H_2O_2 to remove any organics that may have been added from the resin. Samples were once again dried down. Due to problems with residual Na and sometimes Fe contamination, a clean-up step using a PrepFAST-MC was used. Samples were then dissolved in 6M HNO3 and Na and Fe were eluted. Sample U was eluted, collected, and measured using a Neptune MC-ICP-MS at Arizona State University.

The U-isotopic composition is reported as $\delta^{238}U$ in standard per mil (‰) notation. The $\delta^{238}U$ value is calculated against standard reference material CRM112 using the formula:

$$\delta^{238}U = [(^{238}U/^{235}U)_{sample} / (^{238}U/^{235}U)_{CRM112} - 1] \times 1000, \text{ (equation 4.2)}$$

All data are provided in Table A7. Trace metal measurements discussed here were all within less than 5% error for U. Error in isotopic measurements are given as 2 standard deviations (2SD).

4.4.4 Late–Devonian Seawater Average $\delta^{238}U$ Calculation

To determine the degree of U-isotope fractionation from seawater, the late Devonian seawater composition was calculated. Since carbonates are considered to hold a record of the U-isotopic composition of seawater, carbonate U-isotopic values in Late Devonian carbonates reported in White et al. (2018) are used to give an approximation of Late Devonian seawater composition for comparison purposes. It was recently observed in recent Bahamian carbonates that diagenesis imparts a positive isotopic fractionation in carbonate rock of, on average, 0.27‰ (Chen

et al., 2018). This correction is applied to $\delta^{238}U$ values reported in White et al. (2018), which were then averaged to give an approximation of Late Devonian seawater composition.

4.5 Results

4.5.1 Woodford Shale

In the George and Poe cores, U content ranges from ~8ppm to ~50ppm with TOC content between 0.4 and 12 wt.% (Figure 4.2, Table A7). The George core has U/TOC ratios ranging from 2.7 to 5.9 and $\delta^{238}U$ values between -0.46 (+/- 0.23‰; 2SD) to +0.3 (+/- 0.10‰; 2SD, Figure 4.2A). Poe has highly variable U/TOC ratios ranging from 0 to 45 with the largest U/TOC ratios in the shallowest section. Poe $\delta^{238}U$ values from -0.21‰ (± 0.13‰; 2SD) to 0.38 (± 0.13‰; 2SD, Figure 4.2B).

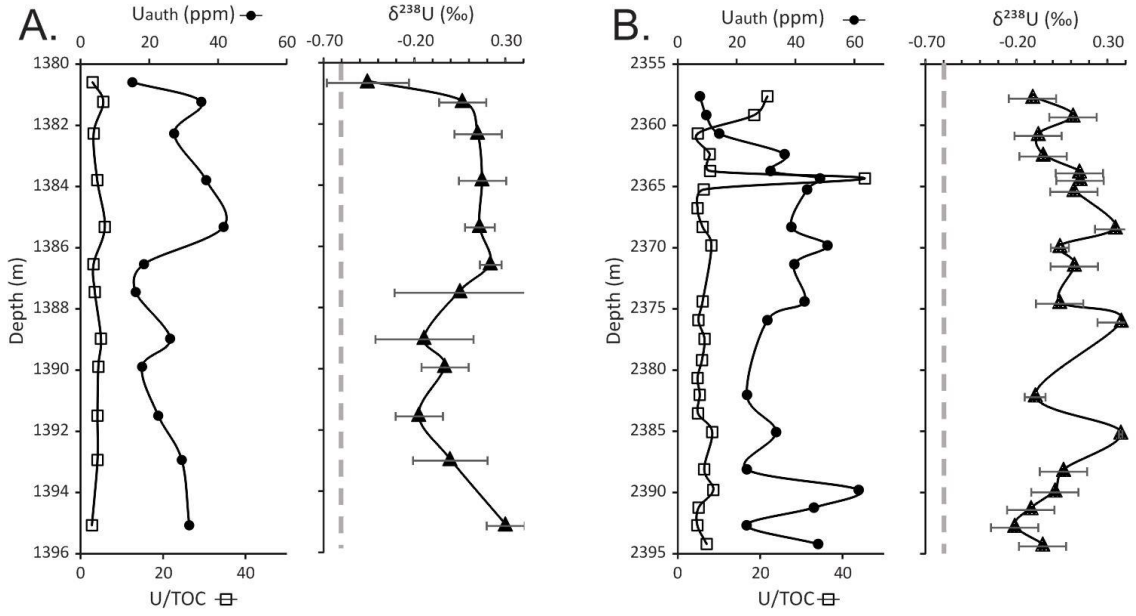

Figure 4.2. Authigenic uranium (U_{auth}), U/TOC ratio, and $\delta^{238}U$ values (Error bars = 2SD) in the Woodford Shale cores (A) George and (B) Poe. Dashed grey line on isotope plot represents the

mean $\delta^{238}U$ of Late Devonian seawater calculated from reported carbonate values in White et al. (2018).

4.5.2 Cleveland Shale

Within core K-566765, the Cleveland Shale U content ranges from 1.3 ppm to 22.9 ppm with TOC content between 0.5 and 8 wt.%. Within the examined core, U/TOC ratios range from 1 to 7 with an average of 3 and $\delta^{238}U$ values are between -0.22‰ (± 0.16‰; 2SD) and 0.21‰ (± 0.13‰; 2SD, Figure 4.3, Table A7).

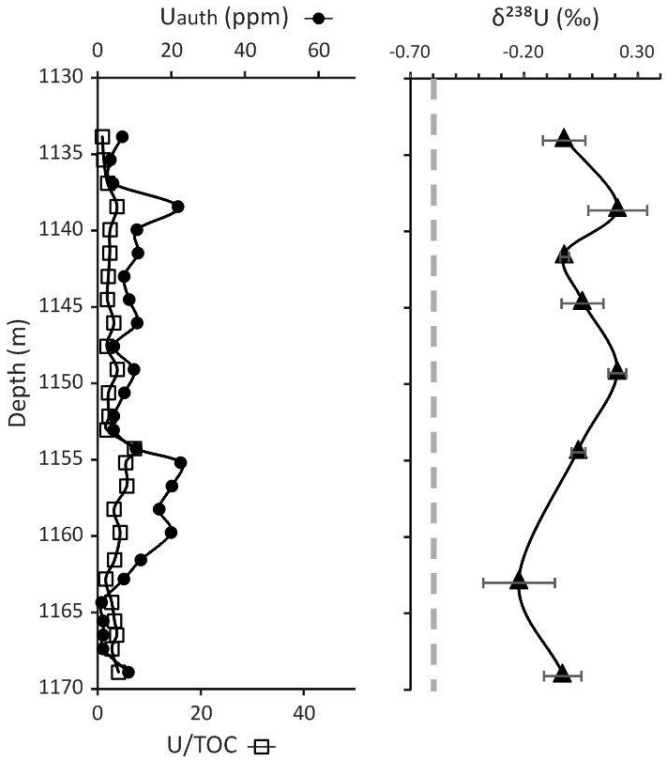

Figure 4.3. U_{auth}, U/TOC ratio, and $\delta^{238}U$ (Error bars = 2SD) with depth in the Cleveland Shale core K-566765. Blue bar on isotope plot indicates calculated mean $\delta^{238}U$ of Late Devonian seawater from reported values in White et al. (2018).

4.5.3 Bakken Shale

Trace metal and TOC contents of the Bakken Shale samples used in this study were previously reported in the supplementary material of Scott et al. (2017). The U/TOC ratios in the Bakken Shale core E701 range from 2 to 7 (average 3) in the Upper Bakken Shale, which has a range of $\delta^{238}U$ values between +0.12‰ (± 0.04‰, 2SD) to +0.27‰ (± 0.09‰, 2SD). The U/TOC ratios in the Lower Bakken Shale range from 2 to 13 (average 6) with $\delta^{238}U$ values in between +0.07‰ (± 0.19‰, 2SD) and +0.36‰ (± 0.05‰, 2SD; Figure 4.4, Table A7).

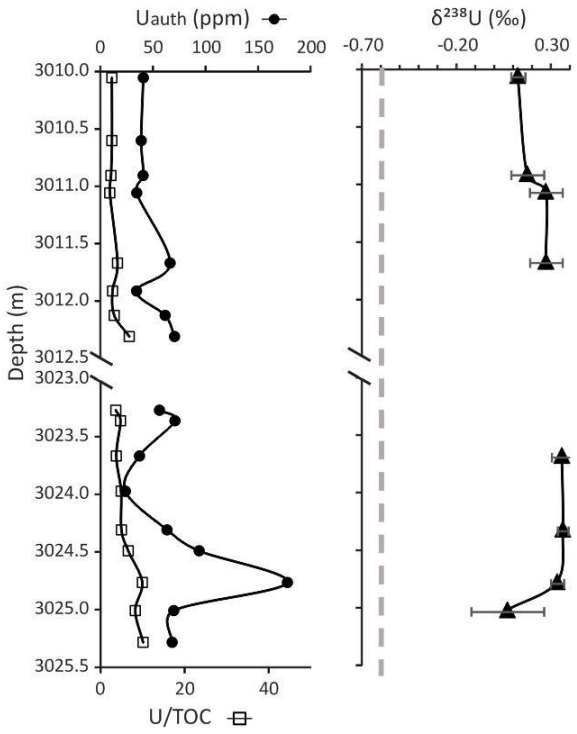

Figure 4.4. U_{auth}, U/TOC ratio, and $\delta^{238}U$ (Error bars = 2SD) with depth in the Upper and Lower Bakken Shale in core E701. The U and TOC data are previously reported by Scott et al. (2017). Blue bar on isotope plot indicates calculated mean $\delta^{238}U$ of Late Devonian seawater from reported values in White et al. (2018).

4.6 Discussion

The oceanographic conditions of the Late Devonian basins of North America can be differentiated by the distinct relationship between U and TOC found in the black shales contained within. The Woodford Shale contains a relatively linear relationship between U and TOC (Figure

4.5) with a general increase in U enrichment with increasing TOC content. Scatter in these data may reflect post-depositional changes and/or catagenesis as this rock is considered mature throughout the areas where cores for this study were obtained (Cardott, 2012).

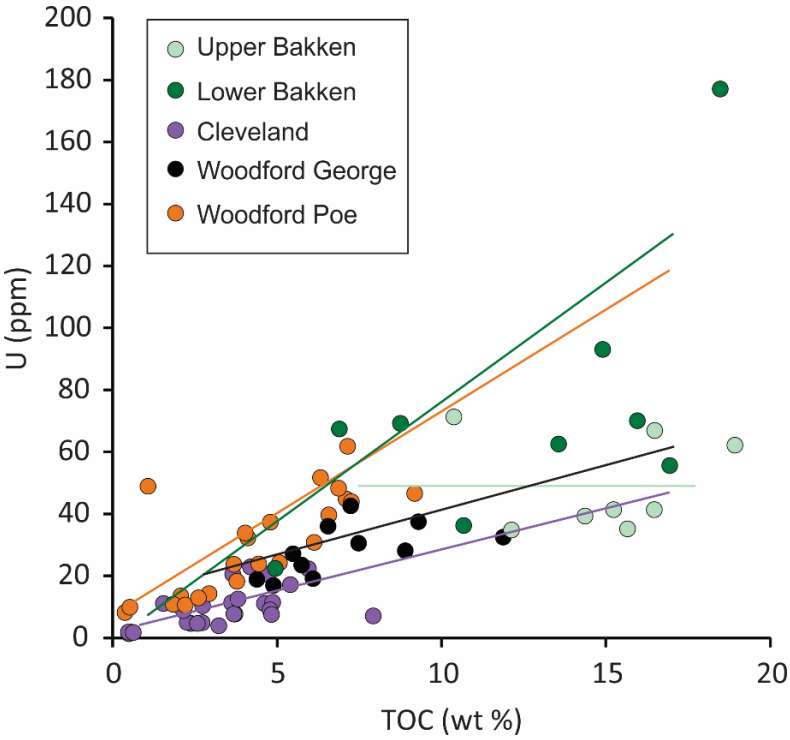

Figure 4.5. The association between U and TOC in Woodford, Cleveland and Bakken shales. Bakken shale data are from Scott et al. (2017). Cleveland and Woodford shale data are from this study.

The large enrichment of U in the sediments and general positive correlation between U and TOC is in agreement with previous interpretations of deposition in an anoxic benthic environment (e.g. Heckel, 1977; Algeo and Tribovillard, 2009; Comer, 2008; Turner and Slatt, 2016).

Since the TOC contents of both Woodford Shale cores are similar, the difference in U content could be due to a higher accumulation rate on the present-day Cherokee Platform (George core), which may be a consequence of the shallower and more proximal setting (Puckette et al., 2016). The higher U content in the Woodford Shale from the Arkoma Basin (Poe core) may be due

to the proximity of the sample location to past upwelling (Lowe, 1975; Heckel and Witzke, 1979; Ettensohn and Barron, 1981; Parrish, 1982; Comer, 1991, 2008), which may have provided more nutrients to surface waters, driving primary productivity and highly reducing bottom water conditions (Comer, 1991), although this is not evidenced by an increase in TOC content. However, the Woodford Shale from the Arkoma Basin (Poe core) does contain elevated nickel (Ni) and copper (Cu) contents (Table A8), relative to the Woodford Shale from the Cherokee Platform (George core), which is possible evidence of enhanced productivity is similar to what is observed in modern sediments from upwelling areas (e.g. Borchers et al., 2005).

The geochemical signals in the Woodford Shale are comparable to those observed in modern shelf sediments of the upwelling Namibia Continental Margin where there is good correlation between U and TOC and U/TOC ratios are high. Additionally, the average $\delta^{238}U$ values from the Woodford Shale and Namibia shelf sediments show similar fractionation from seawater ($\Delta^{238}U$) approaching +0.6‰, which is indicative of U-reduction taking place in an anoxic, open setting (Anderson et al., 2014). It is also possible that the lower U content and higher TOC content on the Cherokee Platform indicates some basin restriction within a sub-basin, as proposed by Turner and Slatt (2016). However, there are not enough data from this study to draw any further conclusions about sub-basins on the present-day Cherokee Platform.

Similar to the Woodford Shale, the Cleveland Shale exhibits a positive covariation between U and TOC (Figure 4.5). The ratios of U to TOC in the Cleveland Shale are, however, slightly lower with an average ratio of ~3, when compared to the Woodford Shale (Table 4.1). These lower ratios are controlled primarily by lower U content and not TOC. A decrease in the rate of U incorporation into sediments may be a symptom of basin restriction if the watermass was depleted of metals due to persistent bottom water anoxia with little deepwater renewal (Algeo and Rowe, 2012). In previous work it was suggested that the mechanism for lower trace metal content in the Cleveland Shale is strong restriction of the Appalachian Basin and the extensive global trace metal

drawdown during the Late Devonian (e.g. Algeo et al., 2007; Algeo and Rowe, 2012). However, the $\delta^{238}U$ values of the Cleveland Shale are very similar to the $\delta^{238}U$ values of Woodford Shale (Table 4.1, A7) with an approximate $\Delta^{238}U$ of +0.6‰. This degree of fractionation would imply that the Appalachian Basin, while possibly partially restricted, was not restricted enough, or over a long enough time interval, to alter the isotopic composition of the reduced U. For example, in the highly-restricted Black Sea, the bottom water $\delta^{238}U$ is lower than that of average seawater due to the extensive drawdown of the heavier isotope into anoxic sediments (Rolison et al., 2017) resulting in Black Sea sediments with lower $\delta^{238}U$ values than expected for highly reducing environments (Andersen et al., 2014). Samples in the previous Appalachian Basin studies were collected from the deeper basin. Thus, due to the location of our Cleveland Shale sample site, and because a definitive U-isotopic signature of basin restriction is not apparent in the sediments, we propose that the cause for the lower U content of the Cleveland Shale in the studied core may be post-depositional oxidation due to a change in the level of the pycnocline, as proposed by Ettonsohn et al. (1988). A similar geochemical signal has been observed in some Antrim Basin shales and was attributed to the effects of a fluctuating pycnocline on sediments deposited in a shallow basin-rim setting (Formolo et al., 2014).

The Lower and Upper Bakken shales, while lithologically similar to each other (Meissner, 1984, Webster, 1984; Egenhoff and Fishman, 2013, Borcovsky et al., 2017), have very different relationships between U and TOC (Figure 4.5). Interestingly, the difference in U/TOC ratios (Lower Bakken average U/TOC = 6; Upper Bakken average U/TOC = 3, Table 4.1) is not reflected in the isotopic composition. It should be noted, however, that the Upper Bakken contains Lower Mississippian-aged sediments for which no seawater compositional data are presently available. In the Lower Bakken Shale, there is significant fractionation from interpreted seawater values on the order of ≥ 0.7‰. These findings are consistent with reduction and U-isotope fractionation occurring above the sediment-water interface and subsequent accumulation in the sediments (Andersen et al.,

2017), coupled with back-diffusion of isotopically light U into the water column. This is similar to the isotopic fractionation observed in the highly-restricted Black Sea water column and sediments (Montoya-Pino, 2010; Rolison et al., 2017; Anderson et al, 2017) where U-isotopic fractionation from seawater increases to +0.42‰ in Unit I and +0.62‰ in Unit II (Weyer et al., 2008; Montoya-Pino et al., 2010). In this case, the combination of high U/TOC ratios, coupled with the large U-isotopic fractionation from Devonian seawater indicates highly sulfidic redox conditions in the stratified bottom waters with enough surface water connection to the open ocean to replenish the supply of nutrients and trace metals into the basin. This is in good agreement with conclusions made by Scott et al. (2017) which surmised that the ancient Williston Basin contained persistent sulfidic bottom waters, which resulted in the large enrichments of trace metals and organic carbon within the Bakken Shale. Carbon loss, either during early diagenesis or catagenesis, may also contribute to a decoupling of U and TOC (e.g. Lüning and Kolonic, 2003), however, in the case of the Bakken Shale in core E701, the shale is thermally immature (Ro = 0.7-0.8, USGS), thus significant catagenetic carbon loss is unlikely.

While there is some difficulty in describing the geochemical conditions of an entire basin based on limited sample locations, the findings of this study are typically in agreement with past studies of the investigated shales: High TOC and U contents, moderate to high *m* values (Table 4.1), and $\Delta^{238}U$ values of up to +0.6‰ suggest that the Woodford Shale was deposited in a predominantly open ocean setting. However, the lower U/TOC ratios in sediments from the George core suggest that these sediments may have been deposited in a semi-restricted sub-basin, as proposed by Turner and Slatt (2016).

Table 4.1. Comparison of the average U_{auth}, TOC, U/TOC, Slope, and $\delta^{238}U$ for Woodford, Cleveland, and Bakken shales. *Italicized* values are calculated using data from Scott et al. (2017).

Unit	U_{auth} Avg. (ppm)	TOC Avg. (wt. %)	U/TOC Avg.	Slope (*m*)	$\delta^{238}U$ (‰)
Woodford (Poe)	34.4	4.4	9.1	5	0.06
Woodford (George)	26.5	6.9	4.0	2	0.02
Cleveland	9.1	3.4	3.0	2	0.03
Upper Bakken	*48.4*	*14.9*	*3.4*	*0*	0.21
Lower Bakken	*71.9*	*12.3*	*6.0*	*3*	0.28

The Cleveland Shale was deposited along the margin of the semi-restricted Appalachian Basin, which may have been strongly affected by sea-level fluctuations (e.g. Pashin and Ettonsohn, 1995, Algeo et al., 2007, Algeo and Rowe, 2012) and a fluctuation pycnocline. Because the reoxidation of U after deposition does not significantly alter the U-isotopic composition of sediments (Abshire et al., 2020), the heavier isotopic composition of the Cleveland Shale in core K-566765, coupled with the low U/TOC ratios (Table 4.1) support a fluctuating pycnocline and a change in redox conditions along the basin margin, rather than basin restriction, as the primary cause for the observed low U content. Like the Woodford and Cleveland shales, the geochemistry of the Upper and Lower Bakken Shales both indicate a reducing environment; the high U and TOC content, lower average U/TOC ratio, isotopically-heavy U-isotopic composition, and *m* value of 0 in the Upper Bakken Shale (Table 4.1) indicates a very strongly reducing water column with sulfidic conditions above the sediment-water interface, comparable to the highly-restricted Black Sea (Murray et al., 1989). Thus, it is likely that the conditions responsible for the decoupling of U and TOC in the Upper Bakken may be related to intense metal drawdown with limited bottom water renewal under persistent euxinic conditions.

4.7 Conclusion

The combination of the U/TOC ratio and the U-isotopic compositions reported in this study provides further refinement to past paleoenvironmental interpretations of the degree of basin restriction and redox conditions within the Late Devonian epicontinental seas of North America. In the case of the examined shales in the study, while lithologically similar, there were stark contrasts in U content and U/TOC ratios in each shale indicating that each studied basin had unique oceanographic conditions ranging from an open continental margin setting to a stratified euxinic basin. The degree of U-isotope fractionation recorded in each shale assisted in identifying the differences between each of the depositional environments. The result of this study is a more refined understanding of the various environments of black shale deposition and new geochemical proxy tools which can be used to influence depositional models and improve the ability to predict the spatial distribution of organic-rich shales in the subsurface.

4.8 Acknowledgements

This manuscript is based upon work supported by the National Science Foundation (NSF) Graduate Research Fellowship Program under Grant No. 1746055. Any opinions, findings, and conclusions or recommendations expressed in this manuscript are those of the authors and do not necessarily reflect the views of the National Science Foundation. The authors would like to express gratitude to G. Gordon and T. Martin at the METAL lab at Arizona State University, A. Kuzminov and S. Severmann for guidance with the measurement of U-isotopes in the Woodford samples, the United States Geological Survey for contributing Bakken Shale samples and maturity data from the Core Research Center, and F. Ettonsohn for insightful conversation.

CHAPTER V

CONCLUSIONS

This thesis represents a geochemical study of a modern, organic-rich dynamic depositional system, which examines the pathways of trace metals into organic-rich sediment and evaluates the effects of lateral transport and post-depositional oxidation on trace metal contents. The results of the modern study are compared to ancient black shales. Historically, many have looked to the Black Sea and other enclosed anoxic basins as the closest analogues for the depositional environment of an organic-rich shale (e.g. Pompeckj, 1901; Brumsack, 2006, and references therein). The assumption is that the restriction of the Black Sea caused stagnation and anoxic bottom waters, facilitating the preservation of organic matter (e.g. Demaison and Moore, 1980). The sediments and organic matter then accumulated in the basin, eventually becoming deeply buried and forming black shale. However, there are parts of the modern ocean floor that contain large amounts of buried organic carbon, such as secondary depositional centers, which can form along passive margin shelfs in upwelling areas (e.g. Mollenhauer et al., 2002). The high primary productivity and oxygen depleted waters within oxygen minimum zones is ideal for the accumulation and preservation of organic matter. However, large quantities of organic matter can also accumulate and be preserved under an oxic water column, away from the area of highest surface productivity (e.g. Mollenhauer et al., 2002, 2007; Inthorn et al., 2006a,b). The transport and redeposition of organic matter leaves behind a unique geochemical signature that, when preserved over time, can fingerprint areas where

redeposition has taken place beneath an oxygen minimum zone.

In this study, we (1) determined that the cause of the decoupling of U and TOC in sediment of the NCM is the disproportionate loss of U during transport and subsequent oxidation; (2) revealed that, despite a loss of U in redeposited sediments, the remaining U remains strongly enriched in the heavier U-isotope, maintaining the isotopic signature of the sediments' primary deposition under anoxic conditions; (3) defined a geochemical signature of a redepositional zone using redox-sensitive metals Fe, Mn, Mo, V, and U and productivity-related metals Ni, Cu, and Ag; and (4) determined the depositional and oceanographic conditions of three Late Devonian shales based on U content, U/TOC ratios, and U-isotopic composition compared to modern organic-rich systems.

Due to a changing climate and a current loss of oxygen from the oceans (Benson and Krause, 1980; Matear and Hirst, 2003; Keeling et al., 2011), there are growing concerns about the threat of ocean deoxygenation to marine ecosystems (Diaz, 2001; Diaz and Rosenberg, 2008). Furthermore, major global anoxia has been considered one of the primary causes for past mass-extinction events (Meyer and Kump, 2008). Therefore, it is critical to understand how the oceans have responded to extreme changes in the past. Due to the sensitivity of some inorganic geochemical proxies to changes in productivity and redox conditions, these proxies are invaluable tools for reconstructing past ocean conditions. Our interpretation of the geochemical composition of the dynamic Namibian Continental Margin has provided a window into the depositional conditions which may have been present in the ancient oceans. While this work focused heavily on sediments from the Namibian Continental Margin, literature suggests that the results are highly applicable to other highly productive continental margin settings (e.g. Jahnke et al., 1990; Arthur et al., 1998, Scholz et al., 2011). This thesis presents new insight into the incorporation and accumulation of metals in sediments under dynamic depositional conditions and provides tools which may be used to influence depositional models, potentially allowing for the discovery of large

areas of organic carbon preserved in ancient redepositional zones. Furthermore, the results of this thesis will help to refine paleo-environmental interpretations and develop new depositional models. Considering the impact of sediment transport and post-depositional oxidation on organic matter distribution and geochemical signals allows for well-informed interpretations of paleoenvironments and improves predictions of the impacts of future climate changes on marine environments.

REFERENCES

Abshire, M. L., Romaniello, S. J., Kuzminov, A. M., Cofrancesco, J., Severmann, S., and Riedinger, N. (2020). Uranium isotopes as a proxy for primary depositional redox conditions in organic-rich marine systems. Earth and Planetary Science Letters 529, 115878.

Algeo, T. (2004). Can marine anoxic events draw down the trace element inventory of seawater? Geology, 32, 1057-1060, doi: 10.1130/G20896.1.

Algeo, T. and Lyons, T. (2006). Mo–total organic carbon covariation in modern anoxic marine environments: Implications for analysis of paleoredox and paleohydrographic conditions. Paleoceanography, 21(1), doi: 10.1029/2004PA001112.

Algeo, T. J, and Rowe, H. (2012). Paleoceanographic applications of trace-metal concentration data. Chemical Geology, 324, 6-18, doi: 10.1016/j.chemgeo.2011.09.002.

Algeo, T. J. and Maynard, J. B. (2004). Trace-element behavior and redox facies in core shales of Upper Pennsylvanian Kansas-type cyclothems. Chemical Geology 206, 289-318.

Algeo, T. J., and Tribovillard, N. (2009). Environmental analysis of paleoceanographic systems based on molybdenum–uranium covariation. Chemical Geology, 268(3-4), 211-225.

Algeo, T. J., Heckel, P. H., Maynard, J. B., Blakey, R., Rowe, H., Pratt, B. R., and Holmden, C. (2008). Modern and ancient epeiric seas and the super-estuarine circulation model of marine anoxia. Dynamics of Epeiric seas: sedimentological, paleontological and geochemical perspectives. St. John's, Canada: Geological Association of Canada, Special Publication, 48, 7-38.

Algeo, T. J., Lyons, T. W., Blakey, R. C., and Over, D. J. (2007). Hydrographic conditions of the Devono–Carboniferous North American Seaway inferred from sedimentary Mo–TOC relationships. Palaeogeography, Palaeoclimatology, Palaeoecology, 256(3-4), 204-230.

Aller, R. C. (1994). Bioturbation and remineralization of sedimentary organic matter: effects of redox oscillation. Chemical Geology, 114(3-4), 331-345.

Andersen, M. B., Romaniello, S., Vance, D., Little, S. H., Herdman, R., and Lyons, T. W. (2014). A modern framework for the interpretation of $^{238}U/^{235}U$ in studies of ancient ocean redox. Earth and Planetary Science Letters, 400, 184-194.

Andersen, M. B., Stirling, C. H., and Weyer, S. (2017). Uranium isotope fractionation. Reviews in Mineralogy and Geochemistry, 82(1), 799-850.

Andersen, M. B., Vance, D., Morford, J. L., Bura-Nakić, E., Breitenbach, S. F., and Och, L. (2016). Closing in on the marine $^{238}U/^{235}U$ budget. Chemical Geology, 420, 11-22.

Anderson, R. F. (1987). Redox behavior of uranium in an anoxic marine basin. Uranium, 3(2-4), 145-164.

Anderson, R.F. (1982). Concentration, vertical flux, and remineralization of particulate uranium in sea-water: Geochimica et Cosmochimica Acta 46, p. 1293-1299. https://doi.org/10.1016/0016-7037(82)90013-8

Angulo, S., and Buatois, L. A. (2009). Sedimentological and ichnological aspects of a sandy low-energy coast: Upper Devonian–Lower Mississippian Bakken Formation, Williston Basin, southeastern Saskatchewan. Summary of Investigations, 1, 2009-4.

Arthur, M. A., Brumsack, H. J., Jenkyns, H. C., and Schlanger, S. O. (1990). Stratigraphy, geochemistry, and paleoceanography of organic carbon-rich Cretaceous sequences. In Cretaceous resources, events and rhythms (pp. 75-119). Springer, Dordrecht.

Arthur, M. A., Dean, W. E., and Laarkamp, K. (1998). Organic carbon accumulation and preservation in surface sediments on the Peru margin. Chemical Geology, 152(3-4), 273-286.

Arthur, M. A., Schlanger, S. T., and Jenkyns, H. C. (1987). The Cenomanian-Turonian Oceanic Anoxic Event, II. Palaeoceanographic controls on organic-matter production and preservation. Geological Society, London, Special Publications, 26(1), 401-420.

Azetsu-Scott, K., Johnson, B. D., and Petrie, B. (1995). An intermittent, intermediate nepheloid layer in Emerald Basin, Scotian Shelf. Continental shelf research, 15(2-3), 281-293.

Bacon, M. P., and van der Loeff, M. M. R. (1989). Removal of thorium-234 by scavenging in the bottom nepheloid layer of the ocean. Earth and Planetary Science Letters, 92(2), 157-164.

Bailey, G. W. (1991). Organic carbon flux and development of oxygen deficiency on the modern Benguela continential shelf south of 22 S: spatial and temporal variability. Geological Society, London, Special Publications, 58(1), 171-183.

Barling, J., Arnold, G. L., and Anbar, A. D. (2001). Natural mass-dependent variations in the isotopic composition of molybdenum. Earth and Planetary Science Letters, 193(3-4), 447-457.

Barnes, C.E. and Cochran, J.K. (1990). Uranium removal in oceanic sediments and the oceanic U balance: Earth and Planetary Science Letters v. 97, p. 94-101.

Basu, A., Sanford, R. A., Johnson, T. M., Lundstrom, C. C., and Löffler, F. E. (2014). Uranium isotopic fractionation factors during U (VI) reduction by bacterial isolates. Geochimica et Cosmochimica Acta, 136, 100-113.

Baudin, F. (2005). A Late Hauterivian short-lived anoxic event in the Mediterranean Tethys: the 'Faraoni Event'. Comptes Rendus Geoscience, 337(16), 1532-1540.

Baudin, F., and Riquier, L. (2014). The late hauterivian faraoni 'oceanic anoxic event': an update. Bulletin de la Société Géologique de France, 185(6), 359-377.

Bell, K. G., Goodman, C., and Whitehead, W. L. (1940). Radioactivity of sedimentary rocks and associated petroleum. AAPG Bulletin, 24(9), 1529-1547.

Benson, B. B., and Krause Jr, D. (1980). The concentration and isotopic fractionation of gases dissolved in freshwater in equilibrium with the atmosphere. 1. Oxygen. Limnology and Oceanography, 25(4), 662-671.

Bennett, W. W. and Canfield, D. E. (2020). Redox-sensitive trace metals as paleoredox proxies: A review and analysis of data from modern sediments. Earth-Science Reviews, 103175.

Berger, W., and Wefer, G. (2002). On the reconstruction of upwelling history: Namibia upwelling in context. Marine Geology, 180(1), 3-28.

Berner, R. (1970) Sedimentary pyrite formation. American Journal of Science, 268(1), 1-23.

Berner, R. A., (1982). Burial of organic carbon and pyrite sulfur in the modern ocean: Its geochemical and environmental significance: American Journal of Science 282, p. 451–473.

Bonatti, E., Honnorez-Guerstein, M. B., Honnorez, J., and Stern, C. (1976). Hydrothermal pyrite concretions from the Romanche Trench (equatorial Atlantic): metallogenesis in oceanic fracture zones. Earth and Planetary Science Letters, 32(1), 1-10.

Böning, P., Brumsack, H.-J., Bottcher, M.E., Schnetger, B., Kriete, C., Kallmeyer, J., Borchers, S.V. (2004). Geochemistry of Peruvian near-surface sediments. Geochimica et Cosmochimica Acta 68, 4429–4451.

Böning, P., Cuypers, S., Grunwald, M., Schnetger, B., and Brumsack, H.-J. (2005). Geochemical characteristics of Chilean upwelling sediments at∼ 36° S. Marine Geology, 220(1-4), 1-21.

Böning, P., Shaw, T., Pahnke, K., and Brumsack, H.-J (2015). Nickel as indicator of fresh organic matter in upwelling sediments. Geochimica et Cosmochimica Acta.

Borchers, S. L., Schnetger, B., Böning, P. and Brumsack, H. J. (2005). Geochemical signatures of the Namibian diatom belt: Perennial upwelling and intermittent anoxia. Geochemistry, Geophysics, Geosystems, 6, Q06006.

Borcovsky, D., Egenhoff, S., Fishman, N., Maletz, J., Boehlke, A., and Lowers, H. (2017). Sedimentology, facies architecture, and sequence stratigraphy of a Mississippian black mudstone succession—The upper member of the Bakken Formation, North Dakota, United States. AAPG Bulletin, 101(10), 1625-1673.

Breit, G.N., Wanty, R.B. (1991). Vanadium accumulation in carbonaceous rocks – a review of geochemical controls during deposition and diagenesis. Chemical Geology 91(2), 83–97, doi: 10.1016/0009-2541(91)90083-4.

Bremner, J.M. (1983). Biogenic sediments on the South West African (Namibian) continental margin. *In*: Coastal Upwelling, its Sediment Record, Part B: Sedimentary Records of Ancient Coastal Upwelling, J. Thiede and E. Suess, editors, Plenum, New York, 73-103.

Bremner, J.M. and Willis, J.P. (1993). Mineralogy and geochemistry of the clay fraction of sediments from the Namibian continental margin and the adjacent hinterland. Marine Geology, v. 115, p. 85-116.

Brennecka, G.A., Herrmann, A.D., Algeo, T.J., and Anbar, A.D. (2011a). Rapid expansion of oceanic anoxia immediately before the end-Permian mass extinction. Proceedings of the National Academy of Sciences of the United States of America 108, p. 17631–17634.

Brennecka, G.A., Wasylenki, L.E., Bargar, J.R., Weyer, S. and Anbar, A.D. (2011b). Uranium isotope fractionation during adsorption to Mn-oxyhydroxides. Environmental science and technology 45, 1370-1375.

Bromley, R. G., and Ekdale, A. A. (1984). Chondrites: a trace fossil indicator of anoxia in sediments. Science, 224(4651), 872-874.

Brongersma-Sanders, M. (1966). Origin of trace-metal enrichment in bituminous shales. *In* Advances in Organic Geochemistry Proceedings of the International Congress, 3rd (pp. 231-236). Pergamon Oxford.

Brongersma-Sanders, M., Stephan, K., Kwee, T., and De Bruin, M. (1980). Distribution of minor elements in cores from the Southwest Africa shelf with notes on plankton and fish mortality. Marine Geology, 37(1-2), 91-132.

Brüchert, V., Jørgensen, B. B., Neumann, K., Riechmann, D., Schlösser, M., and Schulz, H. (2003). Regulation of bacterial sulfate reduction and hydrogen sulfide fluxes in the central Namibian coastal upwelling zone. Geochimica et Cosmochimica Acta, 67(23), 4505-4518, doi: 10.1016/S0016-7037(03)00275-8

Brüchert, V., Jørgensen, B. B., Neumann, K., Riechmann, D., Schlösser, M., and Schulz, H. (2003). Regulation of bacterial sulfate reduction and hydrogen sulfide fluxes in the central Namibian coastal upwelling zone. Geochimica et Cosmochimica Acta, 67(23), 4505-4518.

Brüchert, V., Pérez, M. E., and Lange, C.B. (2000). Coupled primary production, benthic foraminiferal assemblage, and sulfur diagenesis in organic-rich sediments of the Benguela upwelling system. Marine Geology, 163(1-4), 27-40, doi: 10.1016/S0025-3227(99)00099-7

Bruland, K. W., and Lohan, M. C. (2006). Controls of trace metals in seawater. The oceans and marine geochemistry 6, 23-47.

Bruland, K.W. (1983). Trace elements in seawater, *In* Chemical Oceanography, vol. 8, edited by J. P. Riley and R. Chester, pp. 158–220, Elsevier, New York.

Brumsack, H. J. (1980). Geochemistry of Cretaceous black shales from the Atlantic Ocean (DSDP Legs 11, 14, 36 and 41). Chemical Geology, 31, 1-25.

Brumsack, H. J. (1986). The inorganic geochemistry of Cretaceous black shales (DSDP Leg 41) in comparison to modern upwelling sediments from the Gulf of California. Geological Society, London, Special Publications, 21(1), 447-462.

Brumsack, H. J. (2006). The trace metal content of recent organic carbon-rich sediments: implications for Cretaceous black shale formation. Palaeogeography, Palaeoclimatology, Palaeoecology, 232(2-4), 344-361.

Brumsack, H.-J. (1989). Geochemistry of recent TOC-rich sediments from the Gulf of California and the Black Sea. Geologische Rundschau, 78(3), 851-882.

Burnett, W. C., and Veeh, H. H. (1977). Uranium-series disequilibrium studies in phosphorite nodules from the west coast of South America. Geochimica et Cosmochimica Acta, 41(6), 755-764.

Byers, C. W. (1977). Biofacies patterns in euxinic basins a general model. SEPM Special Publication 25, 5-17.

Cacchione, D. A., and Drake, D. E. (1986). Nepheloid layers and internal waves over continental shelves and slopes. Geo-Marine Letters, 6(3), 147-152.

Calvert, S. and Price, N. (1983). Geochemistry of Namibian shelf sediments. In Coastal Upwelling Its Sediment Record (pp. 337-375). Springer US.

Calvert, S. E., and Piper, D. Z. (1984). Geochemistry of ferromanganese nodules from DOMES Site A, Northern Equatorial Pacific: Multiple diagenetic metal sources in the deep sea. Geochimica et Cosmochimica Acta, 48(10), 1913-1928.

Calvert, S.E. and Pedersen, T.F. (1993). Geochemistry of recent oxic and anoxic marine sediments: Implications for the geological record. In: R.J. Parkes, P. Westbroek and J.W. de Leeuw (Eds), Marine Sediments, Burial, Pore Water Chemistry, Microbiology and Diagenesis. Marine Geology 113: 67-88.

Canfield, D. E. (1994). Factors influencing organic carbon preservation in marine sediments. Chemical Geology, 114(3), 315-329.

Canfield, D.E. (1989). Sulfate reduction and oxic respiration in marine sediments: implications for organic carbon preservation in euxinic environments. Deep Sea Research 36, 121-138. Doi: 10.1016/0198-0149(89)90022-8

Canfield, D.E. (1989a). Reactive iron in marine sediments. Geochimica et Cosmochimica Acta 53, 619-32.

Cardott, B. J. (2012). Thermal maturity of Woodford Shale gas and oil plays, Oklahoma, USA. International Journal of Coal Geology, 103, 109-119.

Cardott, B. J., and Lambert, M. W. (1985). Thermal maturation by vitrinite reflectance of Woodford Shale, Anadarko basin, Oklahoma. AAPG Bulletin, 69(11), 1982-1998.

Carr, M. E. (2001). Estimation of potential productivity in Eastern Boundary Currents using remote sensing. Deep Sea Research Part II: Topical Studies in Oceanography, 49(1-3), 59-80.

Chapman, P., and Shannon, L. V. (1985). The Benguela ecosystem. II: Chemistry and related processes. Oceanography and marine biology, 23, 183-251.

Chappaz, A., Lyons, TW, Gregory, DD, Reinhard, CT, Gill, BC, Li, C., and Large, RR (2014). Does pyrite act as an important host for molybdenum in modern and ancient sediments? Geochimica and Cosmochimica Acta , 126 , 112-122.

Chen, X., Romaniello, S. J., Herrmann, A. D., Hardisty, D., Gill, B. C., and Anbar, A. D. (2018). Diagenetic effects on uranium isotope fractionation in carbonate sediments from the Bahamas. Geochimica et Cosmochimica Acta, 237, 294-311.

Chen, Z., Osadetz, K.G., Jiang, C., and Li, M. (2009). Spatial variation of Bakken or Lodgepole oils in the Canadian Williston basin: American Association of Petroleum Geologists, Bulletin, v. 93, p. 829–851

Cheng, H., Edwards, R.L., Chuan-Chou, S., Polyak, V.J., Asmerom, Y., Woodhead, J., Hellstrom, J., Wang, Y, Kong, X., Spötl, C., Wang, X., Alexander Jr., E.C. (2013). Improvements in ^{230}Th dating, ^{230}Th and ^{234}U half-life values, and U-Th isotopic measurements by multi-collector inductively coupled plasma mass spectrometry: Earth and Planetary Science Letters 371-372, 82-91.

Cochran, J. K., Carey, A. E., Sholkovitz, E. R., and Surprenant, L. D. (1986). The geochemistry of uranium and thorium in coastal marine sediments and sediment pore waters. Geochimica et Cosmochimica Acta, 50(5), 663-680.

Cofrancesco, J. (2016). Geochemical signatures for redepositional environments beneath oxygen minimum zones: The Benguela upwelling system offshore Namibia. M.S. thesis, Oklahoma State University

Collier, R. W. (1985). Molybdenum in the Northeast Pacific Ocean 1. Limnology and Oceanography, 30(6), 1351-1354.

Collier, R. W., and Edmond, J. M. (1983). Plankton compositions and trace element fluxes from the surface ocean. *In* Trace metals in sea water (pp. 789-809). Springer, Boston, MA.

Comer, J. B. (1991). Stratigraphic analysis of the upper Devonian Woodford formation, Permian basin, west Texas and southeastern New Mexico (Vol. 201). Bureau of Economic Geology, University of Texas at Austin.

Comer, J. B. (2008). Woodford Shale in southern Midcontinent, USA-Transgressive system tract marine source rocks on an arid passive continental margin with persistent oceanic upwelling. AAPG Annual Convention, San Antonio, TX, poster, 3 panels.

Copenhagen, W. J. (1953). The periodic mortality of fish in the Walvis region: a phenomenon within the Benguela Current. South African Journal of Science 49, 330-331.

Corliss, J. B., Dymond, J., Gordon, L. I., Edmond, J. M., von Herzen, R. P., Ballard, R. D., Green, K., Williams, D., Bainbridge, A., Crane, K. and van Andel, T. H. (1979). Submarine thermal springs on the Galapagos Rift. Science, 203(4385), 1073-1083.

Cowie, G. L., and Hedges, J. I. (1992). The role of anoxia in organic matter preservation in coastal sediments: relative stabilities of the major biochemicals under oxic and anoxic depositional conditions. Organic Geochemistry, 19(1-3), 229-234.

Craig, H. (1965). The measurement of oxygen isotope paleotemperatures. Stable isotopes in oceanographic studies and paleotemperatures: Consiglio Nazionale delle Richerche, 161-182.

Cruse, A and Lyons, T. (2004). Trace metal records of regional paleoenvironmental variability in Pennsylvanian (Upper Carboniferous) black shales. Chemical Geology, 206(3), 319-345.

Crusius, J., and Thomson, J. (2003). Mobility of authigenic rhenium, silver, and selenium during postdepositional oxidation in marine sediments. Geochimica et Cosmochimica Acta, 67(2), 265-273, doi: 10.1016/S0016-7037(02)01075-X.

Crusius, J., Calvert, S., Pedersen, T., and Sage, D. (1996). Rhenium and molybdenum enrichments in sediments as indicators of oxic, suboxic and sulfidic conditions of deposition. Earth and Planetary Science Letters, 145(1), 65-78.

Cumberland, S. A., Douglas, G., Grice, K., and Moreau, J. W. (2016). Uranium mobility in organic matter-rich sediments: A review of geological and geochemical processes. Earth-Science Reviews, 159, 160-185.

Dahl, T. W., Boyle, R. A., Canfield, D. E., Connelly, J. N., Gill, B. C., Lenton, T. M., and Bizzarro, M. (2014). Uranium isotopes distinguish two geochemically distinct stages during the later Cambrian SPICE event. Earth and Planetary Science Letters 401, 313-326.

Dahl, T., Connelly, J. N., Kouchinsky A., Gill, B. C., Månsson, S. F., and Bizzarro, M. (2017). Reorganisation of Earth's biogeochemical cycles briefly oxygenated the oceans 520 Myr ago. International Symposium of the Ediacaran and Cambrian Systems.

Dean, W.E. and Gardner, J.V. (1998). Pleistocene to Holocene contrasts in organic matter production and preservation on the California continental margin. Geological Society of America Bulletin, 110(7), 888-899.

Dean, W.E., Gardner, J.V. and Anderson, R.Y. (1994). Geochemical evidence for enhanced perservation of organic matter in the oxygen minimum zone of the continental margin of northern California during the late Pleistocene. Paleoceanography, 9(1), 4761, doi: 10.1029/93PA02829.

Dean, W. E., Gardner, J. V., and Piper, D. Z. (1997). Inorganic geochemical indicators of glacial-interglacial changes in productivity and anoxia on the California continental margin. Geochimica et Cosmochimica Acta, 61(21), 4507-4518.

Demaison, G.J., and Moore, G.T. (1980). Anoxic environments and oil source bed genesis. AAPG Bulletin, 64(8), 1179-1209.

Deuser, W. G. (1971). Organic-carbon budget of the Black Sea. In Deep Sea Research and Oceanographic Abstracts 18(10), 995-1004, Elsevier.

Diaz, R. J. (2001). Overview of hypoxia around the world. Journal of Environmental Quality, 30(2), 275-281.

Diaz, R. J., and Rosenberg, R. (2008). Spreading dead zones and consequences for marine ecosystems. Science 321(5891), 926-929.

Dymond, J., Corliss, J. B., and Heath, G. R. (1977). History of metalliferous sedimentation at Deep Sea Drilling site 319 in the South Eastern Pacific. Geochimica et Cosmochimica Acta, 41(6), 741-753.

Dymond, J., Suess, E. and Lyle, M. (1992). Barium in deep-sea sediment: A geochemical proxy for paleoproductivity. Paleoceanography, 7, 163-181.

Dyrssen, D., and Kremling, K. (1990). Increasing hydrogen sulphide concentrations and trace metal behaviour in the anoxic Baltic waters. Marine Chemistry 30, 193–204, doi:10.1016/0304-4203(90)90070-S.

Edwards, B. D. (1985). Bioturbation in a dysaerobic, bathyal basin: California borderland. In: Curran, H.A. (Ed.), Biogenic Structures: Their Use in Interpreting Depositional Environments. Special Publications – SEPM 35, 309– 331.

Egenhoff, S. O., and Fishman, N. S. (2013). Traces in the dark—Sedimentary processes and facies gradients in the upper shale member of the Upper Devonian–Lower Mississippian Bakken Formation, Williston Basin, North Dakota, USA. Journal of Sedimentary Research, 83(9), 803-824.

Egenhoff, S.O., Van Dolah, A., Jaffri, A., and Maletz, J. (2011). Facies architecture and sequence stratigraphy of the Middle Bakken Member, Williston Basin, North Dakota, in Robinson, L., LeFever, J., and Gaswirth, S., eds., Bakken–Three Forks Petroleum System in the Williston Basin: Rocky Mountain Association of Geologists, Guidebook, p. 27–47

Ekdale, A. A., and Mason, T. R. (1988). Characteristic trace-fossil associations in oxygen-poor sedimentary environments. Geology, 16(8), 720-723.

Emeis, K.C., Brüchert, V., Currie, B., Endler, R., Ferdelman, T., Kiessling, A., Leipe, T., Noli-Peard, K., Struck, U. and Vogt, T. (2004). Shallow gas in shelf sediments of the Namibian coastal upwelling ecosystem. Continental Shelf Research, 24(6), 627-642.

Emerson, S. (1985). Organic carbon preservation in marine sediments. The carbon cycle and atmospheric CO_2: natural variations Archean to present, 32, 78-87.

Emerson, S., and Huested, S. (1991). Ocean anoxia and the concentrations of molybdenum and vanadium in seawater. Marine Chemistry, 34(3), 177-196.

Erba, E. (2004). Calcareous nannofossils and Mesozoic oceanic anoxic events. Marine Micropaleontology, 52(1-4), 85-106.

Erickson, B.E., and Helz, G.R. (2000). Molybdenum (VI) speciation in sulfidic waters:: Stability and lability of thiomolybdates. Geochimica et Cosmochimica Acta, 64(7), 1149-1158, doi: 10.1016/S0016-7037(99)00423-8

Ettensohn, F. R. (1987). Rates of relative plate motion during the Acadian Orogeny based on the spatial distribution of black shales. The Journal of Geology, 95(4), 572-582.

Ettensohn, F. R., and Barron, L. S. (1981). Depositional model for the Devonian-Mississippian black-shale sequence of North America: a tectono-climatic approach (No. DOE/ET/12040-2). Kentucky Univ., Lexington (USA). Dept. of Geology.

Ettensohn, F.R., Miller, M.L., Dillman, S.B., Elam, T.D., Geller, K.L., Swager, D.R., Markowitz, G., Woock, R.D. and Barron, L.S. (1988). Characterization and implications of the Devonian-Mississippian black shale sequence, eastern and central Kentucky, USA: Pycnoclines, transgression, regression, and tectonism.

Falkowski, P. G., Algeo, T., Codispoti, L., Deutsch, C., Emerson, S., Hales, B., Heuy, R.B., Jenkins, W.J., Kump, L.R., Levin, L.A., and Lyons, T. W. (2011). Ocean deoxygenation: past, present, and future. Eos, Transactions American Geophysical Union, 92(46), 409-410.

Farrimond, P., Eglinton, G., Brassell, S. C., and Jenkyns, H. C. (1989). Toarcian anoxic event in Europe: an organic geochemical study. Marine and Petroleum Geology, 6(2), 136-147.

Fernex, F., Févrierc, G., Bénaïmc, J., and Arnouxd, A. (1992). Copper, lead and zinc trapping in Mediterranean deep-sea sediments: probable coprecipitation with Mn and Fe. Chemical Geology 98, 293-306. doi: 10.1016/0009-2541(92)90190-G

Fertl, W. H., and Rieke III, H. H. (1980). Gamma ray spectral evaluation techniques identify fractured shale reservoirs and source-rock characteristics. Journal of Petroleum Technology, 32(11), 2-053.

Fisher, N.S., Wente, M. (1993). The release of trace elements by dying marine phytoplankton. Deep-Sea Research I 40, 671–694.

Flegal, A.R., Sanudo-Wilhelmy, S.A., and Scelfo, G.M. (1995). Silver in the eastern Atlantic Ocean. Marine Chemistry, 49(4), 315-320.

Föllmi, K. B., and Grimm, K. A. (1990). Doomed pioneers: Gravity-flow deposition and bioturbation in marine oxygen-deficient environments. Geology, 18(11), 1069-1072.

Formolo, M.J., Riedinger, N., and Gill, B.C. (2014) Geochemical evidence for euxinia during the Late Devonian extinction events in the Michigan Basin (USA). Palaeogeography, palaeoclimatology, palaeoecology, 414, 146-154, doi: 10.1016/j.palaeo.2014.08.024.

Friedl, G., and Pedersen, T. F. (2001). Silver as a new tracer for diatom production. EAWAG News, 52(D), 14-15.

Friedl, G., Pedersen, T.F. (1998). Silver as a palaeo proxy for high productivity. Mineralogical Magazine 62A, 476–477 (Part I), doi:10.1180/minmag.1998.62A.1.252.

Froelich, P., Klinkhammer, G.P., Bender, M.L., Luedtke, N.A., Heath, G.R., Cullen, D., Dauphin, P., Hammond, D., Hartman, B. and Maynard, V. (1979). Early oxidation of organic matter in pelagic sediments of the eastern equatorial Atlantic: suboxic diagenesis. Geochimica et cosmochimica acta, 43, 1075-1090.

Gardner, W. D., Walsh, I. D., and Richardson, M. J. (1993). Biophysical forcing of particle production and distribution during a spring bloom in the North Atlantic. Deep Sea Research Part II: Topical Studies in Oceanography, 40(1-2), 171-195.

Gerhard, L.C., Anderson, S.B., and Fisher, D.W. (1990). Petroleum Geology of the Williston basin, in Leighton, M.W., Kolata, D.R., Oltz, D.T., and Eidel, J.J., eds., Interior Cratonic Basins. American Association of Petroleum Geologists, Memoir 51, p. 507–559.

Gill, B.C., Lyons, T.W., Young, S.A., Kump, L.R., Knoll, A.H., and Saltzman, M.R. (2011). Geochemical evidence for widespread euxinia in the Later Cambrian ocean. Nature, 469, 80-83. doi: 10.1038/nature09700

Gilleaudeau, G.J., and Kah, L.C. (2013). Oceanic molybdenum drawdown by epeiric sea expansion in the Mesoproterozoic. Chemical Geology, 356, 21-37. doi: 10.1016/j.chemgeo.2013.07.004

Giraudeau, J., Bailey, G.W., and Pujol, C. (2000). A high-resolution time-series analysis of particle fluxes in the Northern Benguela coastal upwelling system: carbonate record of changes in biogenic production and particle transfer processes: Deep Sea Research Part II 47, p. 1999-2028.

Giraudeau, J., Monteiro, P., and Nikodemus, K. (1993). Distribution and malformation of living coccolithophores in the northern Benguela upwelling system off Namibia. Marine Micropaleontology, 22(1), 93-110.

Goldschmidt, V. M. (1954). Geochemistry (Vol. 78, No. 2, p. 156). LWW.

Gothmann, A. M., Higgins, J. A., Adkins, J. F., Broecker, W., Farley, K. A., McKeon, R., Stolarski, J., Planavsky, N., Wang, X., and Bender, M. L. (2019). A Cenozoic record of seawater uranium in fossil corals. Geochimica et Cosmochimica Acta, 250, 173-190.

Graf, G., and Rosenberg, R. (1997). Bioresuspension and biodeposition: a review. Journal of Marine Systems, 11(3-4), 269-278.

Gundersen, J. S., Gardner, W. D., Richardson, M. J., and Walsh, I. D. (1998). Effects of monsoons on the seasonal and spatial distributions of POC and chlorophyll in the Arabian Sea. Deep Sea Research Part II: Topical Studies in Oceanography, 45(10-11), 2103-2132.

Hartnett, H. E., Keil, R. G., Hedges, J. I., and Devol, A. H. (1998). Influence of oxygen exposure time on organic carbon preservation in continental margin sediments. Nature, 391(6667), 572-575.

Heckel, P. H. (1977). Origin of phosphatic black shale facies in Pennsylvanian cyclothems of mid-continent North America. AAPG Bulletin, 61(7), 1045-1068.

Heckel, P. H. and Witzke, B. J. (1979). Devonian world palaeogeography determined from distribution of carbonates and related lithic palaeoclimatic indicators. Special Papers in Paleontology 23, 99-123.

Hedges, J. I., and Keil, R. G. (1995). Sedimentary organic matter preservation: an assessment and speculative synthesis. Marine chemistry, 49(2-3), 81-115.

Hedges, J. I., Hu, F. S., Devol, A. H., Hartnett, H. E., Tsamakis, E., and Keil, R. G. (1999). Sedimentary organic matter preservation; a test for selective degradation under oxic conditions. American Journal of Science, 299(7-9), 529-555.

Hedges, J.I., Baldock, J.A., Gélinas, Y., Lee, C., Peterson, M. and Wakeham, S.G., (2001). Evidence for non-selective preservation of organic matter in sinking marine particles. Nature, 409(6822), pp.801-804.

Helz, G. R., Bura-Nakić, E., Mikac, N., and Ciglenečki, I. (2011). New model for molybdenum behavior in euxinic waters. Chemical Geology, 284(3-4), 323-332.

Helz, G., Miller, C., Charnock, J., Mosselmans, J., Pattrick, R., Garner, C., and Vaughan, D. (1996). Mechanism of molybdenum removal from the sea and its concentration in black shales: EXAFS evidence. Geochimica et Cosmochimica Acta, 60(19), 3631-3642.

Henderson, G.M. (2002). Seawater ($^{234}U/^{238}U$) during the last 800 thousand years: Earth and Planetary Science Letters, v. 199, p. 97-110. https://doi.org/10.1016/S0012-821X(02)00556-3.

Hendy, I. L., and Pedersen, T. F. (2005). Is pore water oxygen content decoupled from productivity on the California Margin? Trace element results from Ocean Drilling Program Hole 1017E, San Lucia slope, California. Paleoceanography, 20(4), doi: 10.1029/2004PA001123.

Henrichs, S. M. (1992). Early diagenesis of organic matter in marine sediments: progress and perplexity. Marine Chemistry, 39(1-3), 119-149.

Henrichs, S. M. (1993). Early diagenesis of organic matter: The dynamics (rates) of cycling of organic compounds. In Organic geochemistry (pp. 101-117). Springer, Boston, MA.

Herron, S. L. (1991). In Situ Evaluation of Potential Source Rocks by Wireline Logs: Chapter 13: Geochemical Methods and Exploration.

Hetzel, A., Böttcher, M. E., Wortmann, U. G., and Brumsack, H. J. (2009). Paleo-redox conditions during OAE 2 reflected in Demerara Rise sediment geochemistry (ODP Leg 207). Palaeogeography, Palaeoclimatology, Palaeoecology, 273(3-4), 302-328.

Holland, H. D. (1973). Systematics of the isotopic composition of sulfur in the oceans during the Phanerozoic and its implications for atmospheric oxygen. Geochimica et Cosmochimica Acta, 37(12), 2605-2616.

Holmden, C., Amini, M. and Francois, R. (2015). Uranium isotope fractionation in Saanich Inlet: A modern analog study of a paleoredox tracer: Geochimica et Cosmochimica Acta, 153, p. 202-215.

Horner, T. J., Kinsley, C. W., and Nielsen, S. G. (2015). Barium-isotopic fractionation in seawater mediated by barite cycling and oceanic circulation. Earth and Planetary Science Letters, 430, 511-522. doi: 10.1016/j.epsl.2015.07.027.

Huang, J. H., Huang, F., Evans, L., and Glasauer, S. (2015). Vanadium: Global (bio) geochemistry. Chemical Geology, 417, 68-89.

Huerta-Diaz, M.A., Morse, J.W. (1990). A quantitative method for determination of trace metal concentration in sedimentary pyrite. Marine Chemistry 29, 119-144.

Huerta-Diaz, M.A., Morse, J.W. (1992). The pyritization of trace metals in anoxic marine sediments. Geochimica et Cosmochimica Acta 56, 2681-2702.

Huston, M. A., and Wolverton, S. (2009). The global distribution of net primary production: resolving the paradox. Ecological monographs, 79(3), 343-377.

Inthorn, M. (2005). Lateral particle transport in nepheloid layers-a key factor for organic matter distribution and quality in the Benguela high-productivity area (Doctoral dissertation, Universität Bremen).

Inthorn, M., Mohrholz, V., and Zabel, M. (2006a) Nepheloid layer distribution in the Benguela upwelling area offshore Namibia. Deep Sea Research Part I: Oceanographic Research Papers, 53(8), 1423-1438.

Inthorn, M., Wagner, T., Scheeder, G., and Zabel, M. (2006b). Lateral transport controls distribution, quality, and burial of organic matter along continental slopes in high-productivity areas. Geology 34(3), 205-208.

Jaffey, A. H., Flynn, K. F., Glendenin, L. E., Bentley, W. T., and Essling, A. M. (1971). Precision measurement of half-lives and specific activities of U 235 and U 238. Physical review C, 4(5), 1889.

Jahnke, R. A., Reimers, C. E., and Craven, D. B. (1990). Intensification of recycling of organic matter at the sea floor near ocean margins. Nature, 348(6296), 50-54.

Jarvis, I., Lignum, J. S., Gröcke, D. R., Jenkyns, H. C., and Pearce, M. A. (2011). Black shale deposition, atmospheric CO_2 drawdown, and cooling during the Cenomanian-Turonian Oceanic Anoxic Event. Paleoceanography, 26(3).

Jenkyns, H. C. (2010). Geochemistry of oceanic anoxic events. Geochemistry, Geophysics, Geosystems, 11(3).

Keeling, R. F., Körtzinger, A., and Gruber, N. (2010). Ocean Deoxygenation in a Warming World. Annual Review of Marine Science, 2(1), 199-229.

Kendall, B., Komiya, T., Lyons, T. W., Bates, S. M., Gordon, G. W., Romaniello, S. J., Jiang, G., Creaser, R.A., Xiao, S., McFadden, K., and Sawaki, Y. (2015). Uranium and molybdenum isotope evidence for an episode of widespread ocean oxygenation during the late Ediacaran Period. Geochimica et Cosmochimica Acta, 156, 173-193.

Klinkhammer, G. and Palmer, M. (1991). Uranium in the oceans: where it goes and why. Geochimica et Cosmochimica Acta 55: 1799-1806.

Klump, J., D. Hebbeln, and G. Wefer (2000). The impact of sediment provenance on barium-based productivity estimates, Mar. Geol., 169, 259–271.

Knauer, G. A., and Martin, J. H. (1973). Seasonal variations of cadmium, copper, manganese, lead, and zinc in water and phytoplankton in Monterey Bay, California. Limnology and Oceanography, 18(4), 597-604.

Kolonic, S., Wagner, T., Forster, A., Sinninghe Damsté, J.S., Walsworth-Bell, B., Erba, E., Turgeon, S., Brumsack, H.J., Chellai, E.H., Tsikos, H. and Kuhnt, W. (2005). Black shale deposition on the northwest African Shelf during the Cenomanian/Turonian oceanic anoxic event: Climate coupling and global organic carbon burial. Paleoceanography, 20(1).

Kowalski, N., Dellwig, O., Beck, M., Gräwe, U., Neubert, N., Nägler, T. F., Badewien, H., Brumsack, H.-J., van Beusekom, J.E.E., and Böttcher, M. E. (2013). Pelagic molybdenum concentration anomalies and the impact of sediment resuspension on the molybdenum budget in two tidal systems of the North Sea. Geochimica et cosmochimica acta, 119, 198-211.

Krauskopf, K. B. (1956). Factors controlling the concentrations of thirteen rare metals in sea-water. Geochimica et cosmochimica acta, 9(1-2), 1-B32.

Kristensen, E. (2000). Organic matter diagenesis at the oxic/anoxic interface in coastal marine sediments, with emphasis on the role of burrowing animals. In Life at interfaces and under extreme conditions (pp. 1-24). Springer, Dordrecht.

Kristensen, E., and Holmer, M. (2001). Decomposition of plant materials in marine sediment exposed to different electron acceptors (O_2, NO_3^-, and SO_4^{2-}), with emphasis on substrate origin, degradation kinetics, and the role of bioturbation. Geochimica et Cosmochimica Acta, 65(3), 419-433.

Langmuir, D. (1978). Uranium solution-mineral equilibria at low temperatures with applications to sedimentary ore deposits. Geochimica et Cosmochimica Acta 42, 547-569.

Lau, K. V., Macdonald, F. A., Maher, K., and Payne, J. L. (2017). Uranium isotope evidence for temporary ocean oxygenation in the aftermath of the Sturtian Snowball Earth. Earth and Planetary Science Letters, 458, 282-292.

Lau, K. V., Maher, K., Altiner, D., Kelley, B. M., Kump, L. R., Lehrmann, D. J., Silva-Tamayo, J. C., Yu, M., and Payne, J. L. (2016). Marine anoxia and delayed Earth system recovery after end-Permian extinction. Proceedings of the National Academy of Sciences of the United States of America 113: 2360-2365.

Lau, K. V., Romaniello, S. J., and Zhang, F. (2019). The Uranium Isotope Paleoredox Proxy. Cambridge University Press.

Leckie, R. M., Bralower, T. J., and Cashman, R. (2002). Oceanic anoxic events and plankton evolution: Biotic response to tectonic forcing during the mid-Cretaceous. Paleoceanography, 17(3), 13-1.

Lee, C. (1992). Controls on organic carbon preservation: The use of stratified water bodies to compare intrinsic rates of decomposition in oxic and anoxic systems. Geochimica et Cosmochimica Acta, 56(8), 3323-3335.

Lenniger, M., Nøhr-Hansen, H., Hills, L. V., and Bjerrum, C. J. (2014). Arctic black shale formation during Cretaceous oceanic anoxic event 2. Geology, 42(9), 799-802.

Lev, S. M., McLennan, S. M., and Hanson, G. N. (2000). Late diagenetic redistribution of uranium and disturbance of the U-Pb whole rock isotope system in a black shale. Journal of Sedimentary Research, 70(5), 1234-1245.

Lipinski, M., Warning, B., and Brumsack, H. J. (2003). Trace metal signatures of Jurassic/Cretaceous black shales from the Norwegian Shelf and the Barents Sea. Palaeogeography, Palaeoclimatology, Palaeoecology, 190, 459-475.

Little, S. H., Vance, D., Lyons, T. W., and McManus, J. (2015). Controls on trace metal authigenic enrichment in reducing sediments: insights from modern oxygen-deficient settings. American Journal of Science, 315(2), 77-119.

Lovely, D. R., Phillips, E. J. P., Gorby, J. A. and Landa E. R. (1991). Microbial reduction of uranium. Nature 350, 413–416.

Lovley, D. R. (1993). Dissimilatory metal reduction. Annual Review of Microbiology 47, 263–290.

Lowe, D. R. (1975). Regional controls on silica sedimentation in the Ouachita system. Geological Society of America Bulletin, 86(8), 1123-1127.

Lüning, S. and Kolonic, S. (2003). Uranium spectral gamma-ray response as a proxy for organic richness in black shales: Applicability and limitations. Journal of Petroleum Geology, 153-174.

Lyle, M. (1976). Estimation of hydrothermal manganese input to the oceans. Geology, 4(12), 733-736.

Lyons, T. W., and Severmann, S. (2006) A critical look at iron paleoredox proxies: New insights from modern euxinic marine basins. Geochimica et Cosmochimica Acta, 70(23), 5698-5722.

Lyons, T. W., Werne, J. P., Hollander, D. J., and Murray, R. W. (2003). Contrasting sulfur geochemistry and Fe/Al and Mo/Al ratios across the last oxic-to-anoxic transition in the Cariaco Basin, Venezuela. Chemical Geology, 195(1-4), 131-157.

Lyons, T.W., Anbar, A.D., Severmann, S., Scott, C., and Gill, B.C. (2009). Tracking euxinia in the ancient ocean: A multiproxy perspective and Proterozoic case study. Annual Review of Earth and Planetary Sciences 37, 507-534.

Manheim, F. T. (1961). A geochemical profile in the Baltic Sea. Geochimica et Cosmochimica Acta, 25(1), 52-70.

Mann, U., Leythaeuser, D., and Müller, P. J. (1986). Relation between source rock properties and wireline log parameters: An example from Lower Jurassic Posidonia Shale, NW-Germany, Organic Geochemistry, 10(4-6), 1105-1112.

Martin, J. H., Knauer, G. A., and Gordon, R. M. (1983). Silver distributions and fluxes in north-east Pacific waters. Nature, 305(5932), 306-309.

Martin, J. M., and Meybeck, M. (1979). Elemental mass-balance of material carried by major world rivers. Marine chemistry, 7(3), 173-206.

Matear, R. J., and Hirst, A. C. (2003). Long-term changes in dissolved oxygen concentrations in the ocean caused by protracted global warming. Global Biogeochemical Cycles, 17(4).

McCave, I. N., Hall, I. R., Antia, A. N., Chou, L., Dehairs, F., Lampitt, R. S., Thomsen, L., Van Weering , T. C. E. and Wollast, R. (2001). Distribution, composition and flux of particulate material over the European margin at 47–50 N. Deep Sea Research Part II: Topical Studies in Oceanography, 48(14-15), 3107-3139.

McColloch, M.T. and East, T. (2000). The coral record of last interglacial sea levels and sea surface temperatures: Chemical Geology 169, 107-129.

McKay, J.L. and Pedersen, T.F. (2008). The accumulation of silver in marine sediments: A link to biogenic Ba and marine productivity. Global Biogeochemical Cycles 22, GB4010, doi:10.1029/2007GB003136.

McManus, J., Berelson, W. B., Klinkhammer, G. P., Hammond, D. E., and Holm, C. (2005). Authigenic uranium: relationship to oxygen penetration depth and organic carbon rain. Geochimica et Cosmochimica Acta 69: 95-108.

McManus, J., Berelson, W. M., Severmann, S., Poulson, R. L., Hammond, D. E., Klinkhammer, G. P., and Holm, C. (2006). Molybdenum and uranium geochemistry in continental margin sediments: paleoproxy potential. Geochimica et Cosmochimica Acta, 70(18), 4643-4662.

McManus, J., Berelson, W.M., Klinkhammer, G.P., Kilgore, T.E., and Hammond, D.E. (1994). Remobilization of barium in continental margin sediments. Geochimica et Cosmochimica Acta, 58(22), 4899-4907.

McPhee-Shaw, E.E., Sternberg, R.W., Mullenbach, B., and Ogston, A.S. (2004). Observations of intermediate nepheloid layers on the northern California continental margin. Continental Shelf Research 24, 693–720.

Meissner, F. F. (1984). Petroleum Geology of the Bakken Formation Williston Basin. North Dakota and Montana, 28, 159-179.

Meyer, K. M., and Kump, L. R. (2008). Oceanic euxinia in Earth history: causes and consequences. Annual Review of Earth and Planetary Sciences, 36, 251-288.

Meyer, B. L., and Nederlof, M. H. (1984). Identification of source rocks on wireline logs by density/resistivity and sonic transit time/resistivity crossplots. AAPG bulletin, 68(2), 121-129.

Miller, C. A., Peucker-Ehrenbrink, B., and Schauble, E. A. (2015). Theoretical modeling of rhenium isotope fractionation, natural variations across a black shale weathering profile, and potential as a paleoredox proxy. Earth and Planetary Science Letters, 430, 339-348.

Mo, T., Suttle, A. D., and Sackett, W. M. (1973). Uranium concentrations in marine sediments. Geochimica et Cosmochimica Acta, 37(1), 35-51.

Mollenhauer, G., Inthorn, M., Vogt, T., Zabel, M., Damsté, J., and Eglinton, T. (2007). Aging of marine organic matter during cross-shelf lateral transport in the Benguela upwelling system revealed by compound-specific radiocarbon dating. Geochemistry, Geophysics, Geosystems, 8(9).

Mollenhauer, G., Schneider, R. R., Müller, P. J., Spieß, V., and Wefer, G. (2002). Glacial/interglacial variablity in the Benguela upwelling system: Spatial distribution and budgets of organic carbon accumulation. Global Biogeochemical Cycles, 16(4).

Montoya-Pino, C., Weyer, S., Anbar, A. D., Pross, J., Oschmann, W., van de Schootbrugge, B., and Arz, H. W. (2010). Global enhancement of ocean anoxia during Oceanic Anoxic Event 2: A quantitative approach using U isotopes. Geology, 38(4), 315-318.

Moore, J. N., Ficklin, W. H., and Johns, C. (1988). Partitioning of arsenic and metals in reducing sulfidic sediments. Environmental Science and Technology, 22(4), 432-437.

Morford, J.L. and Emerson, S. (1999). The geochemistry of redox sensitive trace metals in sediments. Geochimica et Cosmochimica Acta 63, 1735-1750.

Morford, J.L., Kalnejais, L.H., Helman P., Yen, G., and Reinard, M. (2008). Geochemical cycling of silver in marine sediments along an offshore transect. Marine Chemistry 110, 77-88.

Morford, J. L., Russell, A. D., and Emerson, S. (2001). Trace metal evidence for changes in the redox environment associated with the transition from terrigenous clay to diatomaceous sediment, Saanich Inlet, BC. Marine Geology, 174(1-4), 355-369.

Morse, J., and Luther, G. (1999). Chemical influences on trace metal-sulfide interactions in anoxic sediments. Geochimica et Cosmochimica Acta, 63(19), 3373-3378.

Müller, P. J., and Suess, E. (1979). Productivity, sedimentation rate, and sedimentary organic matter in the oceans—I. Organic carbon preservation. Deep Sea Research Part A. Oceanographic Research Papers, 26(12), 1347-1362.

Murray, J. W., Jannasch, H. W., Honjo, S., Anderson, R. F., Reeburgh, W. S., Top, Z., Friederich, G. E., Codispoti, L. A., and Izdar, E. (1989). Unexpected changes in the oxic/anoxic interface in the Black Sea. Nature, 338(6214), 411-413.

Naimo, D., Adamo, P., Imperato, M., Stanzione, D. (2005). Mineralogy and geochemistry of a marine sequence, Gulf of Salerno, Italy. Quaternary International 140–141, 53–63. doi: 10.1016/j.quaint.2005.05.004

Nameroff, T. (1996). The geochemistry of redox-sensitive metals in sediments of the oxygen minimum off Mexico (Doctoral dissertation, Ph. D. thesis, University of Washington, Seattle).

Nameroff, T. J., Calvert, S. E., and Murray, J. W. (2004). Glacial-interglacial variability in the eastern tropical North Pacific oxygen minimum zone recorded by redox-sensitive trace metals. Paleoceanography and Paleoclimatology, 19(1).

Nameroff, T., Balistrieri, L., and Murray, J. (2002). Suboxic trace metal geochemistry in the eastern tropical North Pacific. Geochimica et Cosmochimica Acta, 66(7), 1139-1158.

Noordmann, J., Weyer, S., Montoya-Pino, C., Dellwig, O., Neubert, N., Eckert, S., Paetzel, M., and Böttcher, M. E. (2015). Uranium and molybdenum isotope systematics in modern euxinic basins: Case studies from the central Baltic Sea and the Kyllaren fjord (Norway). Chemical Geology, 396, 182-195.

Nordeng, S. H. (2009). The Bakken petroleum system: An example of a continuous petroleum accumulation. DMR Newsletter, 36(1), 21-24.

Oliveira, A., Vitorino, J., Rodrigues, A., Jouanneau, J. M., Dias, J. A., and Weber, O. (2002). Nepheloid layer dynamics in the northern Portuguese shelf. Progress in Oceanography, 52(2-4), 195-213.

Owens, J. D., Reinhard, C. T., Rohrssen, M., Love, G. D., and Lyons, T. W. (2016). Empirical links between trace metal cycling and marine microbial ecology during a large perturbation to Earth's carbon cycle. Earth and Planetary Science Letters, 449, 407-417.

Owens, J.D., Lyons, T.W., Hardisty, D.S., Lowery, C.M., Lu, Z., Lee, B., and Jenkyns, H.C. (2017a). Patterns of local and global redox variability during the Cenomanian-Turonian Boundary Event (Oceanic Anoxic Event 2) recorded in carbonates and shales from central Italy. Sedimentology 64, 168-185.

Owens, J. D., Nielsen, S. G., Horner, T. J., Ostrander, C. M., and Peterson, L. C. (2017b). Thallium-isotopic compositions of euxinic sediments as a proxy for global manganese-oxide burial. Geochimica et Cosmochimica Acta, 213, 291-307.

Pak, H., Codispoti, L. A., and Zaneveld, J. R. V. (1980). On the intermediate particle maxima associated with oxygen-poor water off western South America. Deep Sea Research Part A. Oceanographic Research Papers, 27(10), 783-797.

Parrish, J. T. (1982). Upwelling and petroleum source beds, with reference to Paleozoic. AAPG Bulletin, 66(6), 750-774.

Pashin, J. C., and Ettensohn, F. R. (1995). Reevaluation of the Bedford-Berea Sequence in Ohio and adjacent states: Forced regression in a foreland basin (Vol. 298). Geological Society of America.

Pedersen, T., and Calvert, S. (1990). Anoxia vs. productivity: what controls the formation of organic-carbon-rich sediments and sedimentary Rocks?. AAPG Bulletin, 74(4), 454-466.

Peters, K. E., Moldowan, J. M., Schoell, M., and Hempkins, W. B. (1986). Petroleum isotopic and biomarker composition related to source rock organic matter and depositional environment. Organic Geochemistry, 10(1-3), 17-27.

Philander, S., and Yoon, J. (1982). Eastern boundary currents and coastal upwelling. Journal of Physical Oceanography, 12(8), 862-879.

Piper, D. Z., and Calvert, S. E. (2009). A marine biogeochemical perspective on black shale deposition. Earth-Science Reviews, 95(1-2), 63-96.

Piper, D.Z., and Perkins, R.B. (2004). A modern vs. Permian black shale—the hydrography, primary productivity, and water-column chemistry of deposition. Chemical geology, 206(3-4), 177-197, doi: 10.1016/j.chemgeo.2003.12.006.

Pompeckj, J. F. (1901). Die Jura-Ablagerungen zwischen Regensburg und Regenstauf: ein Beitrag zur Kenntnis der Ostgrenze des Fränkischen Jura. Piloty and Loehle.

Potter, E. K., Stirling, C. H., Andersen, M. B., and Halliday, A. N. (2005). High precision Faraday collector MC-ICPMS thorium isotope ratio determination. International Journal of Mass Spectrometry, 247(1-3), 10-17.

Poulson Brucker, R.L., McManus, J., Severmann, S., and Berelson, W.M. (2009). Molybdenum behavior during early diagenesis: Insights from Mo isotopes. Geochemistry, Geophysics, Geosystems, 10(6).

Puckette, J., Kopaska-Merkel, D., and Walsh, P. (2016). Petrophysics and tight rock characterizaiton for the application of improved stimulation and production technology in shale. Research Partnership to Secure Energy for America (RPSEA).

Raiswell, R., and Canfield, D. (2012). The iron biogeochemical cycle past and present. Geochemical Perspectives, 1(1), 1-2.

Raiswell, R., Berner, R.A. (1985). Pyrite formation in euxinic and semi-euxinic sediments. American Journal of Science 285, 710– 724.

Raiswell, R., Hardisty, D.S., Lyons, T.W., Canfield, D.E., Owens, J.D., Planavsky, N.J., Poulton, S.W. and Reinhard, C.T. (2018). The iron paleoredox proxies: A guide to the pitfalls, problems and proper practice. American Journal of Science, 318(5), 491-526.

Reinhard, C. T., Planavsky, N. J., Robbins, L. J., Partin, C. A., Gill, B. C., Lalonde, S. V., Bekker, A., Konhauser, K.O., and Lyons, T. W. (2013). Proterozoic ocean redox and biogeochemical stasis. Proceedings of the National Academy of Sciences, 110(14), 5357-5362. doi:10.1073/pnas.1208622110.

Rex, R. W., and Goldberg, E. D. (1958). Quartz contents of pelagic sediments of the Pacific Ocean 1. Tellus, 10(1), 153-159.

Riedinger, N., Kasten, S., Gröger, J., Franke, C., and Pfeifer, K. (2006). Active and buried authigenic barite fronts in sediments from the Eastern Cape Basin. Earth and Planetary Science Letters, 241, 876-887, doi: 10.1016/j.epsl.2005.10.032

Robl, T. L., Bland, A. E., Koppenaal, D. W., and Barron, L. S. (1983). Geochemistry of oil shales in eastern Kentucky. ACS Symposium Series 230, 159-290

Röhl, H. J., Schmid-Röhl, A., Oschmann, W., Frimmel, A., and Schwark, L. (2001). The Posidonia Shale (Lower Toarcian) of SW-Germany: an oxygen-depleted ecosystem controlled by sea level and palaeoclimate. Palaeogeography, Palaeoclimatology, Palaeoecology, 165(1-2), 27-52.

Rolison, J. M., Stirling, C. H., Middag, R., and Rijkenberg, M. J. (2017). Uranium stable isotope fractionation in the Black Sea: Modern calibration of the $^{238}U/^{235}U$ paleo-redox proxy. Geochimica et Cosmochimica Acta, 203, 69-88.

Romaniello, S. J., Herrmann, A. D., and Anbar, A. D. (2013). Uranium concentrations and $^{238}U/^{235}U$ isotope ratios in modern carbonates from the Bahamas: Assessing a novel paleoredox proxy. Chemical Geology, 362, 305-316.

Sahoo, S.K., Planavsky, N.J., Jiang, G., Kendall, B., Owens, J.D., Wang, X., Shi, X., Anbar, A.D., and Lyons, T.W. (2016). Oceanic oxygenation events on the anoxic Ediacaran ocean. Geobiology, 14, 457-468.

Savrda, C. E., and Bottjer, D. J. (1986). Trace-fossil model for reconstruction of paleo-oxygenation in bottom waters. Geology, 14(1), 3-6.

Savrda, C. E., and Bottjer, D. J. (1987). The exaerobic zone, a new oxygen-deficient marine biofacies. Nature, 327(6117), 54-56.

Savrda, C. E., and Bottjer, D. J. (1989). Anatomy and implications of bioturbated beds in “black shale” sequences: Examples from the Jurassic Posidonienschiefer (southern Germany). Palaios, 330-342.

Savrda, C. E., Bottjer, D. J., and Gorsline, D. S. (1984). Development of a comprehensive oxygen-deficient marine biofacies model: evidence from Santa Monica, San Pedro, and Santa Barbara Basins, California Continental Borderland. AAPG bulletin, 68(9), 1179-1192.

Schlanger, S. O., and Jenkyns, H. C. (1976). Cretaceous oceanic anoxic events: causes and consequences. Geologie en Mijnbouw, 55(3-4).

Schmidtko, S., Stramma, L., and Visbeck, M. (2017). Decline in global oceanic oxygen content during the past five decades Nature, 542, 335-339,

Schmoker, J. W. (1980). Organic content of Devonian shale in western Appalachian Basin. AAPG Bulletin, 64(12), 2156-2165.

Schmoker, J. W. (1981). Determination of organic-matter content of Appalachian Devonian shales from gamma-ray logs. AAPG Bulletin 65(7): 1285-1298.

Scholz, F. (2018). Identifying oxygen minimum zone-type biogeochemical cycling in Earth history using inorganic geochemical proxies. Earth-Science Reviews 184, 29-45.

Scholz, F., Hensen, C., Noffke, A., Rohde, A., Liebetrau, V., and Wallmann, K. (2011). Early diagenesis of redox-sensitive trace metals in the Peru upwelling area–response to ENSO-related oxygen fluctuations in the water column. Geochimica et Cosmochimica Acta, 75(22), 7257-7276.

Schovsbo, N. H. (2002). Uranium enrichment shorewards in black shales: A case study from the Scandinavian Alum Shale. GFF 124.2: 107-115.

Scott, C. and Lyons, T. (2012). Contrasting molybdenum cycling and isotopic properties in euxinic versus non-euxinic sediments and sedimentary rocks: Refining the paleoproxies. Chemical Geology, 324-325, 19-27.

Scott, C., Slack, J. F., and Kelley, K. D. (2017). The hyper-enrichment of V and Zn in black shales of the Late Devonian-Early Mississippian Bakken formation (USA). Chemical Geology, 452, 24-33.

Seeberg-Elverfeldt, J., Schlüter, M., Feseker, T., and Kölling, M. (2005). Rhizon sampling of pore waters near the sediment/water interface of aquatic systems. Limnology and oceanography: Methods, 3(8), 361-371.

Severmann S., McManus, J., Berelson, W.M., and Hammond, D.E. (2010). The continental shelf benthic iron flux and its isotopic composition. Geochimica et Cosmochimica Acta 74, 3984-4004

Severmann, S., Lyons, T.W., Anbar, A., McManus, J., and Gordon, G. (2008). Modern iron isotope perspective on the benthic iron shuttle and the redox evolution of ancient oceans. Geology 36(6), 487-490.

Shannon, L. V., and Nelson, G. (1996). The Benguela: large scale features and processes and system variability. In The South Atlantic (pp. 163-210). Springer, Berlin, Heidelberg.

Shannon, L.V. (1985). The Benguela ecosystem Part I. Evolution of the Benguela, physical features and processes. Oceanography and Marine Biology - An Annual Review, 23, 105–182.

Shannon, L.V. and Nelson, G. (1996). The Benguela: large scale features and processes and system variability. In The South Atlantic (pp. 163-210). Springer Berlin Heidelberg.

Shaw, T.J., Gieskes, J.M., and Jahnke, R.A. (1990). Early diagenesis in differing depositional environments: The response of transition metals in pore water. Geochimica et Cosmochimica Acta 54, 1233-1246.

Shiller, A.M., Boyle, E.A. (1987). Dissolved vanadium in rivers and estuaries. Earth Planet. Sci. Lett. 86 (2–4), 214–224.

Smith, M. G., and Bustin, R. M. (1996). Lithofacies and paleoenvironments of the upper Devonian and lower Mississippian Bakken Formation, Williston Basin. Bulletin of Canadian Petroleum Geology, 44(3), 495-507.

Spirakis, C. S. (1996). The roles of organic matter in the formation of uranium deposits in sedimentary rocks. Ore Geology Reviews 11, 53-69.

Starinsky, A., Katz, A., and Kolodny, Y. (1982). The incorporation of uranium into diagenetic phosphorite. Geochimica et Cosmochimica Acta, 46(8), 1365-1374.

Stirling, C. H., Andersen, M. B., Potter, E. K., and Halliday, A. N. (2007). Low-temperature isotopic fractionation of uranium. Earth and Planetary Science Letters, 264(1-2), 208-225.

Stirling, C. H., Andersen, M. B., Warthmann, R., and Halliday, A. N. (2015). Isotope fractionation of ^{238}U and ^{235}U during biologically-mediated uranium reduction. Geochimica et Cosmochimica Acta, 163, 200-218.

Stramma, L., Johnson, G.C., Sprintall, J., and Mohrholz, V. (2008). Expanding oxygen-minimum zones in the tropical oceans. Science 320, 655-658.

Stylo, M., Neubert, N., Wang, Y., Monga, N., Romaniello, S. J., Weyer, S., and Bernier-Latmani, R. (2015). Uranium isotopes fingerprint biotic reduction. Proceedings of the National Academy of Sciences, 112(18), 5619-5624.

Summerhayes, C., Kroon, D., Rosell-Melé, A., Jordan, R., Schrader, H., Hearn, J. Villanueva, J., Grimalt, G., and Eglinton, G. (1995). Variability in the Benguela Current upwelling system over the past 70,000 years. Progress in Oceanography, 35(3), 207-251.

Swanson, V. E. (1961). Geology and geochemistry of uranium in marine black shales: a review (pp. 1-110). Washington, DC: US Government Printing Office.

Tissot, F. L. H., Dauphas, N. (2015). Uranium isotopic compositions of the crust and ocean: Age corrections, U budget and global extent of modern anoxia. Geochemica et Cosmochemica Acta 167: 113-143.

Torres, M.E., Brumsack, H.J., Bohrmann, G., and Emeis, K.C. (1996). Barite fronts in continental margin sediments: a new look at barium remobilization in the zone of sulfate reduction and formation of heavy barites in diagenetic fronts. Chemical Geology, 127(1-3), 125-139, doi: 10.1016/0009-2541(95)00090-9.

Tostevin, R., Clarkson, M. O., Gangl, S., Shields, G. A., Wood, R. A., Bowyer, F., Penny, A.M. and Stirling, C. H. (2019). Uranium isotope evidence for an expansion of anoxia in terminal Ediacaran oceans. Earth and Planetary Science Letters, 506, 104-112.

Tourtelot, H. A. (1979). Black shale—its deposition and diagenesis. Clays and Clay Minerals 27(5): 313-321.

Tribovillard, N., Algeo, T. J., Lyons, T., and Riboulleau, A. (2006). Trace metals as paleoredox and paleoproductivity proxies: an update. Chemical geology, 232(1-2), 12-32.

Tribovillard, N., Ramdani, A., and Trentesaux, A. (2005). Controls on organic accumulation in Late Jurassic shales of northwestern Europe as inferred from trace-metal geochemistry. In: Harris, N. (Ed), The Deposition of Organic-Carbon-Rich Sediments: Models, Mechanisms, and Consequences. SEPM Special Publication, vol. 82, 145-164.

Tribovillard, N., Riboulleau, A., Lyons, T.W., and Baudin, F. (2004). Enhanced trapping of molybdenum by sulfurized organic matter of marine origin as recorded by various Mesozoic formations. Chemical Geology 213, 385-401.

Turekian, K. K., and Wedepohl, K. H. (1961). Distribution of the elements in some major units of the earth's crust. Geological Society of America Bulletin, 72(2), 175-192.

Turner, B. W., and Slatt, R. M. (2016). Assessing bottom water anoxia within the Late Devonian Woodford Shale in the Arkoma Basin, southern Oklahoma. Marine and Petroleum Geology, 78, 536-546.

Tyson, R. V., and Pearson, T. H. (1991). Modern and ancient continental shelf anoxia: an overview. Geological Society, London, Special Publications, 58(1), 1-24.

Tyson, R.V. (1987). The genesis and palynofacies characteristics of marine petroleum source rocks. Geological Society, London, Special Publications, 26(1), 47-67.

USGS National Map. National Geospatial Program. Retrieved from https://www.usgs.gov/core-science-systems/national-geospatial-program/national-map

Van der Sloot, H.A., Hoede, D., Wijkstra, J., Duinker, J.C., and Nolting, R.F. (1985). Anionic species of V, As, Se, Mo, Sb, Te and W in the Scheldt and Rhine estuaries and the Southern Bight (North Sea). Estuarine, Coastal and Shelf Science 21, 633-651.

Van der Weijden, C.H., Reichart, G.J., and Visser, H.J. (1999). Enhanced preservation of organic matter in sediments deposited within the oxygen minimum zone in the northeastern Arabian Sea. Deep Sea Research Part I: Oceanographic Research Papers 46, 807-830.

Veeh, H. H., Calvert, S. E., and Price, N. B. (1974). Accumulation of uranium in sediments and phosphorites on the South West African shelf. Marine Chemistry, 2(3), 189-202.

Volkenborn, N., Hedtkamp, S.I.C., Van Beusekom, J.E.E., and Reise, K. (2007). Effects of bioturbation and bioirrigation by lugworms (Arenicola marina) on physical and chemical sediment properties and implications for intertidal habitat succession. Estuarine, Coastal and Shelf Science 74, 331-343.

Von Breymann, M.T., Emeis, K.C. and Suess, E. (1992). Water depth and diagenetic constraints on the use of barium as a palaeoproductivity indicator. Geological Society, London, Special Publications, 64(1), 273-284.

Von Damm, K. L. (1990). Seafloor hydrothermal activity: black smoker chemistry and chimneys. Annual Review of Earth and Planetary Sciences, 18(1), 173-204.

Walper, J. L. (1977). Paleozoic tectonics of the southern margin of North America: Gulf Coast Association of Geological Societies Transactions 27, 230–239.

Wang, X., Johnson, T.M., and Lundstrom, C.C. (2015). Isotope fractionation during oxidation of tetravalent uranium by dissolved oxygen: Geochimica et Cosmochimica Acta 150, 160-170.

Wang, X., Planavsky, N. J., Reinhard, C. T., Hein, J. R., and Johnson, T. M. (2016). A Cenozoic seawater redox record derived from $^{238}U/^{235}U$ in ferromanganese crusts. American Journal of Science, 316(1), 64-83.

Wanty, R.B., Goldhaber, M.B. (1992). Thermodynamics and kinetics of reactions involving vanadium in natural systems: accumulation of vanadium in sedimentary rocks. Geochimica et Cosmochimica Acta 56, 1471–1483.

Webster, R.L. (1984). Petroleum source rocks and stratigraphy of the Bakken Formation in North Dakota, in Woodward, J., Meissner, F.F., and Clayton, J.C., eds., Hydrocarbon Source Rocks of the Greater Rocky Mountain Region: Denver, Rocky Mountain Association of Geologists, p. 57–81.

Wedepohl, K.H. (1971). Environmental Influences on the Chemical Composition of Shales and Clays. Physics and Chemistry of the Earth, 8, 307-333.

Wedepohl, K.H. (1991). The composition of the upper earth's crust and the natural cycles of selected metals. Metals in natural raw materials. Natural Resources. In: Merian, E.(Ed.), Metals and Their Compounds in the Environment. VCH, Weinheim, 3-17.

Wehrli, B. and Stumm, W. (1989). Vanadyl in natural waters: adsorption and hydrolysis promote oxygenation. Geochimica et Cosmochimica Acta, 53(1), 69-77.

Werne J. P., Sageman B. B., Lyons T. W., Hollander D. J. (2002). An integrated assessment of a type 'euxinic' deposit: Evidence for multiple controls on black shale deposition in the Middle Devonian Oatka Creek Formation. American Journal of Science 302 (2), 110–143.

Westrich, J. T., and Berner, R. A. (1984). The role of sedimentary organic matter in bacterial sulfate reduction: The G model tested 1. Limnology and oceanography, 29(2), 236-249.

Weyer, S., Anbar, A. D., Gerdes, A., Gordon, G. W., Algeo, T. J., and Boyle, E. A. (2008). Natural fractionation of $^{238}U/^{235}U$. Geochimica et Cosmochimica Acta, 72(2), 345-359.

White, D. A., Elrick, M., Romaniello, S., and Zhang, F. (2018). Global seawater redox trends during the Late Devonian mass extinction detected using U isotopes of marine limestones. Earth and Planetary Science Letters, 503, 68-77.

Whitfield, M. (2002). Interactions between phytoplankton and trace metals in the ocean. Advances in Marine Biology 41, 3–120.

Wignall, P.B. and Myers, K.J. (1988). Interpreting benthic oxygen levels in mudrocks: A new approach: Geology 16, 452-455.

Wilson, S., and Weber, J. (1979). An EPR study of the reduction of vanadium (V) to vanadium (IV) by fulvic acid. Chemical Geology, 26(3), 345-354.

Yang, S. and Liu, Y. (2016). Nuclear field shift effects on stable isotope fractionation: a review. Acta Geochimica, 35(3), 227-239.

Zelt, F. B. (1986). Natural gamma-ray spectrometry, lithofacies, and depositional environments of selected Upper Cretaceous marine mudrocks, Western United States, including Tropic Shale and Tununk Member of Mancos Shale. Ph.D. thesis, Princeton University, 284 p.

Zhang, F., Xiao, S., Kendall, B., Romaniello, S. J., Cui, H., Meyer, M., Gilleaudeau, G.J., Kaufman, A.J., and Anbar, A. D. (2018). Extensive marine anoxia during the terminal Ediacaran Period. Science Advances, 4(6), eaan8983.

Zheng, Y., Anderson, R. F., van Geen, A., and Fleisher, M. Q. (2002a). Preservation of particulate non-lithogenic uranium in marine sediments. Geochimica et Cosmochimica Acta, 66(17), 3085-3092.

Zheng, Y., Anderson, R. F., van Geen, A., and Fleisher, M. Q. (2002b). Remobilization of authigenic uranium in marine sediments by bioturbation. Geochimica et Cosmochimica Acta, 66(10), 1759-1772.

Zheng, Y., Anderson, R. F., van Geen, A., and Kuwabara, J. (2000). Authigenic molybdenum formation in marine sediments: a link to pore water sulfide in the Santa Barbara Basin. Geochimica et Cosmochimica Acta, 64(24), 4165-4178.

Zhu, B., Jiang, S., Pi, D., Ge, L., and Yang, J. (2018). Trace Elements Characteristics of Black Shales from the Ediacaran Doushantuo Formation, Hubei Province, South China: Implications for Redox and Open vs. Restricted Basin Conditions. Journal of Earth Science, 29(2), 342 -352.

APPENDICES

Table A1. Uranium, TOC, and isotope composition data from sites 25020 (shelf), GC 4 (shelf break), and GC 5 (slope).

Sample	Depth cm	U ppm	TOC* wt.%	Al* ppm	U_{auth} %	U/TOC	$\delta^{238}U$ ‰	2SD	$\delta^{234}U$ ‰	2SD
25020-11	0.5	5.18	7.78	8667.4	97.49	0.66	-0.56	0.15	126.96	25.43
25020-12	1.5	10.75	8.68	12413.1	98.27	1.24	-0.62	0.04	138.24	8.16
25020-13	3	12.83	7.22	12854.3	98.50	1.78	-0.28	0.09	139.40	12.23
25020-14	5	10.51	8.82	13633.0	98.05	1.19	-0.14	0.15	129.17	25.43
25020-15	7	11.50	8.82	12801.6	98.33	1.30	-0.16	0.19	140.02	3.81
25020-16	9	26.92	8.51	36328.1	97.98	3.16	-0.12	0.13	143.62	10.57
25020-17	13	32.94	10.44	18642.9	99.15	3.15	0.20	0.15	137.83	25.43
25020-18	17	58.35	10.44	-	-	5.59	0.11	0.09	145.63	20.43
25020-19	21	77.69	10.34	21148.9	99.59	7.51	-0.10	0.21	150.60	18.17
25020-20	25	95.85	11.59	31830.3	99.50	8.27	0.09	0.15	145.04	25.43
GC4-21	0.5	39.12	3.27	13788.9	99.47	11.95	-0.36	0.14	15.70	12.35
GC4-22	1.5	38.69	3.38	10381.8	99.60	11.46	-0.18	0.02	17.57	9.15
GC4-23	3	40.12	3.23	12518.0	99.53	12.42	-0.26	0.15	8.90	25.43
GC4-24	5	49.13	3.82	12885.8	99.61	12.86	-0.18	0.15	8.04	25.43
GC4-25	7	46.25	3.13	9979.5	99.68	14.79	-0.23	0.02	14.61	6.33
GC4-26	9	45.68	3.33	12290.5	99.60	13.72	-0.16	0.15	19.23	25.43
GC4-27	13	48.66	3.14	10467.9	99.68	15.52	0.05	0.04	10.95	0.81
GC4-28	19	48.35	3.14	12350.4	99.62	15.39	-0.31	0.14	9.00	27.51
GC4-29	23	50.36	2.51	12520.4	99.63	20.03	-0.21	0.17	14.87	19.00
GC5-30	0.5	6.88	5.79	16763.9	96.34	1.19	0.00	0.01	112.21	21.25
GC5-31	1.5	7.32	6.37	16578.0	96.61	1.15	-0.09	0.15	110.21	25.43
GC5-32	3	7.52	6.04	16049.6	96.80	1.25	-0.11	0.15	109.88	25.43
GC5-33	5	5.99	6.99	16697.7	95.82	0.86	0.17	0.14	108.79	19.30
GC5-34	7	6.78	6.92	14294.6	96.84	0.98	0.08	0.15	115.59	25.43
GC5-35	9	7.48	6.84	16157.7	96.76	1.09	-0.23	0.15	115.87	25.43
GC5-36	13	8.13	7.69	17000.0	96.87	1.06	-0.20	0.13	122.98	26.25
GC5-37	19	10.60	7.44	14000.0	98.02	1.42	-0.26	0.15	110.94	25.43
GC5-38	23	12.47	7.14	16009.0	98.07	1.75	-0.38	0.05	126.57	29.91
NIST2702		7.68	-	79158.1	-	-	-	-	-	-
SDO-1		45.86	-	61957.6	-	-	0.00	0.40	0.27	7.38
BATS SW		-	-	-	-	-	-0.38	0.15	148.35	25.43

*After Cofrancesco, 2016 - indicates value not reported

Table A2. The average shale content of selected elements from Turekian and Wedepohl (1961).

Element	Avg. Shale Content (ppm)
Aluminum (Al)	80,000
Manganese (Mn)	850
Vanadium (V)	130
Iron (Fe)	47,200
Nickel (Ni)	68
Copper (Cu)	45
Molybdenum (Mo)	2.6
Silver (Ag)	0.07

Table A3. Pore water concentrations of Fe, Mo and V from the shelf (25020), shelf break (GC 4), and upper slope (GC 5).

Sample Name	Depth cm	V nM	Fe µM	Ni nM	Cu nM	Mo nM	Mn µM
25020-BW-51	0	19.84	0.15	*	*	114.03	0.00
25020-BW-52	0	16.18	0.25	*	*	107.69	0.00
25020-1-53	0.5	117.30	0.16	*	*	119.52	0.01
25020-3-54	1.5	39.11	3.40	*	*	39.56	0.06
25020-5-55	3	38.29	10.48	*	*	22.29	0.13
25020-7-56	5	50.97	2.53	*	*	25.19	0.15
25020-9-57	7	24.99	0.23	*	*	20.74	0.01
25020-11-58	9	16.55	0.23	*	*	13.25	0.04
25020-13-59	13	35.34	1.44	*	*	0.91	0.10
25020-15-60	17	25.25	0.63	*	*	5.04	0.05
25020-19-61	21	64.59	0.38	*	*	150.59	0.05
25020-21-62	25	664.25	0.20	*	*	106.43	0.02
GeoChe4-BW-63	0	39.93	0.22	*	*	106.32	0.00
GeoChe4-BW-64	0	38.25	0.15	*	*	111.52	0.00
GeoChe4-1-65	0.5	49.78	4.24	*	*	157.49	0.01
GeoChe4-3-66	1.5	53.73	8.49	*	*	189.91	0.01
GeoChe4-5-67	3	22.05	6.12	*	*	194.51	0.03
GeoChe4-7-68	5	57.77	2.31	*	*	291.68	0.03
GeoChe4-9-69	7	53.99	4.64	*	*	246.35	0.02
GeoChe4-11-70	9	44.31	8.83	*	*	144.83	0.14
GeoChe4-15-71	13	72.37	5.85	*	*	408.90	0.09
GeoChe4-19-72	19	127.21	15.87	*	*	1883.61	0.58
GeoChe4-21-73	21	102.85	0.17	*	*	2208.17	0.01
GeoChe5-BW-74	0	47.43	0.00	*	*	123.45	0.00
GeoChe5-BW-75	0	44.31	0.00	*	*	103.80	0.00
GeoChe5-1-76	0.5	44.74	4.51	*	*	345.18	0.05
GeoChe5-3-77	1.5	76.85	3.96	*	*	692.99	0.02
GeoChe5-5-78	3	64.90	5.65	*	*	441.91	0.06
GeoChe5-7-79	5	37.94	15.28	*	*	384.78	0.11
GeoChe5-9-80	7	47.43	16.13	*	*	562.34	0.21
GeoChe5-11-81	9	25.41	6.20	*	*	800.55	0.15
GeoChe5-15-82	13	72.06	0.04	*	*	1560.65	0.06
GeoChe5-19-83	19	83.18	0.00	*	*	2236.06	0.05
GeoChe5-21-84	21	77.94	0.00	*	*	3033.26	0.03

*indicates element was below detection limits

Table A4. Measured TOC and CaCO3 content of sediments from the shelf (25020), shelf break (GC 4), and upper slope (GC 5). TOC data from sites 25020, GC 4 and GC 5 taken from Cofrancesco (2016).

Sample Name	Depth cm	TOC wt%	$CaCO_3$ wt%
25020-11	0.5	7.8	17.1
25020-12	1.5	8.7	13.2
25020-13	3	7.2	17.4
25020-14	5	8.8	10.8
25020-15	7	8.8	7.2
25020-16	9	8.5	9.2
25020-17	13	10.4	11.0
25020-18	-	-	-
25020-19	21	10.3	10.5
25020-20	25	11.6	11.1
GC 4-21	0.5	3.3	26.4
GC 4-22	1.5	3.4	35.2
GC 4-23	3	3.2	36.1
GC 4-24	5	3.8	28.1
GC 4-25	7	3.1	33.1
GC 4-26	9	3.3	35.2
GC 4-27	13	3.1	22.8
GC 4-28	19	3.1	28.6
GC 4-29	23	2.5	30.0
GC 5-30	0.5	5.8	50.5
GC 5-31	1.5	6.4	49.5
GC 5-32	3	6.0	40.8
GC 5-33	5	7.0	54.2
GC 5-34	7	6.9	50.6
GC 5-35	9	6.8	-
GC 5-36	13	7.7	34.8
GC 5-37	19	7.4	63.0
GC 5-38	23	7.1	43.1

- Indicates no measurement collected

Table A5. Solid phase major and trace element content of sediments from the shelf (25020), shelf break (GC 4), and upper slope (GC 5).

Sample Name	Depth cm	Al Wt %	V ppm	Mn ppm	Fe Wt %	Ni ppm	Cu ppm	Mo ppm	Ag ppm
25020-11	0.5	0.72	38.55	38.03	0.53	27.17	18.03	14.85	0.24
25020-12	1.5	1.22	35.00	56.46	0.83	42.93	27.76	17.29	0.38
25020-13	3	0.96	28.93	61.41	0.70	36.84	23.32	11.94	0.35
25020-14	5	1.09	34.22	62.59	0.86	45.21	27.08	17.58	0.38
25020-15	7	-	-	60.84	-	-	-	-	0.25
25020-16	9	1.32	55.12	-	1.02	49.57	30.47	22.46	0.44
25020-17	13	1.76	48.11	86.52	1.30	65.36	40.40	22.01	0.66
25020-18	17	1.97	50.02	-	1.56	78.56	47.08	28.69	0.72
25020-19	21	2.20	59.50	93.40	1.74	93.63	55.54	32.70	0.81
25020-20	25	2.29	124.34	159.74	1.82	99.49	57.41	38.24	0.89
GC4-21	0.5	1.38	30.78	82.47	1.44	53.03	27.54	3.43	0.17
GC4-22	1.5	1.04	25.63	65.10	1.22	44.40	22.29	2.96	0.19
GC4-23	3	1.25	32.58	88.07	1.50	54.45	27.33	3.84	0.17
GC4-24	5	1.29	33.58	92.49	1.66	52.87	24.52	5.00	0.18
GC4-25	7	1.00	29.88	72.63	1.44	51.94	24.02	5.22	0.18
GC4-26	9	1.23	31.65	82.75	1.53	53.02	25.26	4.97	0.17
GC4-27	13	1.05	31.26	76.78	1.37	59.03	28.38	6.45	0.17
GC4-28	19	1.24	32.95	80.33	1.57	53.51	25.18	6.92	0.17
GC4-29	23	1.25	32.10	81.81	1.46	56.43	27.95	8.14	0.17
GC5-30	0.5	1.68	26.61	66.13	1.06	79.23	54.47	1.28	0.83
GC5-31	1.5	1.66	26.16	65.82	1.04	77.97	54.35	1.48	0.83
GC5-32	3	1.60	27.58	67.41	1.07	79.03	54.98	2.11	0.81
GC5-33	5	1.67	27.04	68.70	1.10	79.92	63.79	1.16	0.79
GC5-34	7	1.43	28.55	72.78	1.20	85.40	58.21	2.72	0.86
GC5-35	9	1.62	26.70	67.95	1.11	81.80	54.78	4.74	0.86
GC5-36	13	1.70	33.70	78.50	1.40	47.00	74.30	6.20	0.90
GC5-37	19	1.40	31.60	66.80	1.20	35.20	64.30	7.50	0.95
GC5-38	23	1.60	26.75	61.52	1.01	74.44	51.41	7.33	0.97

- Indicates no measurement collected

Table A6. Calculated enrichment factors for all sample locations.

Sample Name	Mo EF	V EF	Fe EF	Ni EF	Cu EF	Ag EF
25020-11	64	3	1	4	4	38
25020-12	44	2	1	4	4	35
25020-13	38	2	1	4	4	41
25020-14	50	2	1	5	4	40
25020-15	-	-	-	-	-	-
25020-16	52	3	1	4	4	38
25020-17	39	2	1	4	4	43
25020-18	45	2	1	5	4	42
25020-19	46	2	1	5	4	42
25020-20	51	3	1	5	4	44
GC 4-21	8	1	2	5	4	14
GC 4-22	9	2	2	5	4	20
GC 4-23	9	2	2	5	4	16
GC 4-24	12	2	2	5	3	16
GC 4-25	16	2	2	6	4	20
GC 4-26	12	2	2	5	4	16
GC 4-27	19	2	2	7	5	18
GC 4-28	17	2	2	5	4	16
GC 4-29	20	2	2	5	4	16
GC 5-30	2	1	1	6	6	57
GC 5-31	3	1	1	6	6	57
GC 5-32	4	1	1	6	6	57
GC 5-33	2	1	1	6	7	54
GC 5-34	6	1	1	7	7	69
GC 5-35	9	1	1	6	6	61
GC 5-36	11	1	1	3	8	61
GC 5-37	16	1	1	3	8	77
GC 5-38	14	1	1	5	6	69

- Indicates EF not calculated

Table A7. Total organic content (TOC), U, Al, U/TOC and $\delta^{238}U$ data from Woodford, Cleveland, and Bakken shales.

Core	Location		Formation	Depth	TOC	U	Al	U_{auth}	U/TOC	$\delta^{238}U$	2SD
ID	Lat.	Long.	Name	m	Wt %	ppm	ppm	ppm		‰	
George	36.2761	-97.0665	Woodford	1380.6	5.48	16.0	60566	15.1	2.9	-0.46	0.23
				1381.2	6.55	36.0	55445	35.1	5.5	0.06	0.13
				1382.3	8.90	28.1	55199	27.2	3.2	0.15	0.13
				1383.8	9.30	37.4	55774	36.5	4.0	0.17	0.13
				1385.3	7.24	42.5	56633	41.6	5.9	0.16	0.08
				1386.5	6.09	19.1	43911	18.4	3.1	0.22	0.06
				1387.4	4.88	16.8	53377	16.0	3.4	0.05	0.36
				1389.0	5.48	27.0	64059	26.1	4.9	-0.15	0.27
				1389.9	4.38	18.8	63347	17.9	4.3	-0.03	0.13
				1391.5	5.74	23.4	55548	22.6	4.1	-0.18	0.13
				1392.9	7.48	30.6	73827	29.4	4.1	-0.01	0.20
				1395.1	11.87	32.5	58152	31.6	2.7	0.30	0.10
			Average		**6.95**	**27.3**	**57986**	**26.5**	**4.0**	**0.02**	**0.16**
Poe	35.0193	-96.2976	Woodford	2357.6	0.37	8.1	39514	7.5	21.8	-0.11	0.13
				2359.2	0.53	9.8	7048	9.7	18.6	0.11	0.13
				2360.7	2.93	14.2	8095	14.1	4.8	-0.08	0.13
				2362.4	4.80	37.3	63538	36.3	7.8	-0.05	0.13
				2363.7	4.12	32.2	43599	31.5	7.8	0.15	0.13
				2364.3	1.08	48.8	34098	48.3	45.4	0.15	0.13
				2365.2	7.10	44.8	54206	43.9	6.3	0.12	0.13
				2366.8	3.78	18.2	-	-	4.8	-	-
				2368.3	6.58	39.6	65882	38.6	6.0	0.34	0.11
				2369.8	6.33	51.7	53538	50.9	8.2	0.04	0.05
				2371.3	-	40.0	29242	39.6	-	0.12	0.13
				2372.9	4.97	-	-	-	-	-	-
				2374.4	7.26	43.8	48106	43.1	6.0	0.04	0.13
				2375.9	6.13	30.8	18077	30.5	5.0	0.38	0.13
				2377.4	2.07	13.4	-	-	6.5	-	-
				2379.2	1.84	10.8	-	-	5.9	-	-
				2380.6	2.21	10.6	-	-	4.8	-	-
				2382.0	4.45	23.8	18485	23.5	5.3	-0.10	0.06
				2383.5	2.60	12.8	-	-	4.9	-	-
				2385.1	4.04	33.8	26168	33.4	8.4	0.37	0.01
				2386.6	5.80	-	-	-	-	-	-
				2388.1	3.69	23.7	14751	23.5	6.4	0.06	0.13

Table A7. (continued)

Core	Location		Formation	Depth	TOC	U	Al	U_{auth}	U/TOC	$\delta^{238}U$	2SD
ID	Lat.	Long.	Name	m	Wt %	ppm	ppm	ppm		‰	
Poe	35.0193	-96.2976	Woodford	2389.8	7.15	61.8	24101	61.4	8.6	0.01	0.13
				2391.2	9.19	46.5	18540	46.3	5.1	-0.12	0.13
				2392.7	5.07	24.1	51780	23.4	4.8	-0.21	0.13
				2394.2	6.87	48.3	42018	47.7	7.0	-0.05	0.13
			Average		**4.44**	**30.4**	**34778**	**34.4**	**9.1**	**0.06**	**0.11**
K-566765	37.2303	82.7043	Cleveland	1133.9	7.93	7.0	26262	6.6	0.9	-0.03	0.09
				1135.4	3.23	3.8	24133	3.5	1.2	-	-
				1136.9	2.38	4.6	26947	4.1	1.9	-	-
				1138.4	5.96	22.3	29922	21.8	3.7	0.21	0.13
				1140.0	4.62	11.0	28654	10.6	2.4	-	-
				1141.5	4.86	11.3	27163	10.9	2.3	-0.02	0.02
				1143.0	3.73	7.7	32482	7.2	2.1	-	-
				1144.5	4.78	9.0	32088	8.5	1.9	0.06	0.09
				1146.0	3.61	11.3	38126	10.7	3.1	-	-
				1147.6	2.73	4.8	28448	4.4	1.8	-	-
				1149.1	2.73	10.4	35287	9.8	3.8	0.21	0.04
				1150.6	3.69	7.7	25378	7.3	2.1	-	-
				1152.1	2.27	4.9	37485	4.4	2.2	-	-
				1153.1	2.58	4.6	20999	4.3	1.8	-	-
				1154.3	1.54	11.0	40518	10.4	7.1	0.04	0.03
				1155.2	4.19	22.9	20652	22.6	5.5	-	-
				1156.7	3.65	20.5	24149	20.2	5.6	-	-
				1158.2	5.41	17.1	30538	16.7	3.2	-	-
				1159.8	4.72	20.4	33939	19.9	4.3	-	-
				1161.6	3.82	12.4	49926	11.7	3.3	-	-
				1162.8	4.84	7.5	23959	7.1	1.5	-0.22	0.16
				1164.3	0.49	1.3	18464	1.0	2.7	-	-
				1165.6	0.56	1.8	23151	1.5	3.3	-	-
				1166.5	0.48	1.8	21049	1.5	3.7	-	-
				1167.4	0.62	1.7	18361	1.4	2.7	-	-
				1168.9	2.15	8.7	21807	8.3	4.0	-0.03	0.08
			Average		**3.37**	**9.5**	**28457**	**9.1**	**3.0**	**0.03**	**0.08**
E701	48.3794	-104.135	U. Bakken	3010.0	*15.24*	*41.3*	*36300*	40.8	2.7	0.12	0.04
				3010.6	*14.37*	*39.3*	*35100*	38.8	2.7	-	-
				3010.9	*16.47*	*41.3*	*41200*	40.7	2.5	0.17	0.09

Table A7. (continued)

Core	Location		Formation	Depth	TOC	U	Al	U_{auth}	U/TOC	$\delta^{238}U$	2SD
ID	Lat.	Long.	Name	m	Wt %	ppm	ppm	ppm		‰	
E701	48.3794	-104.135	U. Bakken	3011.0	*15.66*	*35.1*	*41500*	34.5	2.2	0.27	0.09
				3011.6	*16.48*	*66.9*	*39700*	66.3	4.1	0.27	0.09
				3011.9	*12.13*	*34.7*	*27600*	34.3	2.9	-	-
				3012.1	*18.92*	*62.1*	*38800*	61.5	3.3	-	-
				3012.3	*10.38*	*71.2*	*38600*	70.6	6.9	-	-
			Average		**14.96**	**49.0**	**37350**	**48.4**	**3.4**	**0.21**	**0.07**
			L. Bakken	3023.3	*16.94*	*55.5*	*56000*	54.7	3.3	-	-
				3023.4	*15.96*	*70.0*	*44200*	69.3	4.4	-	-
				3023.7	*10.68*	*36.2*	*44600*	35.5	3.4	0.36	0.05
				3024.0	*4.95*	*22.4*	*14100*	22.2	4.5	-	-
				3024.3	*13.56*	*62.5*	*48900*	61.8	4.6	0.36	0.03
				3024.5	*14.90*	*93.0*	*46700*	92.3	6.2	-	-
				3024.8	*18.48*	*177.0*	*45500*	176.3	9.6	0.33	0.04
				3025.0	*8.75*	*69.2*	*62000*	68.3	7.9	0.07	0.19
				3025.3	*6.90*	*67.3*	*48900*	66.6	9.8	-	-
			Average		**12.35**	**72.6**	**45655**	**71.9**	**6.0**	**0.28**	**0.08**

- Indicates no measurement collected

Table A8. Nickel (Ni) and Copper (Cu) data collected from Woodford Shale cores George and Poe

Core Name	Depth feet	Depth meters	Ni ppm	Cu ppm
George	**4529.5**	**1380.6**	133.0	64.0
	4531.6	**1381.2**	146.4	111.3
	4535	**1382.3**	157.2	94.8
	4540	**1383.8**	169.4	102.2
	4545	**1385.3**	127.3	78.9
	4549	**1386.5**	102.8	66.2
	4552	**1387.4**	93.3	47.7
	4557	**1389.0**	80.8	44.4
	4560	**1389.9**	70.7	39.1
	4565.25	**1391.5**	90.7	53.7
	4570	**1392.9**	120.3	76.5
	4577	**1395.1**	257.8	131.4
Poe	**7735**	**2357.6**	74.9	44.4
	7740	**2359.2**	26.3	26.8
	7745	**2360.7**	83.3	27.6
	7750.5	**2362.4**	210.6	137.0
	7755	**2363.7**	149.5	84.4
	7757	**2364.3**	284.3	90.7
	7760	**2365.2**	242.9	122.0
	7770	**2368.3**	331.5	89.2
	7775	**2369.8**	204.4	103.7
	7780	**2371.3**	149.3	67.3
	7790	**2374.4**	156.6	99.3
	7795	**2375.9**	66.2	34.9
	7815	**2382.0**	57.6	39.0
	7825	**2385.1**	131.4	80.6
	7835	**2388.1**	48.4	34.7
	7840.5	**2389.8**	182.1	78.4
	7845.25	**2391.2**	240.3	112.0
	7850	**2392.7**	192.4	158.3
	7855	**2394.2**	247.8	187.5

VITA

Michelle Lee Abshire

Candidate for the Degree of

Doctor of Philosophy

Dissertation: DECIPHERING DEPOSITIONAL AND DIAGENETIC PROCESSES IN MARINE SYSTEMS BY APPLICATION OF TRACE METAL AND ISOTOPE GEOCHEMISTRY

Major Field: Geology

Biographical:

Education:

Completed the requirements for the Doctor of Philosophy in Geology at Oklahoma State University, Stillwater, Oklahoma in July, 2020.

Completed the requirements for the Bachelor of Science in Geology at Oklahoma State University, Stillwater, Oklahoma in 2016.

Experience:

Teaching Assistant, Physical Geology, Oklahoma State University 2019-2020

Geoscience Intern, ConocoPhillips, 2019

Adjunct Earth Science Instructor, Northern Oklahoma College 2018

Teaching Assistant, Field Geology, Oklahoma State University 2017-2018

Professional Memberships:

Phi Theta Kappa, American Association of Petroleum Geologists, Association for Women Geoscientists, Geological Society of America, Geochemical Society, American Geophysical Union